



universität
wien

DIPLOMARBEIT

Physiological and molecular characterization of leaf development in *Theobroma cacao* L. (Malvaceae)

verfasst von:

Lisa Haberl

angestrebter akademischer Grad

Magistra der Naturwissenschaften (Mag.rer.nat.)

Wien, 2015

Studienkennzahl lt. Studienblatt: A 190 406 445

Studienrichtung lt. Studienblatt: Lehramtsstudium: Mathematik,
Biologie und Umweltkunde

Betreuer: Univ.Prof. Dr. Wolfram Weckwerth

Acknowledgement

I want to express my gratitude to all members of the MoSys-team –thank you for your help, friendship and moments of laugh. Especially I want to thank my supervisor Wolfram Weckwerth for his guidance and to give me the chance to work on this project. I want to thank Doris Engelmeier, for her ideas, time and support to fulfil this project, Gert Bachmann for his introduction and help with statistical analysis programs as well ionomic measurements, the gardeners and Wolfgang Postl for the support during the thesis.

A special thanks goes to my partner Siegi, who supported me during my whole studies, for his appreciation at all and for enduring my night learning sessions.

Bei meinen Eltern bedanke ich mich für alles was sie mir an Werten mitgegeben haben, sowie für die finanzielle Unterstützung während meines Studiums.

Carmen, Sarah, Theresa, Katrin, Klaus, Michi und Hermann für eure Freundschaft und den gemeinsamen, teilweise kreuzerlbelasteten, Weg durch das Studium.

TABLE OF CONTENT

1. INTRODUCTION	1
1.1. Theobroma cacao	1
1.2. Overview photosynthesis	11
1.3. Photosynthesis pigments and plant pigments	12
1.4. Light absorption	18
1.5. Aim of the thesis	24
1.6. Fluorescence measurements	25
1.7. Photometric measurements	27
1.8. HPLC-UV/VIS.....	28
1.9. Ionomics & voltammetric measurements	30
1.10. Metabolomics	30
2. MATERIAL AND METHODS.....	32
2.1. Plants and their conditions	32
2.2. Climate data	33
2.3. Leaf growth and classification	33
2.4. Fluorescence measurements	34
2.5. Harvesting	37
2.6. Hot-water-extract and acid-hot-water-extract.....	37
2.7. pH measurements.....	38
2.8. Photometry	39
2.9. HPLC-UV/VIS.....	41
2.10. Cation and anion chromatography	42
2.11. Voltammetric measurements.....	43
2.12. LC-MS/MS Orbi XL	43

2.13.	Anatomical studies.....	44
3.	RESULTS	46
3.1.	Climate data and leaf growth.....	46
3.2.	Fluorescence measurements	47
3.3.	pH measurements	49
3.4.	Photometric measurements.....	50
3.5.	HPLC-UV/VIS	54
3.6.	Cation and anion chromatography	57
3.7.	Voltammetric measurements	63
3.8.	Results LC-MS/MS Orbitrap XL	65
3.9.	Anatomical studies	66
3.10.	Statistical analysis.....	70
4.	DISCUSSION	72
5.	OUTLOOK	86
6.	ABSTRACT.....	87
6.1.	Abstract (English).....	87
6.2.	Zusammenfassung (Deutsch)	88
7.	REFERENCES.....	89
8.	APPENDICES	100
8.1.	Results overview - list of cations and anions	100
8.2.	Results overview – fluorescence, photometry, voltammetry and anatomy.....	101
8.3.	List of figures	102
8.4.	List of tables	106
8.5.	Curriculum Vitae et Studiorum	107

1. INTRODUCTION

1.1. *Theobroma cacao*

1.1.1. *Taxonomy and origin*

The genus *Theobroma cacao*, better known as cacao, belongs to the family Malvaceae, former Sterculiaceae (since 1873 –Baillon). In 1753 Carl of Linné gave this tree the name *Theobroma* in his famous book *Species Plantarum* (CUATRECASAS, 1964). It means **food for the Gods**, (theos (θεός): greek for God; bromia (βρωμια): greek for food). The name *cacao* has its origin in Mayan language (PAOLETTI et al., 2012). This family is divided into 6 sections (*Andropetalum*, *Glossopetalum*, *Oreanthes*, *Rhytidocarpus*, *Telmatocarpus* and *Theobroma*) and includes **22 species**. Due to the major number of indigenous cacao species, which are located in the tropical rainforests of Brazil and Colombia, the origin of the cacao is assumed to be there (SANTOS et al., 2011).

1.1.2. *Geographical distribution*

T. cacao is a typical Neotropical under storey plant distributed in the western hemisphere (*Figure 1.1*) between latitude **20 ° North and 20 ° South** (CUATRECASAS, 1964) with temperatures between 20 °C to 30 °C and precipitation of 2000 – 8000 mm (CUATRECASAS, 1964); newer sources saying 1000 – 3000 mm rainfall per year (COLOMBO et al., 2012).

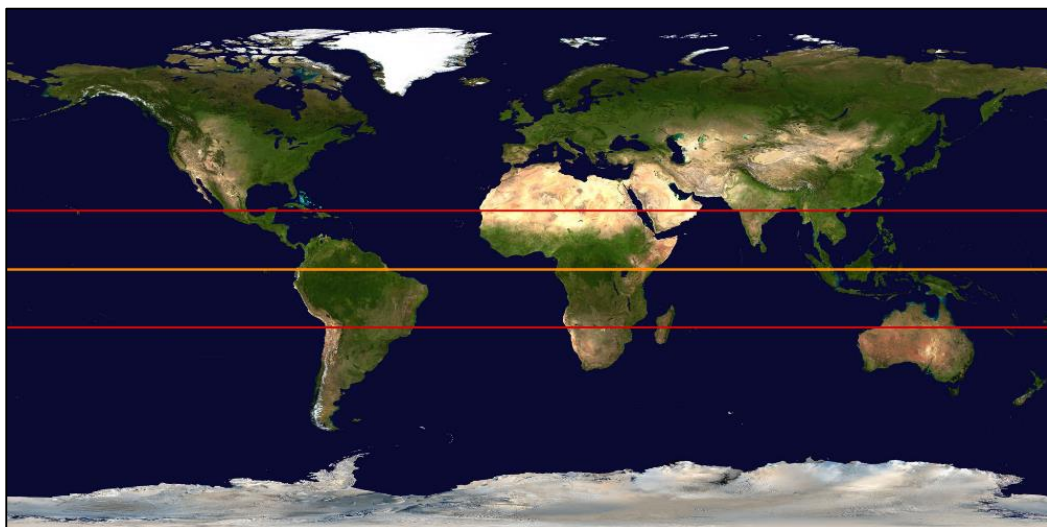


Figure 1.1: In red the latitude from about 20 ° North and South is plotted; the equator is marked in orange. (Adapted with Photoshop from a satellite world map from the NASA: <http://visibleearth.nasa.gov/> 2004)

1.1.3. Botany

The **cacao tree** is a spindly, evergreen growing tree. Under cultivation, a height from 4 to 8 m (CUATRECASAS, 1964) and in natural condition 14 to 20 m is reached (LACHENAUD et al., 1997). Cacao needs constant high humidity and annual temperatures with narrow oscillations and protection (shade) against direct radiation and evaporation. It even doesn't resist short dryness (CUATRECASAS, 1964). At the age of 3 – 6 years the tree reaches its physiological maturation (SAUNDERS et al., 2004).

At the **reproduction stage**, small white to pink flowers with about 1 cm diameter arise in cauliflower clusters at the trunk (*Figure 1.2*).



Figure 1.2: T. cacao flower development: A) Cauliflower cluster at a trunk; B) Flower with anthers; C) Flower bud, flower cross sections and flower top view. (©Engelmeier)

The floral formula is: * S5 P5 A (5+5) G(5) (S = sepalum, P = petalum, A = androeceum G = gynoecium; see picture and drawing in *Figure 1.3*). Flowers are pollinated by tiny flies (midges, diptera) and only 5 % receive enough pollen to start fruit development. In order to that in modern cacao plantations pollination is assisted artificially by hand (CUATRECASAS, 1964; PAOLETTI et al., 2012).

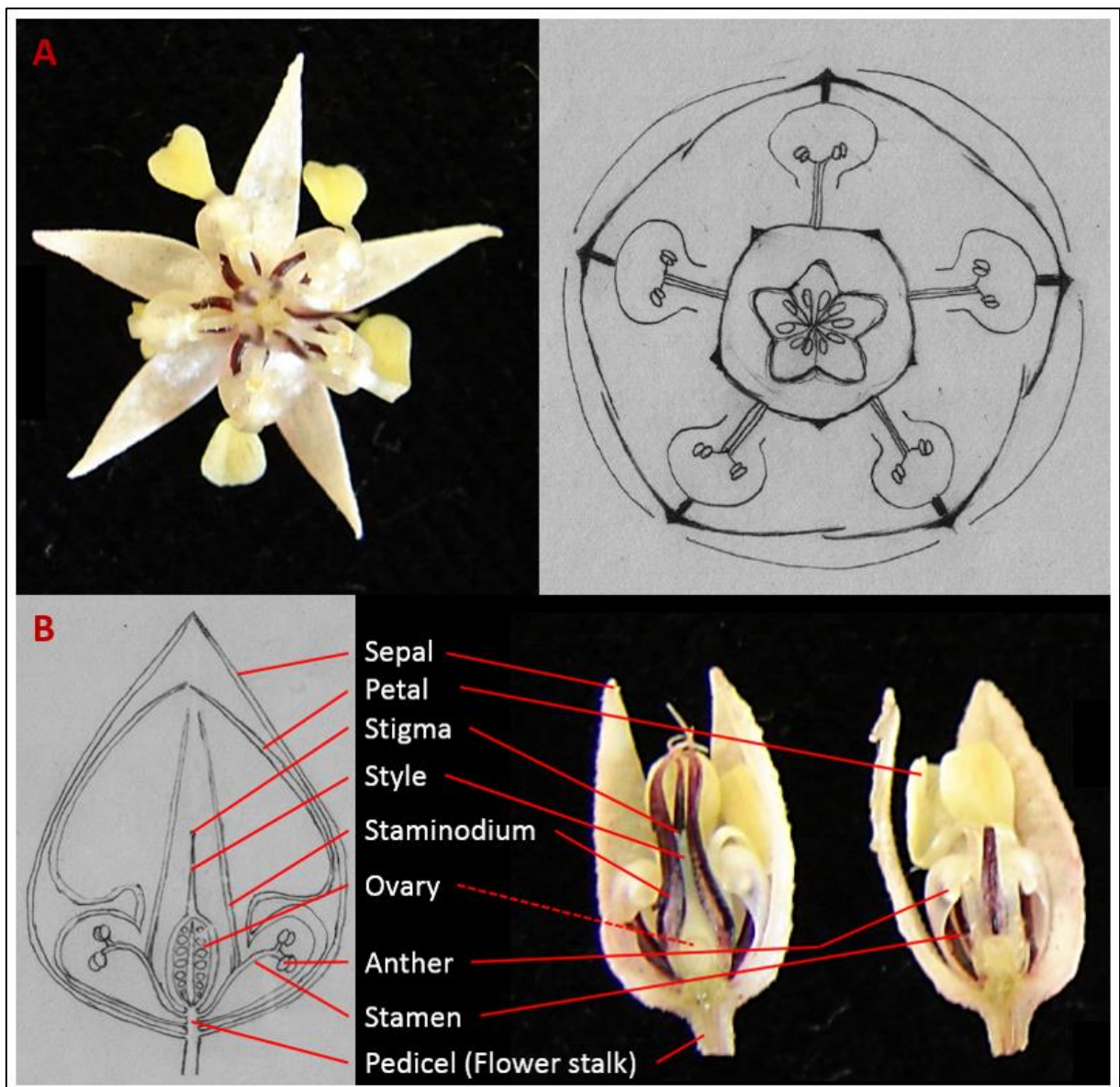


Figure 1.3: *T. cacao* flower development: A) Flower top view with anthers and floral formula drawing of * S5 P5 A(5+5) G(5); B) Drawing and flower cross section through flower bud. (©Engelmeier)

The continuous flower production is very high, each plant can develop between 50.000 to 100.000 flowers per year (PAOLETTI et al., 2012). Cacao fruit develops into a massive **cacao**

pod (dry berry). It will remain up to 3 months on the tree with a size of 15 – 20 cm between the colour range of whitish-green to yellow and red (*Figure 1.4*). This colour range is one identification marker between cacao varieties as Criollo, Forastero, Trinitario and many more.



Figure 1.4: *T. cacao* A) 1 day old Criollo cacao fruit on a trunk 1 cm long, still with petals; B) Forastero cacao fruit, 2 cm long and 3 days old; C) Criollo cacao, 2 months old, 22 cm. Developing and colouring Forastero cacao fruit: D) 2 months old, 19 cm; E) 3 months old, 19 cm. (©Engelmeier)

T. cacao seeds germinate epigeal (*Figure 1.5*) whereas other *Theobroma* species germinate hypogeal (CUATRECASAS, 1964). The cacao pod includes about 30 – 40 seeds surrounded by a bitter-sweet pulp (*Figure 1.5*) (CUATRECASAS, 1964).

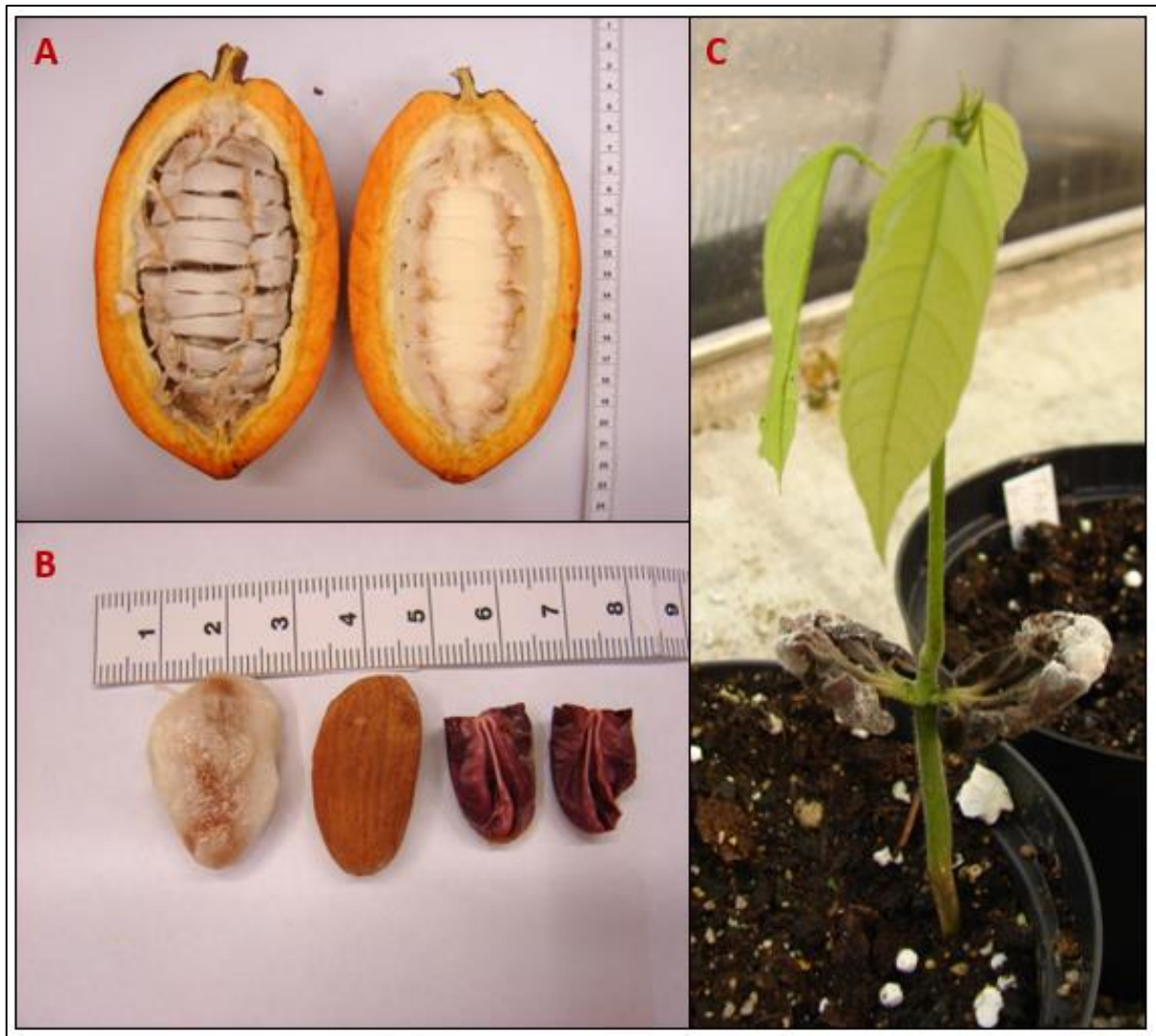


Figure 1.5: *T. cacao* fruit development: A) Opened Forastero cacao fruit with creamy coloured pulp which covers every seed; B) Cacao seed covered with pulp, seed and cross section of anthocyanidin rich seed cotyledons; C) Hypocotyl germination of young *T. cacao* seed. (©Engelmeier)

The **leaf development** of *Theobroma cacao* has been shown to be somewhat different from many temperate plants (BAKER et al., 1975). The dark green leaves are evergreen, shiny, leathery and oval in shape (Figure 1.6). Their size is commonly 20 to 30 cm long and 7 to 10 cm wide (CUATRECASAS, 1964). The maximum leaf size is reached approximately within 8 days. One leaf flushing cycle on a tree takes about 6 weeks and is repeated in both summer and winter (ABO-HAMED et al., 1983). The description of the periodic rhythm of *Theobroma cacao* under normal and under controlled environmental conditions (light and temperature) was the point of interest of GREATHOUSE et al. (1971). A comparison between cacao plants grown in greenhouse environment (ABO-HAMED et al., 1983), grown material under controlled

temperature and light intensity (GREATHOUSE, 1971) and young plants growing outdoor in a shaded tropical environment (VOGEL, 1975) showed similar leaf development, but different durations of development stages.



Figure 1.6: *T. cacao* tree in the greenhouse of the Department: The developing leaves are bright coloured and hanging down vertically, beneath adult dark green leaves in nearly horizontal position.

(©Engelmeier)

Further, during this flushing progress, colour changes can be observed from transparent light green to orange, to red due to presence of anthocyanidins in older immature stages (ORCHARD et al., 1980), to light green and finally to fully expended mature dark green leaves (ALMEIDA & VALLE, 2008). Several development stages of leaf flushing are shown in detail in *Figure 1.7*.

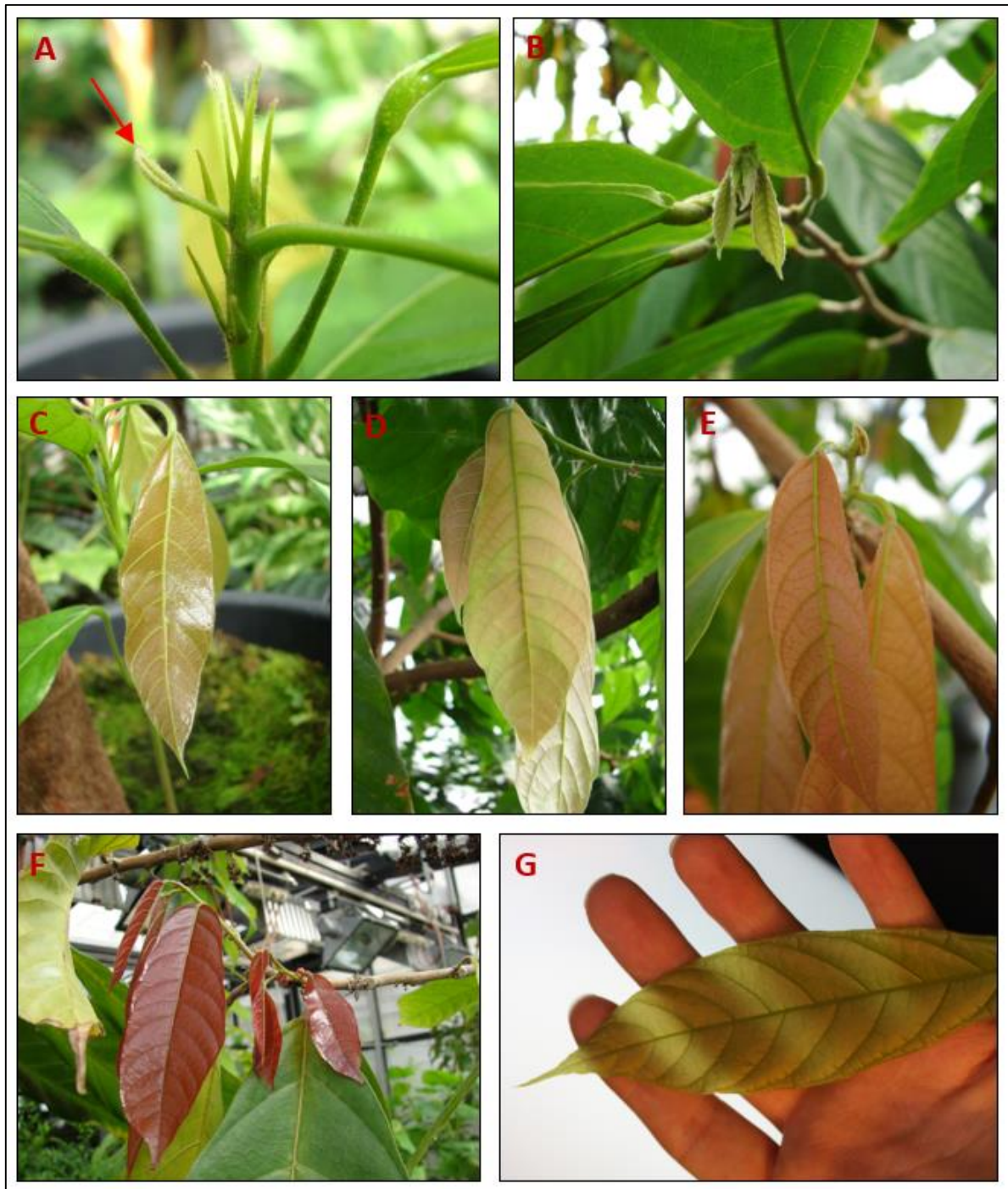


Figure 1.7: *T. cacao* leaf flushing: A) Leaf bud with first flushing leaf (red arrow); B) Leaf expanding during the first days; C) Shiny about one week old leaf coloured in orange; D) 10 days old leaves with anthocyanidin coloured parts and shadowed leaf parts are still transparent greenish; E) 2 week old red to orange leaves with green nerves; F) Red leaves on a twig during expansion, about a week old; G) 1 week old leaf which is still enough transparent to see fingers behind it. (©Engelmeier)

During the flush of young leaves limited stomata development is detected, a reason for this might be the restriction of water loss. Functional stomata are discovered at the age of 4 days old leaves only in midribs. All other stomata in the inter-venial regions start to develop in between 2 to 4 days and opening until leaf expanding phase is finished. Leaf maturation is correlated with stomata opening, maximal cuticle thickness and presence of chlorophyll pigment (ABO-HAMED et al., 1983). Until stomata and leaves are fully developed and the leaves' positions turned horizontal, the young flushed leaves are pendulously (ABO-HAMED et al., 1983). Further, the hypostomatous leaf surface is covered with 4 diverse hair types. There is a discussion going on about their function –they might act as light protection, reduce water loss and protect against herbivores (HARDWICK et al., 1981; ABO-HAMED et al., 1983).

Leaf live from cacao is various. Four major classes of leaf fall were identified by MIYAJI et al. (1997): i) following infection (fungal or bacterial attack); ii) enforced leaf fall (wind, mechanical factors); iii) following injury (90 % of leaf area are eaten by insect larvae); and iv) physiologically (showing a low level of photosynthesis followed by death). In that study observed *T. cacao* trees were grown under shelter trees in a tropical plantation. The leaf longevity was depending on the leaf emergence and the level within the canopy. Life span of upper leaves ranged from 120 to 200 days, in the middle layer from 180 to 250 days and the lower layer from 280 to 370 days. Concluding, leaf longevity of bearing-age cacao trees was longer in the more-shaded lower canopy (MIYAJI et al., 1997).

1.1.4. Brief History before the Spanish conquest

The cacao tree is endemic in **South America** and was domesticated about 3000 years ago (HENDERSON et al., 2007) in Central America (ARGOUT et al., 2011). The beans of cacao also have been consumed by the preclassic Maya. The earliest evidence of cacao could be observed through a 2600 years old pottery (HURST et al., 2002).

In addition, cacao residues were found in local vessels of Chaco Canyon. Cacao was used as currency (money system) during the Aztec state and also by the Mayas (COE, 1994; COE & COE, 1996). Also extensive trade and interaction in Southwest and Mesoamerica in prehistoric time could be monitored with a 'biomarker' of cacao, theobromine – an alkaloid (WASHBURN et al., 2011). The usage of cacao beans as a currency system was still sustained during the

Spanish conquest. For example in Tlaxcala at 1545 AD, for 100 beans you got a slave. Until the 18th century cacao beans had been used as a form of money. This currency system was counted by “load”. Each loads were 24 000 beans and has a worth of 5 – 6 gold pesos (GRIVETTI & SHAPIRO, 2009).

The Aztec had seen in this plant a gift from God Quetzalcoatl. Therefore the seeds were holy and used as a drink. In the ancient time this bitter drink was a mixture of water, cacao, corn, vanilla, cayenne pepper and salt. It was called Xocoatl (= bitter water). It is not sure, if the cacao bean itself or the cacao pulp or both have been used for Xocoatl (GRIVETTI & SHAPIRO, 2009).

Cacao itself is known since ancient times for its health benefits against diseases. Every part was used as medicine. Some Indians disposed cacao for gastro-intestinal diseases and cold medication (DELZENNE, 2001). Also flowers were used against roundworm in eyes (GRAZIANO, 1998) and in bath water to reduce tiredness (DILLINGER et al., 2000). Young leaves were put as antiseptic agent on wounds. Colombian Indians cooked leaves as a tea against heart diseases and took it as urinary agent (GRAZIANO, 1998). Also the fatty part of cacao – cacao butter – was used oral to abate bronchitis, catarrhs and as a cream (DILLINGER et al. 2000).

1.1.5. Cacao over the world previous and today

As the Spanish conquistadors arrived in 1500 Mexico the cacao triumphal procession of cacao over the world has started. The exotic bitter cacao-water was first introduced to the Spanish aristocracy. As sweetened chocolate-drink, it reached the European aristocrats later on the middle class. First the better tasting (mild not bitter, less acid and aromatic) rare cacao cultivar **Criollo** (= native) was cultivated. Nevertheless this cultivar of *T. cacao* was very sensitive against pests. Criollo is a very rare cultivar nowadays too and the best noble and expensive cacao now. Another cultivar called **Forastero** (= foreigner) and hybrids of Criollo and Forastero, which is tasting more bitter and since then, it has been used for commercial chocolate production. Today the **Trinitario** hybrid of Criollo and Forastero is more resistant against pests and it is used for precious chocolate production but it is also as rare as Criollo and therefore comparably expensive. Such Trinitario and Criollo cultivars are very important for noble

chocolate production and have an immense economic importance. In the past also wild relatives of cacao (*T. angustifolium*, *T. bicolor*, *T. grandiflorum*) as well as their pulp have been used for cacao drinks. Today people recognized them again for chocolate production (NOVAK & SCHULZ, 2009). In 1800, the technical revolution started and chocolate and praline production was growing so fast, that chocolate was available for the populace. Various inventions and methods were first leading to chocolate bars and finally to milk chocolate (COE & COE, 1996).

Nowadays cacao is one of the most important perennial crops worldwide. The world production in 2002 is estimated with 2.8 million tons (FAO, 2003). An overview from the production and net exports of cacao beans in year 2005/06 (ICCO, 2006) is shown in *Figure 1.8*. The International Cocoa Organization (ICCO) postulated, that in 2013/14 about **4.16 million tons** of cacao seeds were harvested (ICCO, 2013). Cacao farms are mostly smallholder farms, it is expected that there are over 4.5 million farms. Subsequently, many people having their income from growing cacao beans (World Agroforestry Centre, 2012).

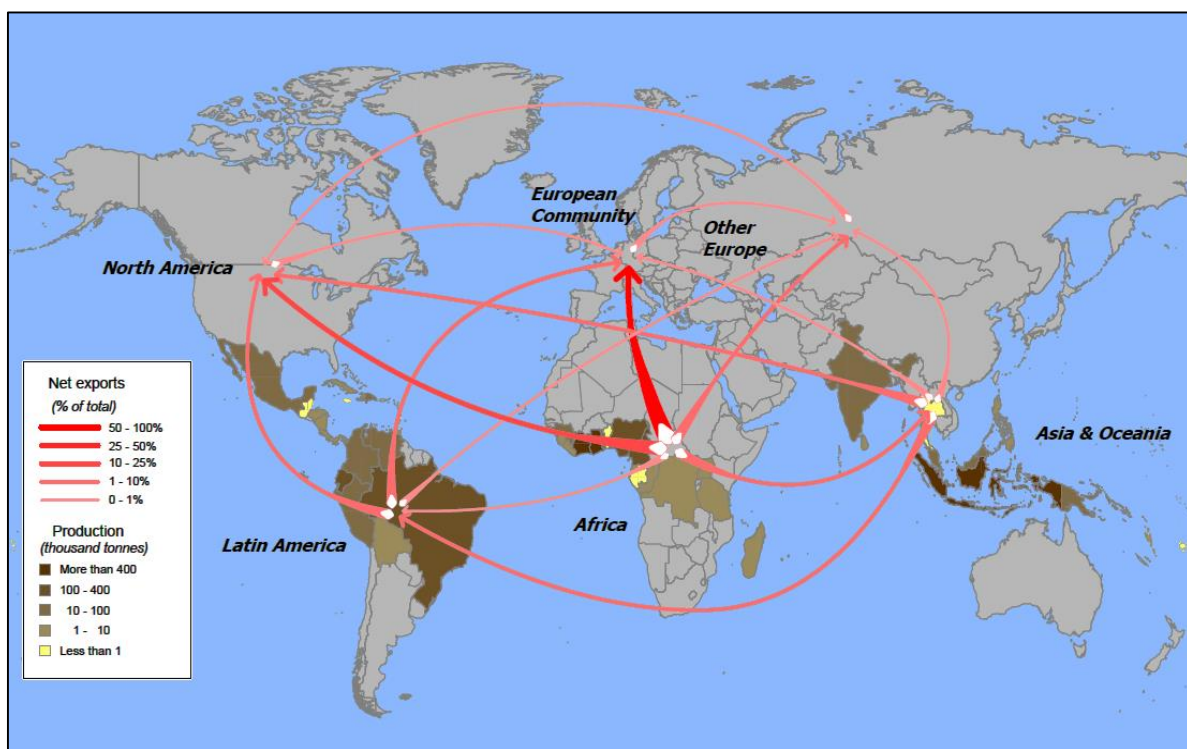


Figure 1.8: Production and net exports of cacao beans in 2005/06 (ICCO, 2006).

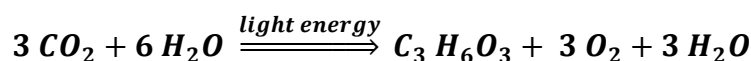
1.1.6. Sequenced genome

In the year 2011 the cacao genome was sequenced (ARGOUT et al., 2011). This knowledge offers new possibilities to study biochemical pathways e.g. flavonoids, disease resistance and new hybrids in detail. All that may also support the development of the future cacao production worldwide (ARGOUT et al., 2008; ARGOUT et al., 2011).

1.2. Overview photosynthesis

The chloroplast is the cell organelle where photosynthesis happens and contains all components of the photosynthesis apparatus.

During photosynthesis light energy is converted into chemical energy and CO₂ is fixated in organic compounds. The gross equation is:



In detail, in the first step light energy is absorbed by pigment molecules. The absorbed light excites electrons of the pigment molecules (located in reaction centres) which are able to reach a higher energy level afterwards. The energy is transferred to the reaction centres of the photosystems. All higher plants possess two photosystems (PS). The evolutionary older PS system, which is PS I, is also used by photoactive bacteria. It is not able to use water as an electron donator (e.g. based on H₂S, green sulphur bacteria).

The various reactions of the photosynthesis are subdivided into two main processes (*Figure 1.9*):

- Reactions of the energy transfer (light reaction)
- Carbon-fixating actions (dark reaction)

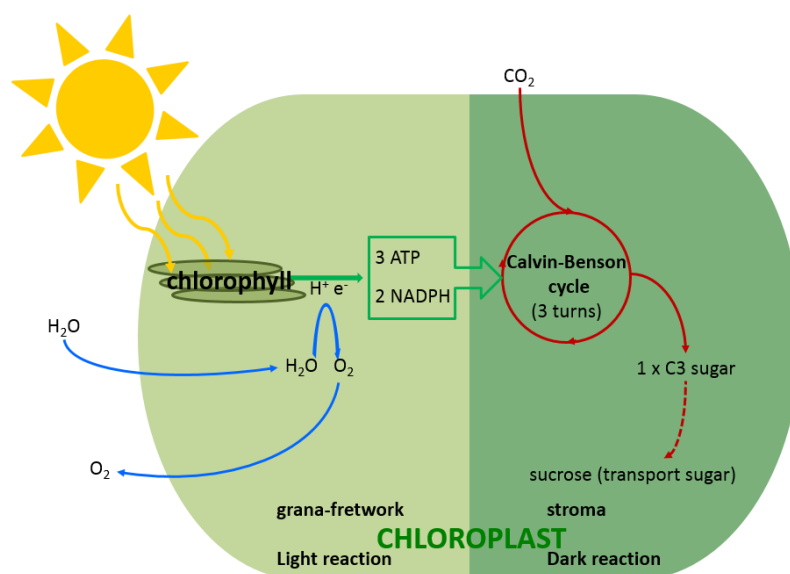


Figure 1.9: Schematical overview of the light and dark reaction in a chloroplast of a C₃ plant. (Based on Engelmeier, unpublished)

Using the energy transported by the photosystems, high energy molecules like ATP (adenosine-tri-phosphate) and NADPH-H⁺ (nicotinamide-adenine-dinucleotid-phosphate) are formed, which are used for carbon fixation.

The carbon fixating actions are starting with the fixation of CO₂ in the reductive pentosephosphat-cycle (Calvin-Benson-cycle). The output of the Calvin-Benson-cycle are carbohydrates, which are primary converted into saccharose and starch (RAVEN et al., 2006).

More detailed information about photosynthesis and other pathways of CO₂ fixation are discussed elsewhere (see references as RAVEN et al., 2006; SCHOPFER & BRENNICKE, 2010).

1.3. Photosynthesis pigments and plant pigments

Pigments which are involved in photosynthesis are chlorophylls, carotenoids, xanthophylls and phycobilines (bacteria and algae). The appearance of photosynthesis pigments in plants, depends on various parameters (e.g. habitat, light intensity). They are adapted as much as possible to various environmental situations. Attributed to the structural formulae of these

pigments – over all called chromophoric system – it is possible to absorb electromagnetic radiation. A chromophore is a system of conjugated double bonds (two $C = C$ – double bonds are separated by a $C - C$ – single bond) (LÜTTGE et al., 2010).

1.3.1. Chlorophyll molecules

The origin of the word chlorophyll is traced back to the Greek word ‘chloros’ (χλωρός), which means yellowish green and ‘phyllon’ (φύλλον), which means leaf. Photosynthesis is the basis of sustaining (autotrophy) life processes in plants (VALEUR & BERBERAN-SANTOS, 2012).

The basic structure is a porphyrin ring, which consists of four pyrrol rings which are linked via methine bridges. From this cyclic tetrapyrrol several further important chemical compounds in organisms (e.g. hemoglobin and cytochrome) derive. In common they contain a metal ion in the centre, which is Mg^{2+} for chlorophyll. In addition, the length of the side chain located at the fourth ring (Figure 1.10 ring D), which is phytol ester, is important for the properties of the structure.

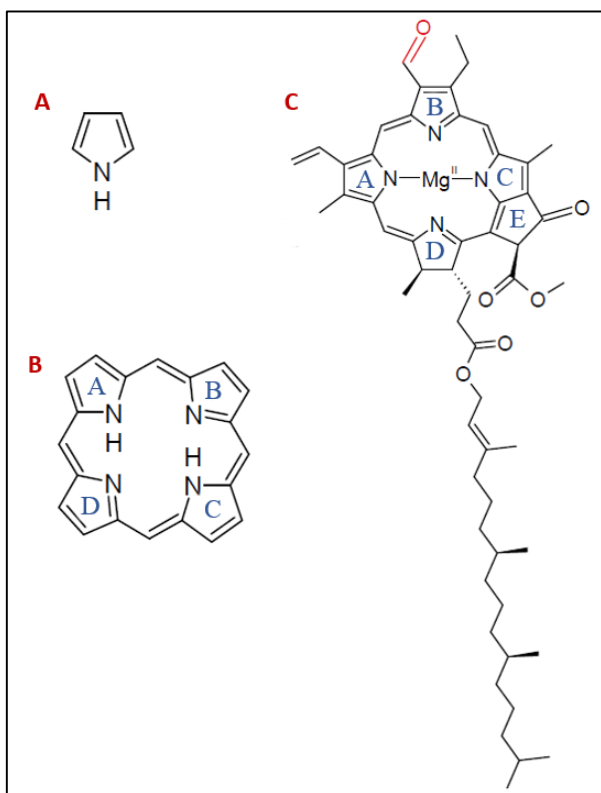


Figure 1.10: Derivation of a chlorophyll molecule A) pyrrol; B) porphyrin; C) chlorophyll a (black) and b (black with COH group in red). Structural formulae are constructed with ChemSketch.

Chlorophyll molecules have a dual nature. The weak hydrophilic part of the chlorophyll molecule originates from the porphyrin ring and the isocyclic structure (E) on the third ring (C). Hence, the strong lipophilic (hydrophobic) character is due to the long hydrocarbon chain – the phytol tail is bound to ring D. In order to that, chlorophyll is soluble in lipophilic organic solvents. Chlorophyll molecules are embedded into the photosystems with the phytol tail showing into the thylakoid membrane of the chloroplasts. Their main function is to absorb light in the light-harvesting complex and the transfer of energy to the reaction centres, those which consist of two embedded chlorophyll a molecules (RICHTER, 1996). For further information see *chapter 1.4.* as well the literature given above.

1.3.2. Carotenoids (*Carotene and Xanthophylls*)

Carotene and xanthophylls are red to yellow coloured pigments. In the chloroplasts of higher plants they are usually covered by green chlorophyll molecules (LÜTTGE et al., 2010).

The molecular structure is a hydrocarbon chain with conjugated double bonds, which is the chromophore. Due to this chromophoric chain the molecules are insoluble in water but soluble in liposoluble liquids (structurally comparable to chlorophyll molecules). The difference between the compounds is the varying number of conjugated double bonds (RICHTER, 1996).

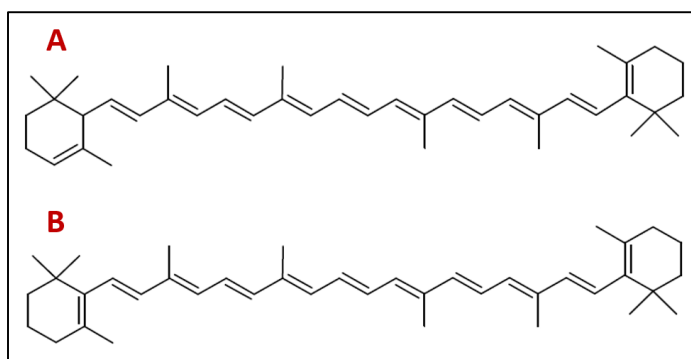


Figure 1.11: Two carotenes A) α -carotene B) β -carotene. Structural formulae are constructed with ChemSketch.

The xanthophylls (*Figure 1.12*) are oxygenated derivatives of carotenes (*Figure 1.11*) (RICHTER, 1996).

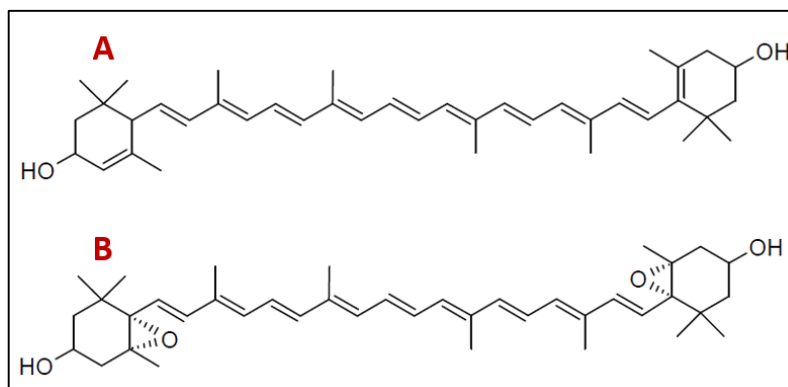


Figure 1.12: Two xanthophylls A) Lutein B) Violaxanthin. Structural formulae are constructed with ChemSketch.

Carotenoids have multifarious functions in plants. They are a part of the light-harvesting system (*chapter 1.4.*) and extend the absorption spectra (*Figure 1.15*). Their main functions are i) protection of the photosystems and especially the chlorophyll molecules from photooxidative damage (RICHTER, 1996). Further tasks are ii) capturing blue/green light and transportation of the energy to chlorophyll, which absorbs it as red light; iii) a special “dark stage” of the carotenoids – a hidden level which is not used for light absorption at all – acts as a mediator and helps to pass energy to chlorophyll pigments (OSTROUMOV et al., 2013); iv) heat transducer; v) colouring flowers for pollination vi) colouring ripened fruits for dispersal by animals; and vii) composition of vitamins and phytohormones (abscisic acid) (OSTROUMOV et al., 2013; RICHTER, 1996; SCHOPFER & BRENNICKE, 2010).

1.3.3. Flavonoids

At least 4000 flavonoids have been described (COOK & SAMMAN, 2008). Flavonoids are yellow coloured (lat. flavus = yellow), colourless or different coloured (e.g. orange, red, blue) phenols. The basic structure of a phenol is an aromatic ring with an OH group (*Figure 1.13*). All flavonoids are based on flavan ($C_6C_3C_6$ -structure). Flavonoids are divided into 14 classes, according to the oxidation level of the central ring C. Most common flavonoid classes are anthocyanins (described in the next chapter), flavones and flavonols. Since 1994, flavonoid biosynthesis is probably the best characterized pathway of secondary metabolites (DAVIES & SCHWINN, 2006).

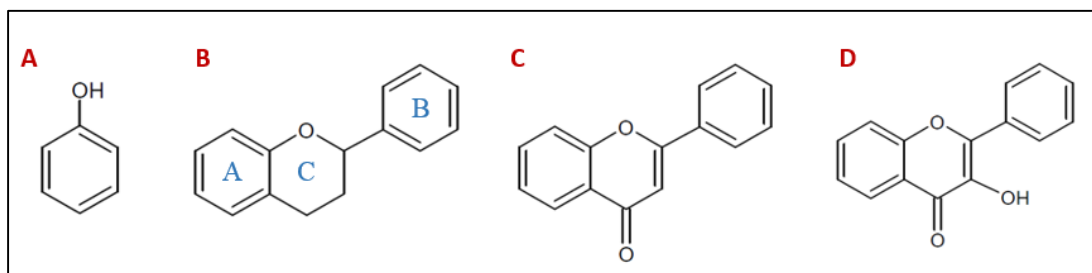


Figure 1.13: A) Phenol B) Flavan – ground structure C) Flavone D) Flavonol. Structural formulae are constructed with ChemSketch.

Most of the flavonoids are glycosides (bound to sugars) and stored in the vacuole. There are also some lipophilic flavonoids found in glandular cells and plant surfaces as root exudate (SEIGLER, 1998). One of the main functions of flavonoids is the protection against UV (ultra violet, 400 nm to 10 nm) radiation and is their antioxidant effect (binding of free radicals) (RICHTER, 1996). Furthermore, they are responsible for colouring flowers and fruits (HARBORNE, 1991).

Flavones and **flavonols** are attracting flower-visiting insects. They are able to stabilize the anthocyanidins and may act as protectors from being eaten by animals. They also contribute to the skill to have an antibacterial and antiviral effect. In the human medicine, flavonoids are maintained to have several positive effects on health (SEIGLER, 1998).

Flavonols are commonly glycosidically bound with rhamnose or glucose. To the group of flavonols belong e.g. kaempferol, quercetin, myricetin, pyranoflavonols and furano-flavonols. Glycosides of the flavanones are responsible for various tastes as acerbic, bitter, unflavoured and sweet, depending on their functional groups (ESAKI et al., 1983; RICHTER, 1996).

1.3.4. Anthocyan and Anthocyanidin

Another colouring component of plant tissue are anthocyan. Anthocyan constitute to one of the 14 classes of flavonoids (see *chapter 1.3.3.* above). Their typical colour is red, purple or blue. They are accumulating in the vacuole sap, where they exist as water soluble glycosides.

Colouring is only due to the sugar free compound – anthocyanidin (*Figure 1.14*), the aglycon part of the anthocyan. The anthocyan are based on flavonoids (RICHTER, 1996).

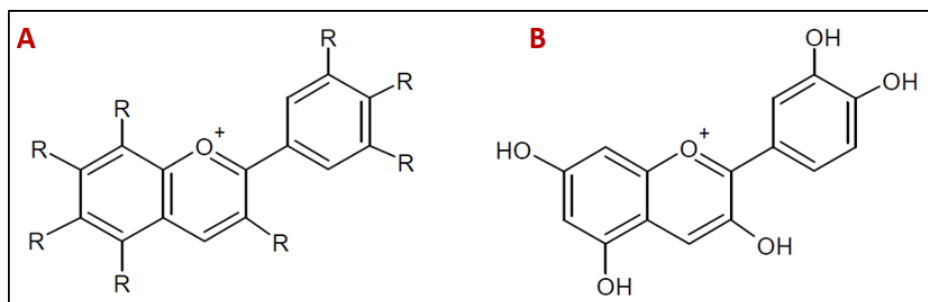


Figure 1.14: A) anthocyanidin, the basic structure of anthocyanins and B) cyanidin. Structural formulae are constructed with ChemSketch.

1.3.5. Protecting functions of phenolic substances

Especially tropical trees have a frequently brilliant colouration associated with the development of foliage (RICHARDS, 1952). Even temperate trees are showing some anthocyanins in young and old leaves (PRICE & STURGESS, 1938). Various hypotheses about the selective advantage of anthocyanic colouration in young leaves of tropical trees have been developed during history. First, SMITH (1909) detected a significant warmer temperature of young leaves tissue. He speculated that there is a rapid development of leaves when temperature is higher (Conflicting reports: NAGORNAYA & KOTSUR (1970) and McCLURE (1975)). Anthocyanin production in leaves is associated with several various physiological processes. LEVIN (1971) described that anthocyanins may be produced in response to various environmental stresses (nutrient deficiency, water stress, physical damage, fungal attack). In senescing autumn leaves of temperate plants, anthocyanins may be associated with the movement of sugars from leaves to other parts of the plant (LEE et al. 1987). The speculation of McCLURE (1975) was that anthocyanins may supporting the photosynthesis, what has not been postulated by good evidence. However, RAUF & SHRAMA (1980) measured increased Hill activity in developing anthocyanic rich leaves in mango. Another hypothesis is a protection against herbivory (many flavonoids are bitter or toxic). Though, anthocyanins are not toxic to higher animals (they are used as food colouring). They can be used to build complexes (where anthocyanins are integrated) and these complexes might be toxic (HARBORNE, 1979). Also the aposematically function of warning potential herbivores about the presence of toxic compounds was discussed by JANZEN (1979). The synthetization with response to intense radiation and the principal UV light could be another reason (LINDOO & CALDWELL, 1978;

YATSUHASHI et al., 1982) and might help to prevent UV-B (280 - 315nm) induced damage (CALDWELL, 1981). The group of LEE et al. (1987) observed the phenomenon of anthocyanins in cacao and mango leaves. They assumed, that the containing anthocyanins (not present in mature leaves) are available in a small proportion compared to the total phenolic concentration. In order to that and other reasons, they postulated that anthocyanins do not seem to be important in the developing leaves as: i) a protection screen against UV radiation; ii) a mechanism for elevating leaf temperature; iii) a prevention against herbivory; and iv) a part of any postulated physiological mechanism, as photosynthesis. They concluded that anthocyanic colouration might be a by-product of the metabolism of other flavonoid compounds in these rapidly growing organs.

However, in 2001 BIEZA & LOIS performed further experiments with *Arabidopsis* mutants, which were more sensitive against UV-B light than the wild type. The protective effect of colourless, yellowish or reddish flavonoids and other UV absorbing phenolic substances as a filter against short wavelength irradiation have been shown. The sensitive mesophyll cells are protected against UV and light stress through the phenolic substances.

1.4. Light absorption

Photosynthesis is initiated by light absorption. One of the central molecules that absorbs sunlight is chlorophyll a (GOVINDJEE, 2004).

1.4.1. Absorption spectra

In the thylakoid membranes of chloroplasts, several pigments as chlorophyll a, chlorophyll b and carotenoids are located. An extinction spectra of these molecules describes the dependence of absorbed light quanta from the spectral range. The absorption spectra of different chlorophyll-protein complexes with another ratio of chlorophyll a and b molecules can differ (SCHOPFER & BRENNICKE, 2010).

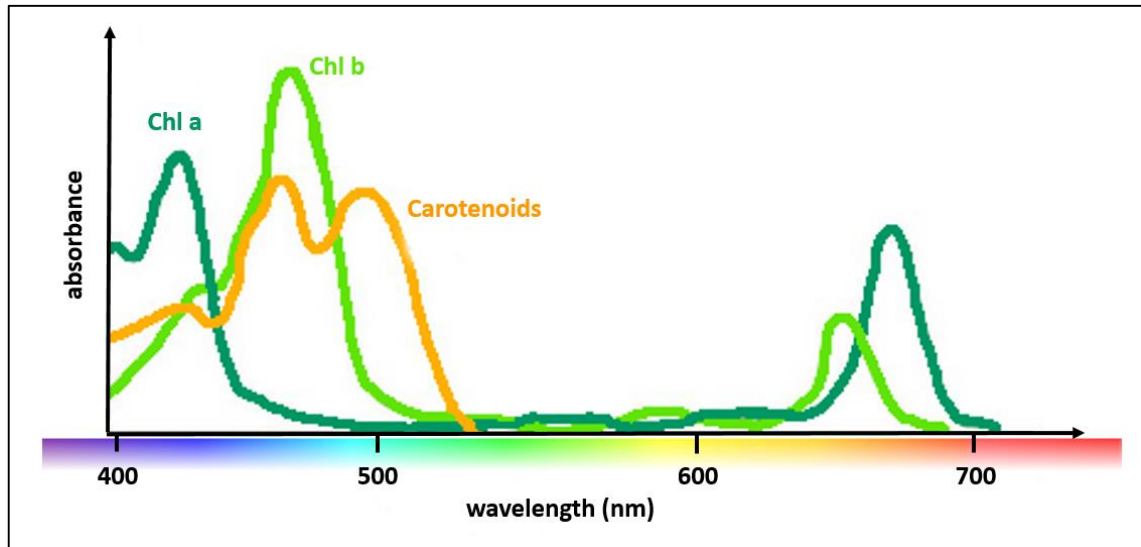


Figure 1.15: Absorption spectra of chlorophyll a, b and carotenoids. The maximal absorbances are typically in the region of blue and red. Around green light, there is less absorbance (green-gap). (Based on CAMPBELL et al. 2009)

The efficiency of the single pigments for the photosynthetic energy transformation can be demonstrated by action spectra (e.g. the photosynthetic intensity is measured through O_2 production and CO_2 uptake at a quantum flow [$mol\ m^{-2}\ s^{-1}$]) (SCHOPFER & BRENNICKE, 2010). The percentage of the absorbance (Figure 1.15) of blue or red light by plant leaves is up to 90 % and that one of green light is about 70 – 80 % (green gap) (TERASHIMA et al., 2009). The green gap is reduced by carotenoids and xanthophylls, which are absorbing about 30 % of the light quanta (SCHOPFER & BRENNICKE, 2010; LÜTTGE et al., 2010).

1.4.2. Chlorophyll fluorescence, Perrin and Jablonski scheme

Luminescence (= generic word for all types of light emission) was first observed by N. Monardes, within the clearest discovery of the phenomena of fluorescence by Sir J. Herschel in a solution of quinine sulphate. The name fluorescence was given by Sir G.G. Stokes, which is well known for the Stokes shift which is named after him. Emission bands are shifted to longer wavelengths than the absorption bands (GOVINDJEE, 1995).

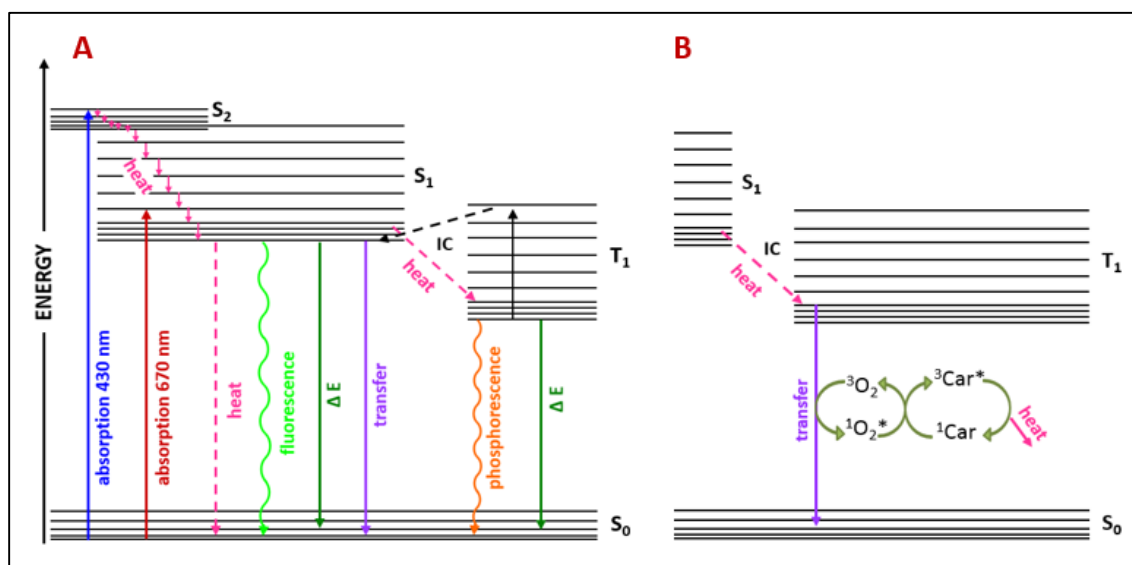


Figure 1.16: A) Perrin and Jablonski scheme: Different possibilities for an excited Chl *a* molecule (Chl *a**) to return to the electronic ground state S_0 . B) During deactivation of triplet chlorophyll molecules, excited singlet oxygen ($^1O_2^*$) is formed. It is transformed to original stage (3O_2) with usage of singlet carotene (1Car), which is then transformed to triplet carotene ($^3Car^*$). The triplet carotene is formed to singlet carotene by the release of thermal energy. (Based on HÄDER & TEVINI, 1987 and SCHOPFER & BRENNICKE, 2010)

The chlorophyll *a* molecules, which are situated in the chl-protein complexes of photosystem (PS) II, reach their excited singlet state (Chl *a**) during the absorption of light. They can decay to the ground state by several pathways (GOVINDJEE, 2004). The pathways from the excited singlet state to the ground state were described from Perrin and Jablonski (VALEUR & BERBERAN-SANTOS, 2012). At Figure 1.16 (A) there is the simplified term scheme of chlorophyll *a*. When a **blue quant** is hitting chlorophyll *a* molecules, the electron is coming up to the S_2 singlet state. This state is very unstable (half-life $\tau_{1/2} \approx 10^{-12}$ s) and no chemical work is possible. Hence there is an overlap of S_2 and S_1 it is possible that there is a fall back through rotation and vibration to state S_1 – radiationless – only with emission of thermal energy (internal conversion). At state S_1 also the absorption of the **red light quants** is taking place (in order to this, there is no difference between the stimulation of chlorophyll molecules with blue or red light). At the state S_1 the electrons are more stable (half-life $\tau_{1/2} \approx 10^{-9}$ s) and the transition from S_1 to S_0 is possible within different energy conversions. A possibility is the transformation of rotational and vibrational energy into **thermal energy**. Another return to lower energy level is possible through emission of a light quant (= **fluorescence**). Considering the Stokes shift, the

fluorescence light possesses at a longer wavelength. By the emission of a high-energy electron to primary acceptors and accordingly processing it through the electron transport chain, **photochemical work** (ΔE) is done. Another option is a radiationless **energy transfer** to a nearby chlorophyll molecule, which is then excited (exciton transfer) on the return to the S_0 state.

The **intersystem crossing (IC)** from S_1 to T_1 (overlap) combines both radiation of thermal energy and a transition to an excited triplet state, including a spin reversal. This state has a quite long half-life time ($T_1 \rightarrow S_0$: $\tau_{1/2} \approx 10^{-2}$ s). According to that, there is a long duration of light emission (= **phosphorescence**, $\lambda_{\max} \approx 750$ nm). Another way back from T_1 to S_1 (means $S_1 \rightarrow T_1 \rightarrow S_1$) is feasible because of the overlap from T_1 and S_1 . Consequently, a **delayed fluorescence** may occur. At high light conditions there is more light energy absorbed from the photosynthetic apparatus than can be used for the biochemical dark reaction. This tailback results from the transfer of energy to the acceptors. One of these acceptors is the plentiful O_2 . At the triplet state, the deactivation of the triplet chlorophyll molecule is done by forming **excited singlet oxygen** ($^3O_2 \xrightarrow{Chl^* \rightarrow Chl} ^1O_2$).

This oxygen radical formation possesses a huge damage potential at the pigment-protein-complex at the thylakoid membrane. To transfer the excited oxygen back to normal configuration, carotenoids are involved. This transfer process emits thermal energy (*Figure 1.16 B*) and finally no damage of the chloroplasts occurs (SCHWEDT, 1996; LÜTTGE et al., 2010; SCHOPFER & BRENNIKE, 2010).

1.4.3. *Light harvesting antenna system and electron transport chain*

The functional, clustered arrangement of light absorbing pigments and their electron carriers in the thylakoid membranes is called photosystem (PS). The PS II is quite well analysed and it is described below (the evolutionary older PS I reaction centres are quite similar to PS II).

At the three dimensional light harvesting antenna the pigments absorb photons and pass them to their neighbour pigment molecules and finally transfer them to the reaction centres (*Figure 1.17*). To achieve a short transfer to the reaction centres, the exciting energy of neighbouring molecules towards the centre is less. As a consequence, chlorophyll b molecules which need

higher energy to be excited by red light than chlorophyll a molecules (see Figure 1.15), are located at the outer edge of the antenna.

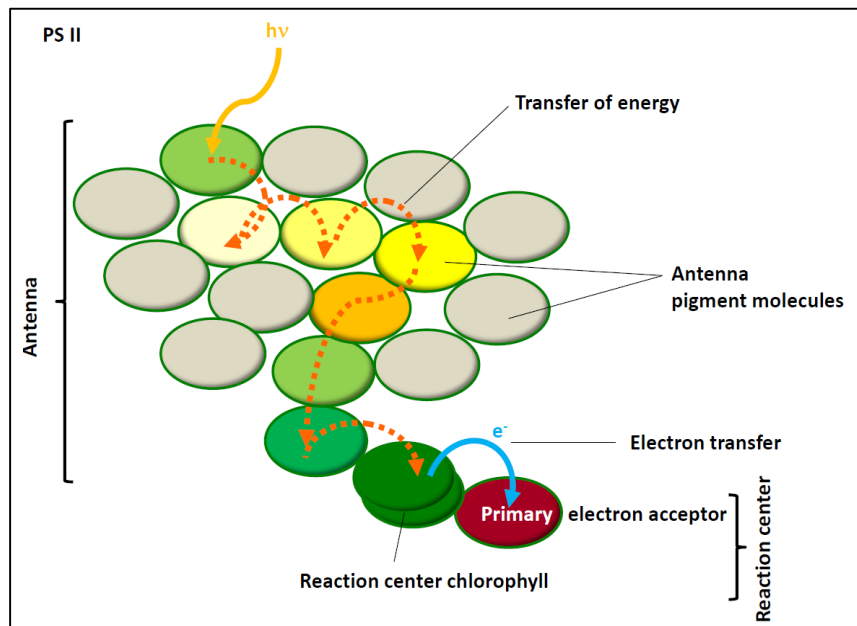


Figure 1.17: Energy transfer from the antenna to the reaction centre (© Engelmeier, unpublished).

In total at a ratio of 1:300 there are two different functional pigment collectives:

- Photochemical active chlorophyll a molecules from the reaction centres
- Photochemical inactive chlorophyll a and b molecules, antenna pigments

Two photochemical active chlorophyll a molecules at the reaction centres a pair is formed which is connected by proteins. The transfer of the exciting energy from the antenna pigments to the reaction centres is quite fast (10^{-12} s). A reason for the fast dispatch is the dense arrangement of the pigment molecules at the thylakoid membranes. Therefore this system is faster than fluorescence and in order to that hardly energy is lost.

In the reaction centre, which is located at the inner antenna (core-area), an electron acceptor gets the electron from the pigment molecule and leads it to the electron transport chain. The electron acceptor is reduced by the electron release and an electron donator is needed. During the reaction centre is working it is closed and no energy could be taken up anymore. With increasing quant flow the probability that a reaction centre is not available becomes higher. By

filling quant flow the reaction centres are permanent closed the system is saturated (SCHOPFER & BRENNICKE, 2010; NULTSCH, 2000; LÜTTGE et al., 2010).

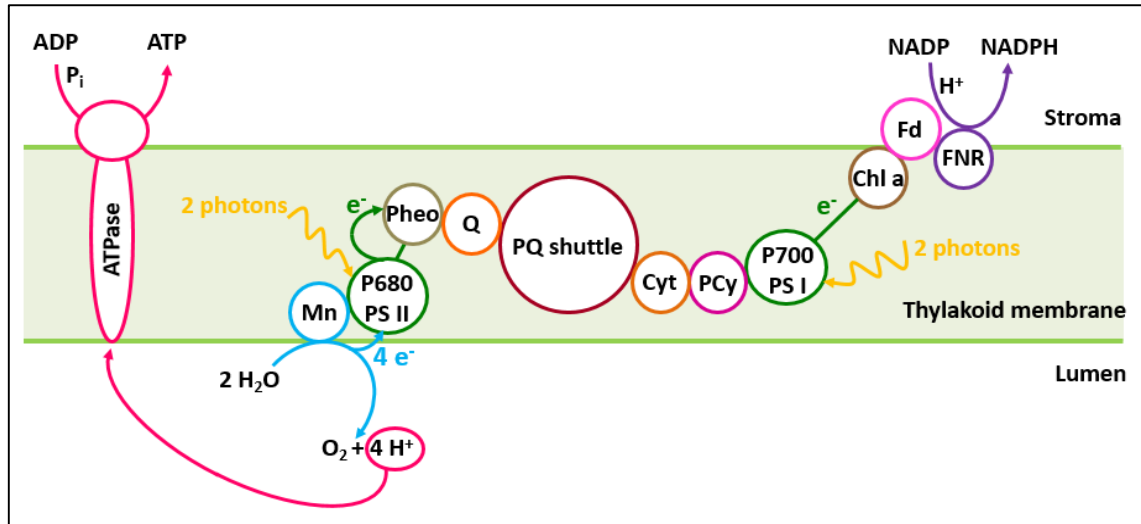
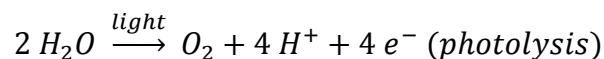


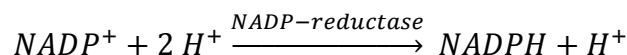
Figure 1.18: Not cyclic electron chain. Mn for manganese cluster; P680 for a pair of chlorophyll a at the reaction centre; Pheo for pheophytin for primary electron acceptor of PS II; Q for plastocinone electron acceptor of PS II; PQ for plastocinone pool; Cyt for cytochrome; Pcy for plastocyanin; P700 for a pair of Chl a; Chl a for primary electron acceptor of PS I – monomer; Fd for ferredoxin; FNR for ferredoxin - NADP reductase. (Adapted from Engelmeier, unpublished)

Simple description of not cyclic electron chain:

With the antenna systems electrons are absorbed from the pigment molecule Chl a P680 which is then excited (P680*) in the photosystem II (Figure 1.18). The P680* is donating the molecules to different acceptors (quinon –proteins). According to this there is a gap of electrons and the electrons for the pigment P680 are originating from photolysis. In photolysis, water is dissociated under release of molecular oxygen:



Electron pairs are moving ‘downhill’ in the electron transport chain to the Photosystem I via different proteins (quinons, cytochromes). The photosystem I has its own antenna. The pigment molecule Chl a P700 from PSI is excited to P700*. The NADP⁺ (nicotinamide-adenine-dinucleotid-phosphate) is rebuilt through NADP-reductase to NADPH.



Through the ATPase



a phosphate molecule is suspended, so that a high-energy ATP (adenosine-tri-phosphate) is built up. The ATPase works, because the electron transport chain pumps protons from the luma into the stroma, creating a pH-gradient (RAVEN et al., 2006).

1.5. Aim of the thesis

The aim of this thesis is to give an overview of physiological, morphological and molecular differences during leaf development in *Theobroma cacao*. A focus of the work is whether the photosynthetic performance correlates with stomata growth, photoactive pigments (as chlorophyll a and b, carotenoids) and in the flavonoid class on anthocyanidins. Deviations or stability levels of inorganic-, organic ions and metabolites during life span should be shown and described. The physiological fluorescence measurements were performed by two methods: Imaging Pulse Amplitude Measurements (PAM) and Plant Efficiency Analyser (PEA). The detection of the content of chlorophyll molecules as well as carotenoids and anthocyanidins was done by photometric analysis. Metabolites (metabolomics) were detected by Liquid Chromatography coupled with Mass Spectrometry (LC-MS/MS) and High Performance Liquid Chromatography (HPLC) coupled with UV/VIS detection. The intention of applying voltammetry measurements was to get insights into the molecular redox potentials. Via Anion & Cation Chromatography (ionomics) the different distribution of ions should be gauged. Anatomical cuttings, especially stomata prints, were performed. An overview of the working steps is given in *Figure 1.19*.

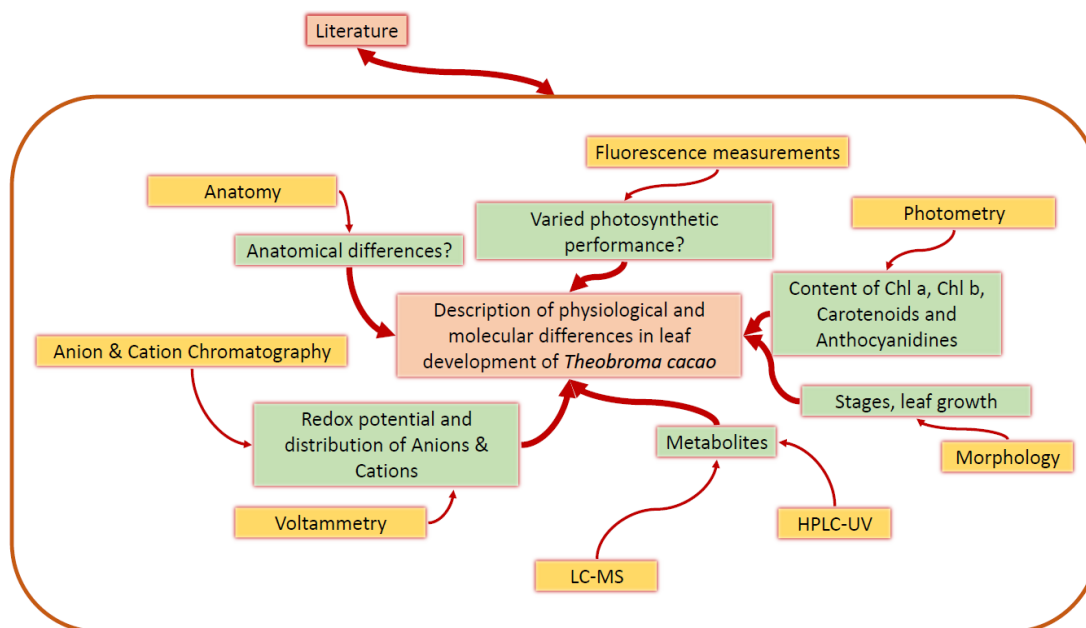


Figure 1.19: Overview of the working steps.

For a better understanding of the mechanisms and important facts of different measuring methods, the next few chapters will give a short explanation.

1.6. Fluorescence measurements

Considering the competition of photochemical energy conversion (see *chapter 1.4.2.*) with fluorescence, two extreme situations are possible (assuming the yield of heat degradation). At a normal dark-adapted state all reaction centres supposed to be open. The other possibility is that all reaction centres are closed (e.g. in saturating light). According to that, the fluorescence yield is between the minimum (F_0) or the maximum (F_m) (*Figure 1.20*) (SCHREIBER, 2004).

Abbreviations which are used in the context of fluorescence measurements are shortly explained in *Table 1.1*.

F_0	Initial fluorescence, minimal fluorescence yield of a dark adapted state	
$F_{0'}$	Minimal fluorescence yield of a light-adapted state	
F_t	Current fluorescence yield	
F_m	Maximum fluorescence yield of a dark adapted state	
$F_{m'}$	Maximum fluorescence yield of light-adapted state	
F_v	Variable fluorescence of a dark adapted state	$F_v = F_m - F_0$
F_v/F_m	Maximal PS II quantum yield (photochemical efficiency) of a dark adapted state	$\frac{F_v}{F_m} = \frac{(F_m - F_0)}{F_m}$
ΔF	Variable fluorescence of a light adapted state	$\Delta F = F_{m'} - F_t$
Φ_{PSII}	Effective quantum yield from PS II of a light adapted state	$\Phi_{PSII} = \frac{\Delta F}{F_{m'}}$ $= \frac{F_{m'} - F_0}{F_{m'}}$

Table 1.1: Overview and definition of fluorescence concerning abbreviations (GENTY et al., 1989; SCHREIBER et al., 1994)

The most used term is the F_v/F_m value. The kinetics of the fluorescence rise provides information on various steps of photosynthetic electron transport (STRASSER, 2004).

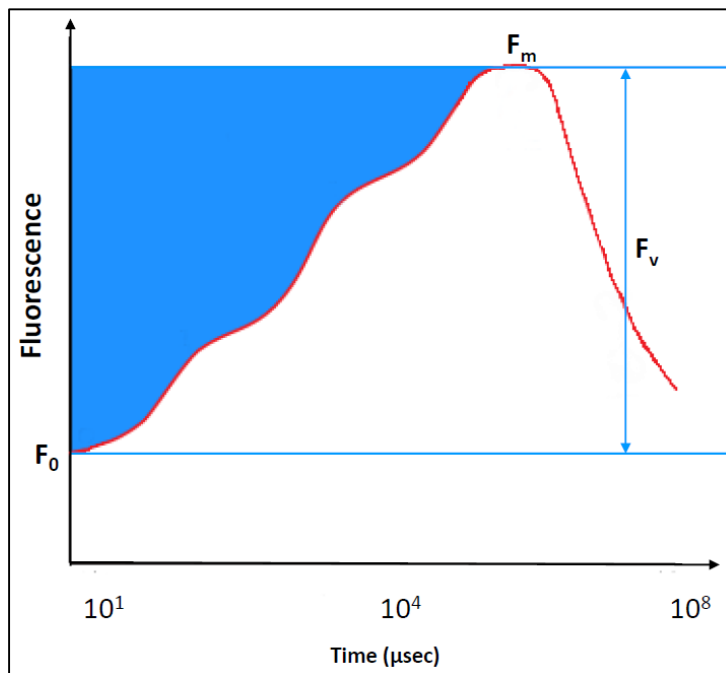


Figure 1.20: At the F_0 state, reaction centres are opened, the leaf is illuminated with saturating light till all reaction centres are closed (F_m). (Adapted from: HANSATECH INSTRUMENTS Ltd, 2014)

1.7. Photometric measurements

A photometric analyser detects the attenuation of a ray of monochromatic light through an absorbing liquid. The set-up of a photometric analyser is shown in *Figure 1.21*. The optical part contains a light source, a monochromatic illuminator and a light detector combined with a signal amplifier (SCHOPFER, 1986).

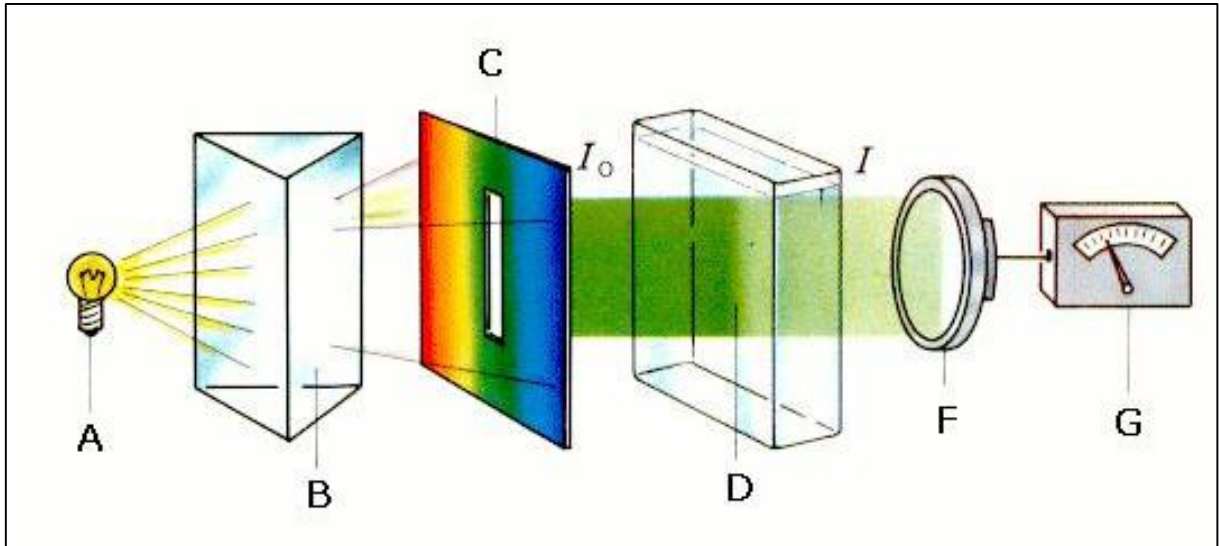


Figure 1.21: Set-up of a photometric analyser. A) Light source; B) Monochromatic illuminator (prism or grating); C) Aperture; D) Cuvette with the liquid sample; F) Light detector; G) Measuring amplifier with the extinction outcome E_λ ; I_0) Intensity of the irradiating light; I) Intensity of the transmitted light.

© SEESING & TAUSCH (2004)

The background of the photometric measurements is the Lambert-Beer law. The law based on Bouguer (1728), Lambert (1760) and Beer (1852) describes the decrease of the intensity of monochromatic light radiation during passing through an absorbing media and the dependence on the concentration ($c \leq 10^{-2}$ mol/l) of the absorbing substances and the thickness of the layer (HESSE et al., 1995; SCHOPFER, 1986):

$$E_\lambda = \log \frac{I_0}{I} = \varepsilon_\lambda * c * d$$

E_λ is the extinction (absorbance of the material for light at the wavelength λ)

I_0 is the intensity of the irradiating light [W/m^2]

I_1 is the intensity of the transmitted light [W/m^2]

c is the concentration of the amount of the absorbing substance in the liquid [mol/m^3]

ϵ_λ is the decade extinction coefficient (specific absorbance coefficient) at the wavelength λ (depending on pH and solvent)

d is the distance the light travels through material [m]

By irradiating a molecule at a basic state (ψ_0) at a specific frequency ν (e.g. VIS (visible) light 400-750 nm) it is able to absorb light. With this absorbance the molecule is at an electric stimulated state (ψ_1), because the valence electrons are excited and according to that raised to a higher energy level. The energy of the absorbed photon ($h\nu$) has to be the same as the energy difference of the two states ψ_0 and ψ_1 :

$$\Delta E = E(\psi_1) - E(\psi_0) = h * \nu$$

This resonance condition is the base of every spectrometric method. For the absorbance also the angular momentum has to stay constant (HESSE et al., 1995).

1.8. HPLC-UV/VIS

The name HPLC is an abbreviation for High Performance Liquid Chromatography and former called High Pressure Liquid Chromatography. The mobile phase of the column transports sample substances from one end of the column to the other one where they are detected in dependence on their migration time. The different components of the samples have different migration times, because of physical interactions with the column stationary phase. Briefly the setting of a HPLC system is shown in *Figure 1.22*.

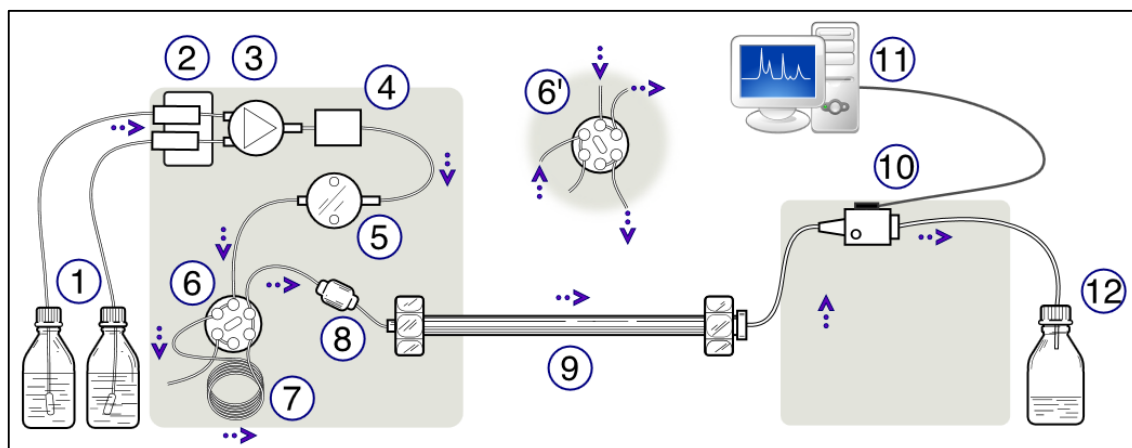


Figure 1.22: Schematic Diagram of a High Performance Liquid Chromatograph.

1) Solvent reservoirs (solvent A and solvent B); 2) Solvent degasser; 3) Gradient valve; 4) Mixing vessel for delivery of the mobile phase; 5) High-pressure pump; 6) Switching valve in 'inject position'; 6') Switching valve in 'load position'; 7) Sample injection loop; 8) Pre-column or guard column; 9) Analytical column; 10) Detector (i.e. UV-VIS); 11) Data acquisition; 12) Waste collector. (Adapted from MRABET, 2009)

In this study an UV/VIS photodiode array detector was used. A photodiode array detector allows simultaneous monitoring of a range of wavelengths (here: $\lambda = 220 \text{ nm}$ to 590 nm). The schematic function is illustrated in Figure 1.23.

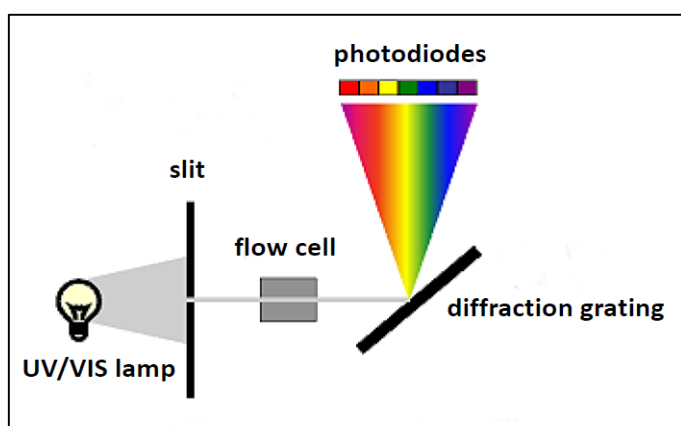


Figure 1.23: Simple illustration of a photodiode array detector (PDA), which is linked to the HPLC system and detected with a photodiode (light sensor). (Adapted from: LC RESOURCES, 2005)

Accordingly to the explanation of photometric measurements in *chapter 1.7*. (HESSE et al., 1995), also the UV/VIS measurements are based on the same physical effects.

1.9. Ionomics & voltammetric measurements

The ionome is defined as the mineral nutrient and trace element composition of an organism. It is representing the inorganic component of cellular and organismal systems. Ionomics, the studies of the ionome, have a high throughput and a low cost in analysis. The plant tissue is not homogenous in ionomics. Leaves, which are just a week apart in age can show significant differences. The elemental composition of living organisms, their changes in this composition in response to physiological stimuli, developmental state and genetic modifications is the point of interest (SALT et al., 2008). The detection of the content of dissolved anions and cations was done by chromatography.

Voltammetric measurements are based on the application of voltage steps on a redox-active system and the detection of the occurring electrical current flow. The electrochemical process is related to a redox reaction. The oxidation takes place at the anode and the reduction at the cathode. At the anode side either positive or negative charge carriers could pass the phase boundary between the metal and the solution (OTTO, 2000).

1.10. Metabolomics

Plants possess a large plurality of chemical compounds and use them for primary and secondary metabolism for their purposes. The corresponding research field is named metabolomics after the metabolome, as it is proteomics for research of proteins. The sum of all chemical compounds of a plant is called metabolome and describes the enormous variety of organic substances that are elaborated and accumulated by plants. The metabolome deals with the chemical structure, their biosynthesis, turnover and metabolism, natural distribution and their biological function. This various functions are for example interaction with enzymes, catalytic activity, or defence and interaction with the environment (HARBORNE, 1973).

For metabolomics, the analysis of the chemical processes involving metabolites (compare proteomics, genomics), several methods are established. To study the metabolome there is a need for a method efficient identification of explorative plant metabolites with limited material.

Chromatographic methods are a common choice for such analysis: i) GC/MS – gas chromatography coupled with mass spectroscopy for analysing volatile compounds, sugars, amino-, fatty- and organic acids, hydrocarbons and further other small molecules; ii) LC coupled with UV/VIS detectors (HPLC-UV/VIS) for detecting chromophoric substances or coupled with a mass spectroscopy (LC/MS) to distinguish all metabolites (untargeted examination) or monitor a selected set of metabolites (targeted examination). For structure evaluation and identification iii) NMR (nuclear magnetic resonance) spectroscopy and iv) IR (infrared spectrophotometry) are used (WECKWERTH, 2003).

2. MATERIAL AND METHODS

Leaf samples of two *Theobroma cacao* Criollo hybrid trees were taken. In total more than 60 leaves were harvested. It was the intention to apply as many methods as possible for all single samples, but in the manner of less plant material, some methods couldn't be applied consequently. Subsequently, the two trees were called Criollo 1 (C1) and Criollo 2 (C2). Some of the measurements were done with healthy, intact leaves as well with frozen plant material.

2.1. *Plants and their conditions*

2.1.1. *Facility greenhouse*

In the Fervidarium greenhouse of the Department of Molecular Systems Biology, University of Vienna, several *T. cacao* species, besides many other plants, grow. A team of gardeners take care of all plants there. In the greenhouse there has to be maintained a continuous cycle of temperature and humidity, what is monitored with several analysers (see *chapter 2.2.*).

2.1.2. *Criollo hybrids C1 and C2*

It is not exactly known where the two *T. cacao* Criollo hybrids in the greenhouse were actually coming from. It is estimated that they might originate from South America and that both are about 20 years old. Although the two trees are the same species, the colour of the young, developing leaves is different (C1 young stages are looking in colour bright red, the leaves of C2 are more orange – see *Figure 2.1*).

2.2. *Climate data*

The climate data before and after the harvesting days were taken continuously from three different placed analysers. Two of the analysers were USB-loggers (EL-USB-2 RH/ TEMP DATA LOGGER, Lascar, U.K.) which were located at different branches on the cacao trees. The third analyser was located near the plant pots (DELTA LOGGER, Δ-T Devices, Burwell-Cambridge-U.K.). Consequently, temperature and humidity data were measured and recorded all 5 minutes.

2.3. *Leaf growth and classification*

During some periods the growth of single leaves was continuously measured with a common tape measure. The length along the midrib and the width of the widest position of the leaf blade were measured.

Additionally a short time lapse movie was made. For this time lapse movie a camera (Canon, EOS 40D) with an automatic releaser was installed. Every hour five pictures were taken. Following programs were used to create the movie from single pictures: Adobe Bridge, Adobe Camera RAW, Adobe Premiere Pro and Adobe Media Encoder. The movie will be available online soon at <http://www.univie.ac.at/mosys/>.

The classification of the different leaf stages is adjusted from ORCHARD et al. (1980), GREATHOUSE et al. (1971) and ABO-HAMED et al. (1983). The classification is described below, symbol pictures can be seen in *Figure 2.1*.

Flushing period 1 (F-1): Stipules surrounding terminal bud, leaf initiation and unfolding, leaf colour may be lightly green

Flushing period 2 (F-2): Leaves expand with anthocyanin, mid rip is green, leaves are thin and supple. This section is divided into two substages:

F-2-a (red < 10): Leaves are red, mid rip is green, length is smaller than 10 cm

F-2-b (red > 10): Leaves are red, mid rip is green, length is taller than 10 cm

Interflush period 1 (I-1): Leaf expansion is going to be completed, lamina is going to be green. Further, this section is divided into two substages:

I-1-a (green-red): Leaves are turning from red to pale green

I-1-b (pale-green): Leaves are pale green

Interflush period 2 (I-2): Leaf expansion completed (adult leaves) and they are fully stiff. Further, this section is divided into two substages:

I-2-a (green): No leaf expansion, leaves are dark green ('fully green')

I-2-b (aging): Leaf senescence is visible by yellow and brown fields

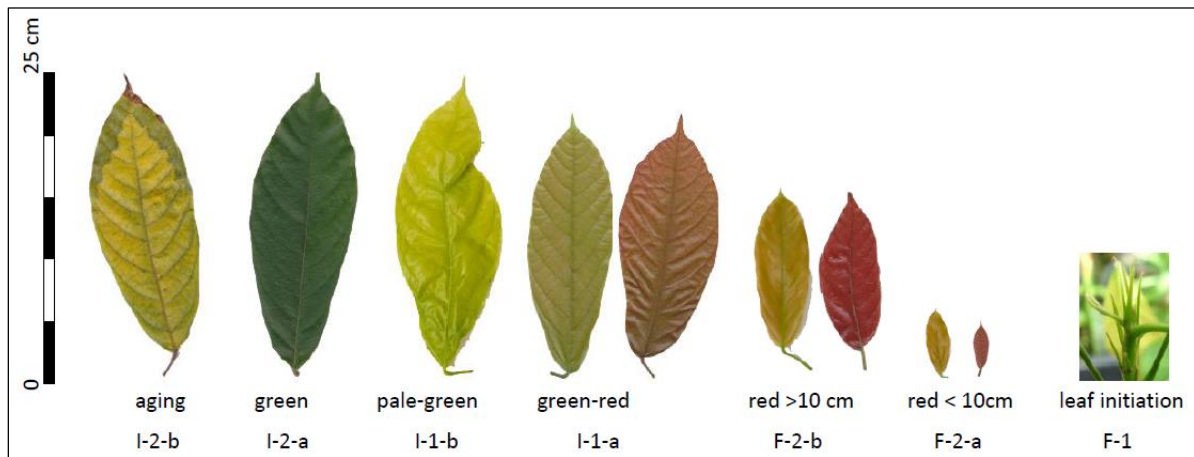


Figure 2.1: The classification of the different leaf stages. At the stages F-2 to I-1-a differences between the two trees can be determined (right: C1 and left: C2). The picture of the leaf initiation (F-1) is enhanced.

2.4. Fluorescence measurements

Measurements of chlorophyll a fluorescence are widely used as a non-invasive and rapid technique for estimating photosynthetic performances in plants (GOVINDJEE, 1995; OXBOROUGH & BAKER, 1997). Two different analysers were used to get an idea of the efficiency of the photosynthetic apparatus. There is a general agreement that at room

temperature, chlorophyll a fluorescence of plants in the spectral range of 680 to 740 nm, is emitted mainly by PS II (STRASSER, 2004).

2.4.1. Plant efficiency analyser PEA – workflow

The plant efficiency analyser (PEA, Hansatech Instruments, Kings Lynn, U.K.) consists of three parts: a leafclip, a sensor unit and a control box. To obtain indications about the F_v/F_m of the single intact leaves at the harvesting day, the up- and bottom side of the leaves were measured. According to preliminary experiments, the measurements were taken with 80 % light intensity, then the leaves were shaded with the shutter of the leafclips for 30 minutes. Red light ($1200 \mu\text{mol}/\text{m}^2\text{s}$) was used for excitation. The measurements were taken for 3 seconds from the dark adapted leaves. The measuring point of time was chosen to be about noon and was measured for all samples in between one hour. The data evaluation was done with Microsoft Excel.

Healthy, fully green plant leaves typically show a F_v/F_m ratio of 0.8, which varies depending on the particular plant and physiological conditions (SCHREIBER, 2004). From shadow leaves as *T. cacao* lower values were observed (LOVELOCK et al., 1998).

2.4.2. Imaging Pam

The Imaging PAM (pulse amplitude modulated) analyser is a chlorophyll fluorometer, which is specialised in the two-dimensional study of photosynthetic activity. For this work an Imaging PAM Mini (Walz GmbH, Effeltrich, Germany) was used. It applies pulse-amplitude-modulated measuring light (for assessment of chlorophyll fluorescence yield) as well as actinic illumination (driving photosynthesis) and saturation pulses. It provides a non-destructive analysing of the photosynthetic performance of plants through energy conversion at PS II reaction centres. The Imaging PAM Mini is able to assess the characteristic fluorescence levels F_o , F_m and F_m' . In order to that, the PS II quantum yield F_v/F_m ($\Delta F/F_m'$), induction curves as well as light saturation curves with quenching analysis can be determined. The detection head is equipped with an extremely powerful ring array of LEDs (light emitting diode), which are illuminating an area from 24 mm x 32 mm. At the measuring head there is a CCD (charge-coupled-device) camera employed, which shows via the software 'Imaging Win' (Walz GmbH,

Effeltrich, Germany) the measurement curves and fluorescence pictures of the sample at a glance. To start the measurements the system was calibrated to the standard loadings. The measurements themselves were taken at the upside of the intact leaves and direct measuring at the main rip was avoided to make them comparable. Of special interest were the ETR (electron transport rate) parameters. The advantage of the ETR measurements is the possibility of measuring a plant in situ under natural light conditions (SCHREIBER, 2004). The photosynthetic electron transport rate is calculated from different fluorescence parameters as follows:

$$ETR = Yield \times PAR \times 0.5 \times Absorptivity [\mu mol \text{ of electrons } m^{-2} s^{-1}]$$

The absorptivity parameter describes the fraction of incident light which is absorbed. In most studies the determination was carried out with standard PAM fluorometers. It has been assumed that the absorptivity is around 0.84, which is determined by the mean value for a large number of normal, healthy green leaves. With increasing chlorophyll content the red signal decreases, while the near-infrared signal remains constant. The term PAR means the photosynthetically active radiation. The PAR-absorption can be expressed as a , which is calculated pixel by pixel according to the equation

$$a = 1 - \frac{\text{red signal}}{\text{near infrared signal}}.$$

For example, if the near-infrared signal is 5 times more intense than the red signal, then $a = 0.8$, which means that 80 % of the incident red light is absorbed. The actual photosynthetic activity depends on chlorophyll content and the absorbed PAR (SCHREIBER, 2004). Usually it can be assumed that 84 % of the incident photons are absorbed (BJÖRKMAN & DEMMIG, 1987). According to this, the Imaging PAM system is automatically calculating with this value. The factor 0.5 takes into account that only half of the absorbed quanta are distributed to PS II, because the transport of one electron requires absorption of two quanta (MEYER et al., 1997). The ETR was measured at different PAR-values in a different area due to the leaf-size (PAR values from 0 to 784 $\mu mol \text{ quanta } m^{-2} s^{-1}$). It has to be considered, if the turnover rates of PS I and PS II are equal, that there is no negative influence for the calculation. Nevertheless, the cyclic electron transport around PS I and PS II causes some deviations. Despite the absolute values of PS II absorbance and PS II quantum yield are almost uncertain, the relative changes

of ETR with environmental parameters may be very informative (SCHREIBER, 2004). The evaluation was done with the software Imaging Win and Microsoft Excel.

2.5. *Harvesting*

2.5.1. *Workflow*

The leaves were cut at the end of the petiole with a steel scissor, afterwards the fresh weight of the samples was determined. Further, leaves were scanned to determine the area (cm²) and pictured for documentation. Accordingly, circles (d = 0,5 cm) were punched with a cork drill for analysis of the content of chlorophyll and carotenoids. A small part (< 1 cm) from the end of the bigger leaves was cut off with a ceramic knife for anatomical studies. Previous methods were accomplished quite fast, because samples had to be ground as soon as possible with a ceramic mortar and pistil in liquid nitrogen until there was a fine powder to prohibit further metabolism. The powdered plant material was frozen at – 80 °C for the use for further treatments.

2.6. *Hot-water-extract and acid-hot-water-extract*

The hot-water-extract (HE) and acid-hot-water-extract (AE) at different extracting levels were used for various measurements (e.g. HPLC-UV/VIS, Photometry). In case of it was necessary to follow a step by step schedule.

2.6.1. *Workflow for hot-water-extract (HE)*

HE-1 (hot-water-extract 1)

For extract preparation about 150 mg of the at –80 °C frozen and ground plant material were taken into cooled safe lock Eppendorfer (Epi) tubes (2.0 ml), diluted in 1.5 ml MilliQ-water

(ultrapure) vortexed afterwards. Then all samples were extracted for 30 minutes in a water bath at + 80 °C. Following, the samples were cooled and centrifuged.

HE-2 (hot-water-extract 2)

From the HE-1 500 µl were transferred into a 10 ml Falcon tube and diluted with 10 ml MilliQ-water. Afterwards the samples were acidified with 100 µl 0.2 N HNO₃ to avoid microorganism growth.

Until further use the extracts were stored in the fridge at + 4 °C.

2.6.2. Workflow for the acid-hot-water-extract (AE)

AE 1 (acid-hot-water-extract 1)

For the acidic extracts approximately 80 mg of frozen and ground plant material were taken into a cooled down safe-lock Epi tube, diluted with 1.5 ml 1 N HCl and vortexed afterwards. As for the HE-1, the acidic extracts were stored in a water bath for 30 minutes at + 80 °C and then cooled and centrifuged.

AE 2 (acid-hot-water-extract 2)

From the AE-1 250 µl were transferred into a 10 ml Falcon tube and diluted with 10 ml MilliQ-water. To make sure that the dilution is not too less acidified, there were again 100 µl 0.2 N HNO₃ added to the samples. The extracts were stored in the fridge at + 4 °C until further use.

2.7. pH measurements

2.7.1. Measurement and sample preparation

From the undiluted and not acidic HE-1 100 µl were pipetted onto the membrane of the measurement electrode, which has previously been calibrated (Sentron SI Series pH-Meter SI

400 7400-010 s/n 20207, Netherlands). From the measured pH-values the μval concentration was calculated with Microsoft Excel.

2.8. Photometry

The detection of chlorophyll, carotenoids and anthocyanidins content was done with a photometer (Tecan, infinite M200, Switzerland). This instrument allows to measure samples either with a cuvette or microtitre plate.

2.8.1. Extraction with DMF (chlorophyll, carotenoids)

Considering the paper of MORAN & PORATH (1980), the advantage of the use of Dimethylformamide (DMF) instead of acetone is that plant material has not to be ground and therefore no loss of plant material due to sample preparation has to be expected. Additionally, DMF extracts are quite stable. As mentioned in *chapter 2.5. (Harvesting)*, five circles were punched from leaf samples to detect the absolute content of chlorophyll and carotenoids. This was done by a cork drill ($d = 0.5 \text{ cm}$) at areas which were representative for the particular leaves. It had to be provided that no midvein and side veins were drilled out. The circles were left in 2 ml DMF for extraction. The extraction took some days. To avoid expose to light, the samples were stored in brown glass bottles (10 ml) in a fridge at $+4^\circ\text{C}$.

2.8.2. Measuring and evaluating chlorophyll- and carotenoid content

For measuring the chlorophyll and carotenoid content 1 ml of DMF-extracts were transferred into a normalized glass cuvette ($d = 1 \text{ cm}$; Rotilabo-precision glass cuvette, micro, Roth, Karlsruhe, Germany). ZIEGLER & EGGLE (1965), SCHOPFER (1989) and PORRA et al. (2002) proposed different wavelengths for the measurement 480 nm, 645 nm, 647 nm, 663 nm and 664 nm (rounded off). The concentration of photosynthesis pigments was calculated according to Lambert-Beer's law (see *chapter 1.7.*).

For quantification of chlorophyll a and chlorophyll b in DMF, the following formulae were used (PORRA, 2002):

$$c_{chl\ a} = -3.11 E_{647} + 12.00 E_{664} \left[\frac{\mu g}{l} \right]$$

$$c_{chl\ b} = 20.78 E_{647} - 4.88 E_{664} \left[\frac{\mu g}{l} \right]$$

$$c_{chl\ a+b} = 17.67 E_{647} + 7.12 E_{664} \left[\frac{\mu g}{l} \right]$$

For the determination of the total amount of carotenoids following formula was used frequently (SCHOPFER (1989) based on KIRK & ALLEN (1965)):

$$[E_{480}^{car}] = E_{480} - 0.638 E_{645} + 0.114 E_{663}$$

This formula includes the assumption that customarily appearing carotenoids in chloroplasts show similar extinction coefficients at 480 nm. Accordingly, there is no exact value for the extinction coefficient. The common way to compare the content of carotenoids is the $[E_{480}^{car}]$ designation (SCHOPFER, 1989). Further SCHOPFER (1989) also recommends that there may exist no other disturbing pigments (e.g. anthocyanidins) in the extract. Nevertheless, the extraction here in the present work was done with different solutions. The assumption is that to the chemical structure and lipophilic behaviour of DMF no disturbance of anthocyanidins, which are mainly water soluble, may occur.

2.8.3. *Extraction with 1N HCl AE 1 (Anthocyanidins)*

For the measurement of anthocyanidins the samples of AE-1 (*chapter 2.6.2.*) were used.

2.8.4. *Measuring and evaluating Anthocyanidins*

From AE-1 100 µl were pipetted into a U-bottom microtitre plate with 96 wells (GREINER BIO ONE, Austria). For blanks 1 N HCl was taken. The known anthocyanidin in cacao is cyanidin. To draw comparisons, a serial dilution of cyanidin (Extrasynthese, Lyon, France) from 1 mg/ml to $1.9 \cdot 10^{-7}$ mg/ml was made and a calibration curve was calculated. Through

different declarations in literature (HARBORNE, 1967; PÉREZ-GREGORIO et al., 2011) a spectrum 465 to 559 nm (with an interval of 2 nm) was chosen. The evaluation and calculation was done in Microsoft Excel and Statgraph (regression curve).

2.9. HPLC-UV/VIS

2.9.1. Sample preparation and measurements

From the acidic extract AE-1 (*chapter 2.6.2.*) 100 µl were diluted in glass vials (with inserts, IVA Analysentechnik, Meerbusch, Germany) with 100 µl 1 N HCl to obtain a concentration of 1 mg/ml. In addition, standards of cyanidin derivatives (Extrasynthese, Lyon, France) of different concentrations were measured (from 1 mg/ml to 0.00195 mg/ml). The system was calibrated 30 minutes before use. The software which was used is Chromeleon. The HPLC System is a Dionex Summit equipped with a photodiode array detector (PDA, UVD170U/340U, Dionex) and an autosampler (Famos). The column was a Phenomenex Synergi Max C12, 150 mm x 2 mm, 4 µl particle size. The column oven was adjusted to 40 °C, with a flow rate of 0.2 µl/minute. Two different solvents were injected. Solvent A started with 100 % for 2 minutes and then the gradient linearly changed to 100 % of B within 98 minutes. Solvent A was MilliQ-water : MeOH(Methanol) : 85 % o-phosphoric acid (9:1:0.5 [v/v/v]) and solvent B was pure MeOH ultra solve. In total, 5 µl were injected and detected, UV/VIS spectra were recorded from 220 nm to 590 nm. The analysis of data was done with Chromeleon and Microsoft Excel.

2.10. Cation and anion chromatography

2.10.1. Method anion chromatography

The anion chromatography is a liquid chromatographic method, in which the sample ions interact with the stationary phase, which is an ion resin exchanger. The column is purged with a mobile phase (electrolyte, e.g. diluted base) and consecutively an elution of the sample ions at the stationary phase is processed.

2.10.2. Sample preparation and measurements – Anions

For the anion chromatography 1.5 ml of HE-2 samples were filled into glass vials and measured with the Dionex ICS-3000 system. Additionally internal standards in different concentrations (100 mg/l to 0.098 mg/l –dilution 1:2) were measured in between (chloride, nitrate, quinic acid, malic acid, sulphate, oxalic acid, phosphate, citrate, vanillic acid, ferulic acid and cumaric acid; all supplied from Sigma Aldrich). In this experiments the anion exchanging column was an IonPac AS11, 10 µm, 25 cm x 4 mm inner diameter. The precolumn was an IonPac AS11-guard, 13 µm, 5 cm x 4 mm inner diameter. The eluent was 0.5 mM NaOH to 37.5 mM NaOH with a flow time of 18 minutes and an eluent generator EG40. The flow rate was 2 ml/minute at a temperature of + 35 °C.

2.10.3. Method cation chromatography

The cation chromatography is a liquid chromatographic method, in which the sample cations are separated at a cation exchanger were separated. The column is purged with the mobile phase (an electrolyte, here diluted tartaric acid).

2.10.4. Sample preparation and measurements – Cations

Cations were measured with 881 Compact IC pro (Metrohm, Switzerland). Therefore 2 ml of the HE-2 and AE-2 were diluted in 20 ml MilliQ water.

2.11. Voltammetric measurements

2.11.1. Sample preparation and measurements

For these measurements 5 ml of the diluted HE-2 were filled into the round bottom flask of the 797 VA Computrace (Metrohm, Suiss). Protective gas was argon; 10 ml of acetic acid sodium acetate puffer (pH = 3.8) were added to each sample.

The diluted sample solution was mixed together with an acetic-acid-Na-acetate buffer (measuring solution) into a measuring cell. The measuring cell consists of the working electrode, a reference electrode and a counter electrode. In dependency to an external voltage between counter and working electrode, which is controlled in time-dependent steps and allows a certain current, the corresponding potential difference between working and reference electrode is monitored (OTTO, 2000).

2.12. LC-MS/MS Orbi XL

2.12.1. Sample preparation and measurements

Samples for LC-MS/MS were prepared from 40 – 80 mg of fresh weight powder and 1 ml of the extraction mix (MeOH : 1 N HCl = 99 : 1 [v : v]). The extraction took about 10 minutes (in between the samples were vortexed) and then centrifuged for 5 minutes with 14800 r/min. Afterwards the liquid part was transferred into another Epi (*Figure 2.2*), the remaining pellet was frozen again at – 80 °C for further experiments (e.g. proteomics). The supernatant was again centrifuged for 5 minutes with 14800 r/min. In glass vials with insert (IVA Analysentechnik, Meerbusch, Germany) 90 µl of internal standard mixture (2 µl reserpine, 10 µl 1 % formic acid, 78 µl U-H₂O) were put to 10 µl of the supernatant.

In this study the samples were measured with an LC-MS/MS system (Orbitrap XL, Thermo Fischer Scientific, US), HPLC-UV/VIS system and anion and cation chromatography for detecting metabolites. For the LC-MS/MS system, the molecules are separated on a column, with an ion source the particles get charged and detected afterwards. In our case the column is

a reversed phase LC column (unpolar stationary phase). The reversed phase column, an unpolar stationary phase, consists of alkanes substituted with silanes bonded to Si-OH groups. The advantage of a reversed phase column is that the column is able to operate with watery eluents (most biological samples arise from a water-based background). The ion source here is the electrospray ionisation (ESI). The Orbitrap mass analyser combines a linear ion trap with a specialized electrode. This electrode is surrounded by the charged molecules in oscillating waves, which can be displayed in a frequency spectrum and after a Fourier transformation a mass spectrum is available (DÖRFLER, 2011). Gradient for measurements see MARI et al. (2013).

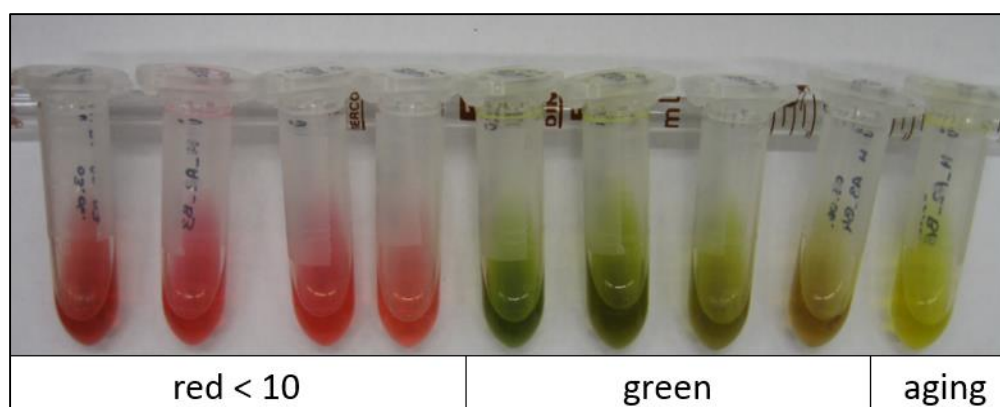


Figure 2.2: Extraction of metabolites – individual colouring during maturity.

2.13. Anatomical studies

2.13.1. Sample preparation and measurements – Stomatal imprints

For representation of stomata, some so called ‘stomata prints’ were done. Therefore round circles were punched with a cork drill. The plant circles (upside and bottom side) were fixed with methyl-ethyl-ketone (Merck, Germany) at a special plastic object slide (Wettlinger Kunststoffe, Vienna, Austria). Considering GITZ & BAKER (2009) methyl-ethyl-ketone is cheap, but they were not pleased with the quality of the results compared to other methods. However, this method was suitable for determining solely the number of stomata. The plant material was weighed down with little lead cylinders until the methyl-ethyl-ketone was

evaporated. Afterwards the plant material was scraped off and a negative imprint remained at the slide. For analysing the slides a microscope (Nikon, Eclipse 55i) with a microscopy camera (Nikon, DS-5M) was used. Analysis was done with the NIS Elements software (Nikon).

3. RESULTS

Most of the results are summarised in *Table 8.1* and *Table 8.2*.

3.1. Climate data and leaf growth

The climate in the greenhouse was in a quite rhythmic state during harvesting and experimental time. Higher relative humidity and higher temperature were alternating (*Figure 3.1*).

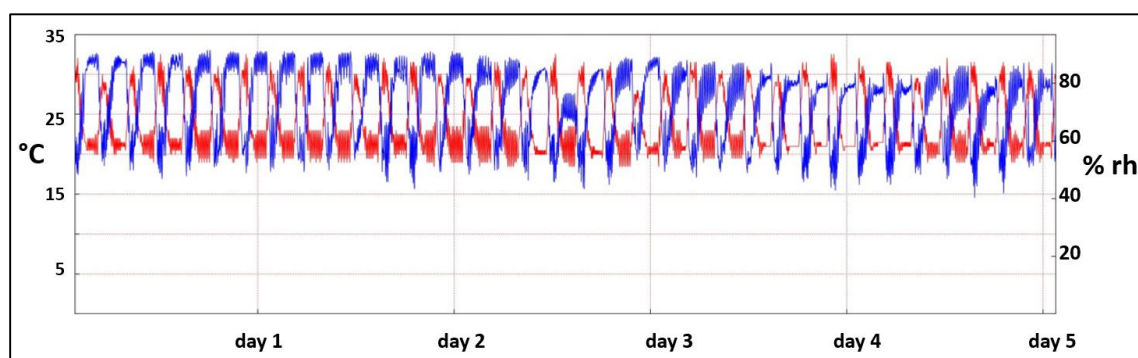


Figure 3.1: Climate plotting of temperature (°C, red) and relative humidity (% rh, blue) analysed by Temp Data logger, 5 days are zoomed out in scheme.

Due to individual differences between leaves, the leaf growth may only be explained qualitatively (*Figure 3.2*). The young leaf is convoluted and is surrounded by stipules. Some leaves remain in this position for some days. This often happens when young leaves getting succeeding yellow, followed by brown and finally are dying.

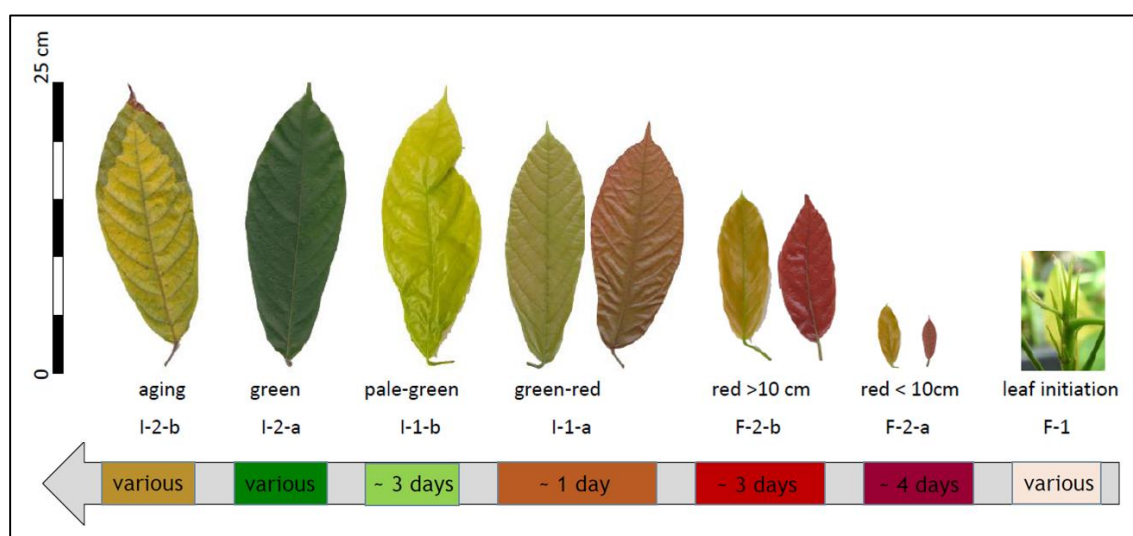


Figure 3.2: Leaf classification with an approximate time bar. Leaf initiation is zoomed out.

During leaf growth the leaf opening or unfolding stage starts at a length of about 1.5 cm. The expanding takes about 2 to 3 days – at the first day it was usually half opened, at the second day normally $\frac{3}{4}$ opened (or completely opened) and at the third day it was entire opened and had reached approximately 2 cm. Until leaves expand to 4 cm, their rate of length growth is close to 1 cm per day. Afterwards a fast growing could be observed – the length increases up to 3 cm per day. The width of the leaves changes more slowly, but almost 50 % of the rate of length growth. Colour changes and classifications are described in *chapter 2.3*.

3.2. Fluorescence measurements

The Plant Efficiency Analyser (PEA) measurements are illustrated in *Figure 3.3*. The F_v/F_m values of the stage I-2-a (green) is about 0.8, which is expected for normal, healthy leaves. All other stages showed a lower F_v/F_m value compared to the adult I-2-a (green). The medians of the developing leaves (F-2, I-1) were clearly under this ones of the I-2-a (green) stage and obtained a value around 0.6.

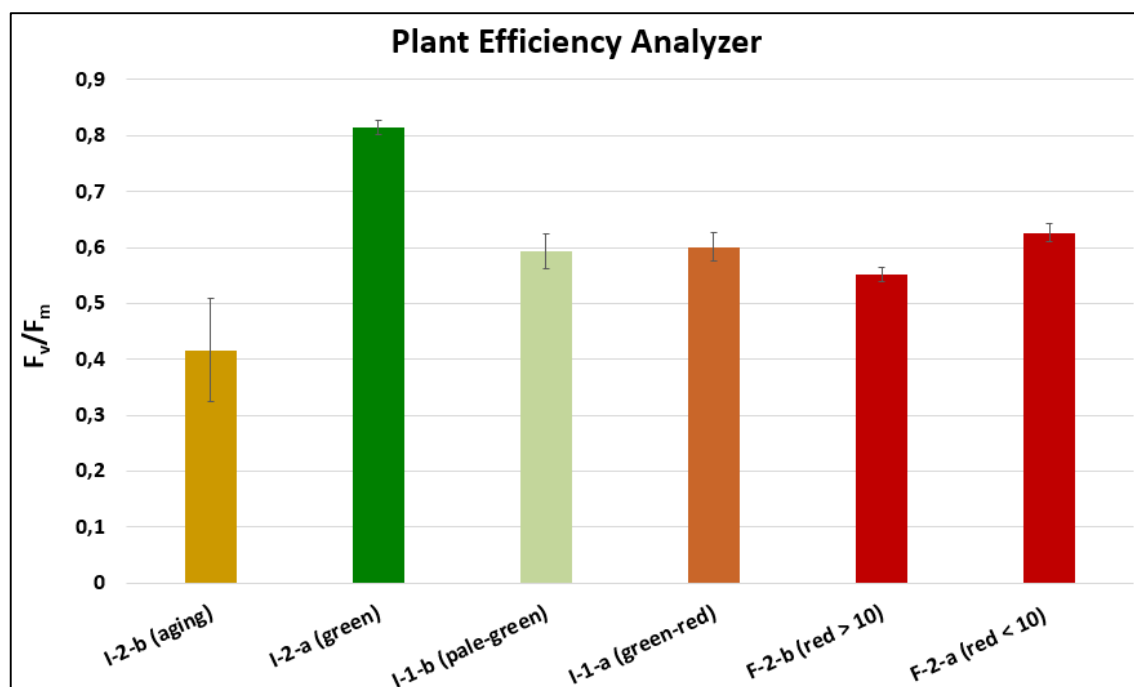


Figure 3.3: Results of PEA measurements: the shown data represent the median; error bars correspond to the 95 % confidence interval (t-values).

At advanced senescence the median was comparably lower, but at the same time the relative error increased. The error bar resulted from the classification of stage I-2-b (aging).

The F_v/F_m values of PEA are in good agreement to the data of the ETR (Imaging PAM) measurements (Figure 3.4).

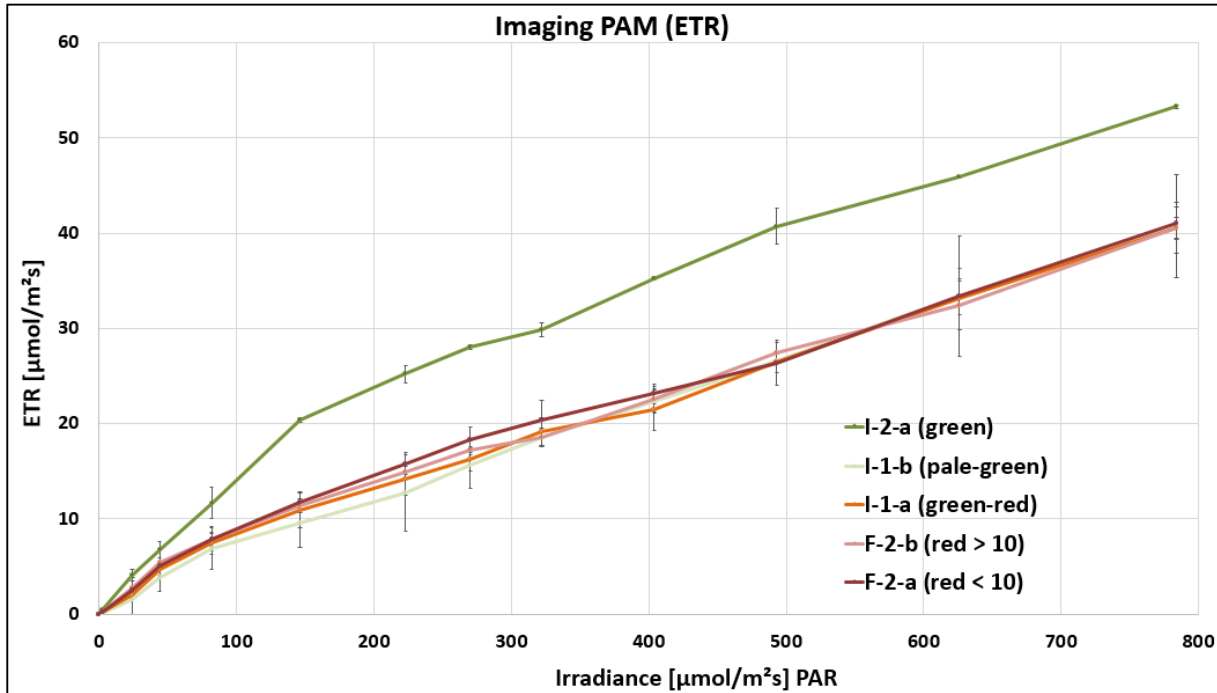


Figure 3.4: Imaging PAM: the data points are the medians; the 95 % confidence interval corresponds to the error bars.

The relative electron transport rates (ETR) of developing leaves at stages F-2 and I-1 are fairly the same (at an irradiance of 784 μmol quanta $\text{m}^{-2}\text{s}^{-1}$ the medians have an ETR value of about 40). The results of pale green leaves (I-1-b) were not clearly between the reddish (F-2, I-1-a) and the green ones (I-2-a) – but the error bars, especially those ones of measurements between the irradiance 600 to 784 PAR were showing fluctuations at the stage pale-green and green-red. At higher PAR values the deviations between different stages become more constant.

3.3. pH measurements

The pH values of the hot-water-extracts-1 were determined. They varied between 5.4 and 6.0 and are summarized in *Table 3.1* with their standard deviation (SD, σ).

Leaf stage	pH \pm SD (σ)
I-2-b (aging)	5.4 \pm 0,1 (n = 7)
I-2-a (green)	5.7 \pm 0,1 (n = 19)
I-1-b (pale-green)	5.7 \pm 0,1 (n = 5)
I-1-a (green-red)	5.7 \pm 0,2 (n = 10)
F-2-b (red > 10)	6.0 \pm 0,0 (n = 6)
F-2-a (red < 10)	5.7 \pm 0,2 (n = 4)

Table 3.1: Arithmetic means and standard deviations (σ) of pH measurements.

The proton concentrations are shown in *Figure 3.5*.

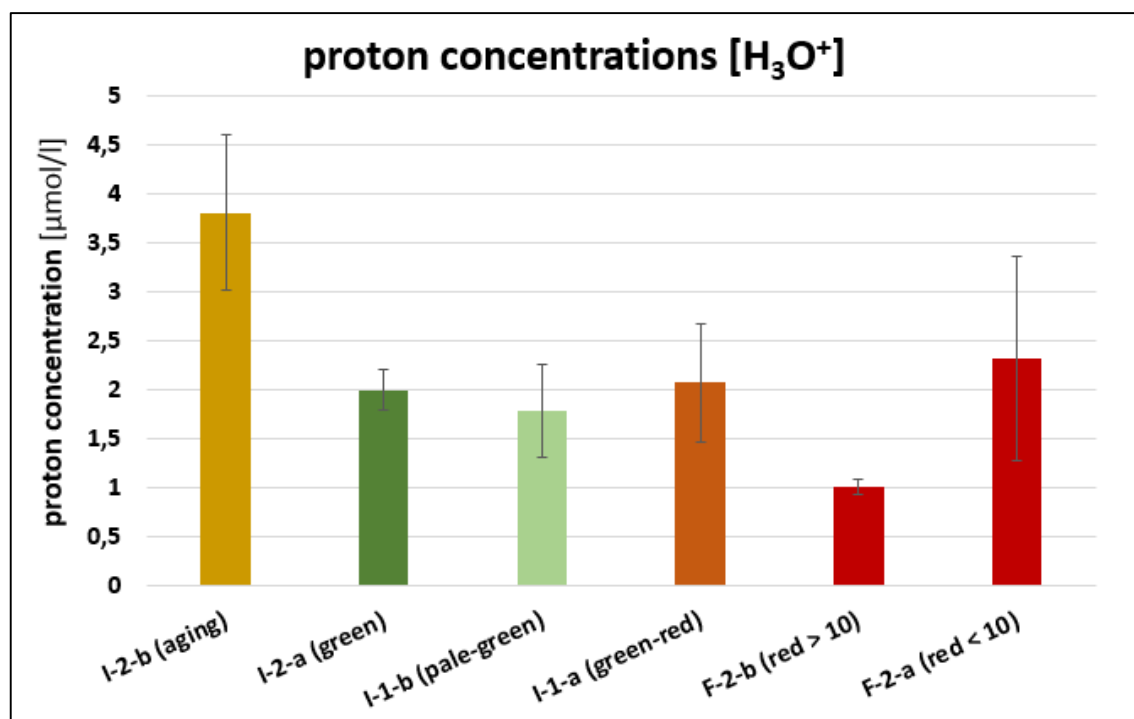


Figure 3.5: Median and 95 % confidence interval (error bar) of the calculated proton concentrations [$\mu\text{mol/l}$].

The overall error bars were rather large. This could be either explained by differences between proton concentrations of the two different trees C1 and C2 (*Table 3.2*), or insignificance due to too less samples (at F-2-a just 4 samples were measured).

Leaf stage	Tree C1 c(H ₃ O ⁺) [μmol/l]	Tree C2 c(H ₃ O ⁺) [μmol/l]
I-2-a (green)	2.1 ± 0.2	1.6 ± 0.3
I-1-a (green-red)	3.4 ± 0.7	1.2 ± 0.4

Table 3.2: Differences from stages green and green-red in between the two trees C1 and C2 (medians ± 95 % confidence interval).

3.4. Photometric measurements

The concentrations of chlorophyll a, chlorophyll b and carotenoids [E_{480}^{car}] was measured in DMF-extracts. The results are shown in *Figure 3.6*.

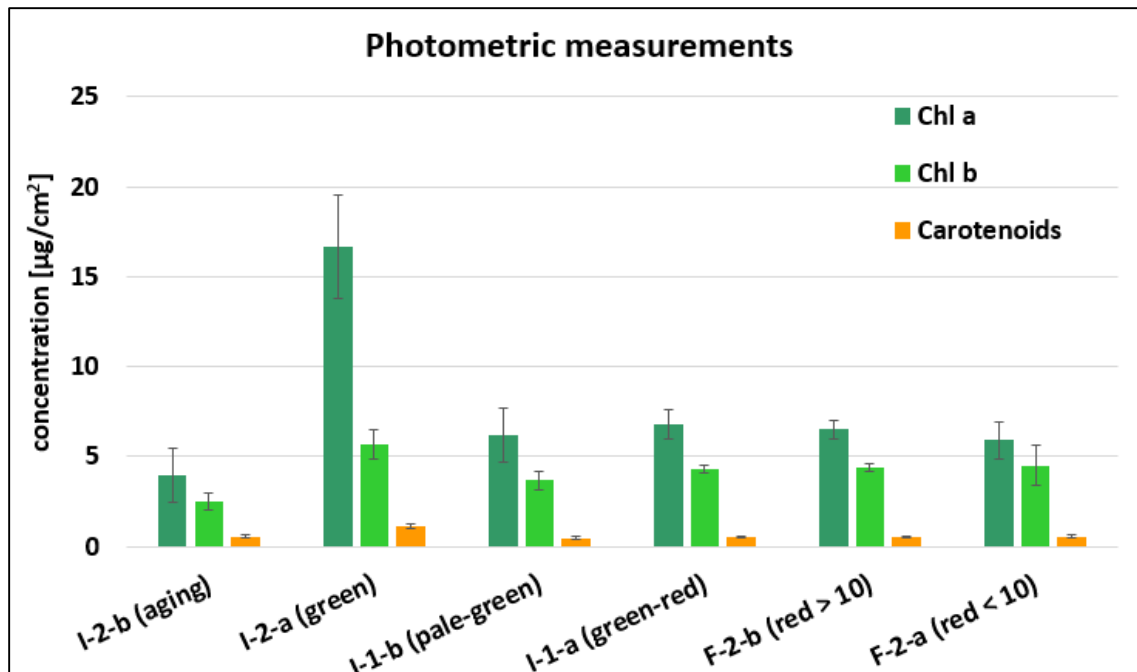


Figure 3.6: Median and 95 % confidence interval (error bars) of concentrations of chlorophyll a (Chl a), chlorophyll b (Chl b) and carotenoids.

The highest amount of the three categories was detected for the stage I-2-a (green) with a median and a 95 % confidence interval value of 16.7 ± 2.9 [$\mu\text{g}/\text{cm}^2$] chlorophyll a, chlorophyll b reached 5.7 ± 0.8 [$\mu\text{g}/\text{cm}^2$] and carotenoids 1.1 ± 0.2 [$\mu\text{g}/\text{cm}^2$]. Due to the fairly tall error bar of the stage I-2-a (green) in *Figure 3.6* a separation of the analysed leaves was done for the different trees C1 and C2 in *Figure 3.7*.

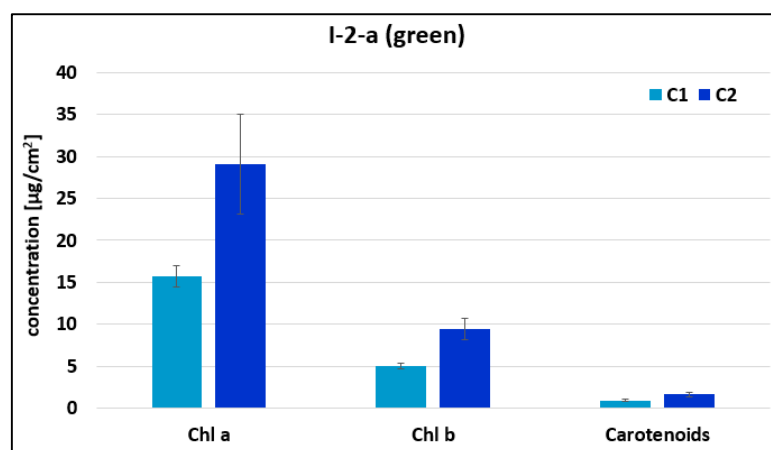


Figure 3.7: Comparison between the two trees C1 (n = 14) and C2 (n = 5) in stage I-2-a (green). Medians and 95 % confidence intervals (error bars) are shown.

The differences between trees were not so inherent for other stages like in stage I-2-a (green). The ratio of Chl a to Chl b (*Figure 3.8*) seems to be rather constant (around 1.5) at the developing leaf stages (F-2 and I-1) and a similar ratio was nearly reached from the stage I-2-b (aging).

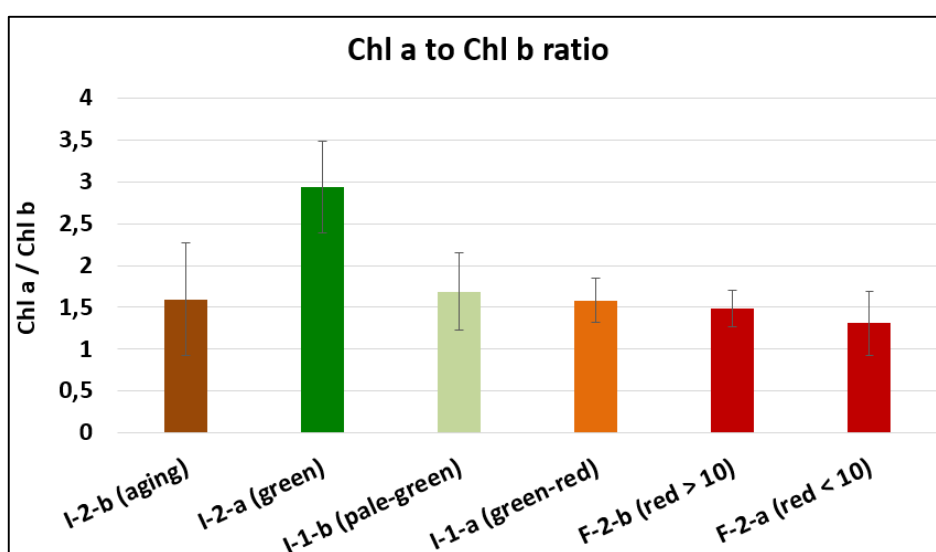


Figure 3.8: Chl a to Chl b ratio; error bars are calculated with error propagation.

The content of carotenoids per square centimeter is quite stable during leaf development stages F-2 and I-1-b (Figure 3.9). Again, there is no smooth transition between the stages pale green (I-1-b) and green (I-2-a) observable.

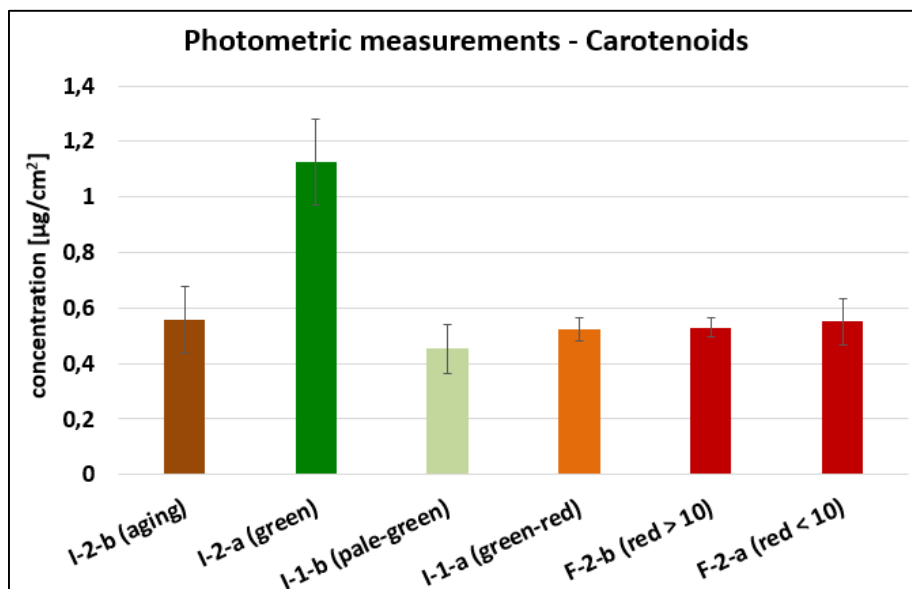


Figure 3.9: Carotenoids photometry of different development stages; medians and 95 % confidence intervals (error bars) are shown (zoomed out of Figure 3.6).

The ratio between mass concentrations [µg/cm²] of carotenoids to chlorophyll (a + b) is shown in Figure 3.10. The calculation was made with error propagation, which causes comparatively large error bars. However, it could be shown that the ratio of carotenoids per chlorophyll a and b is relatively constant.

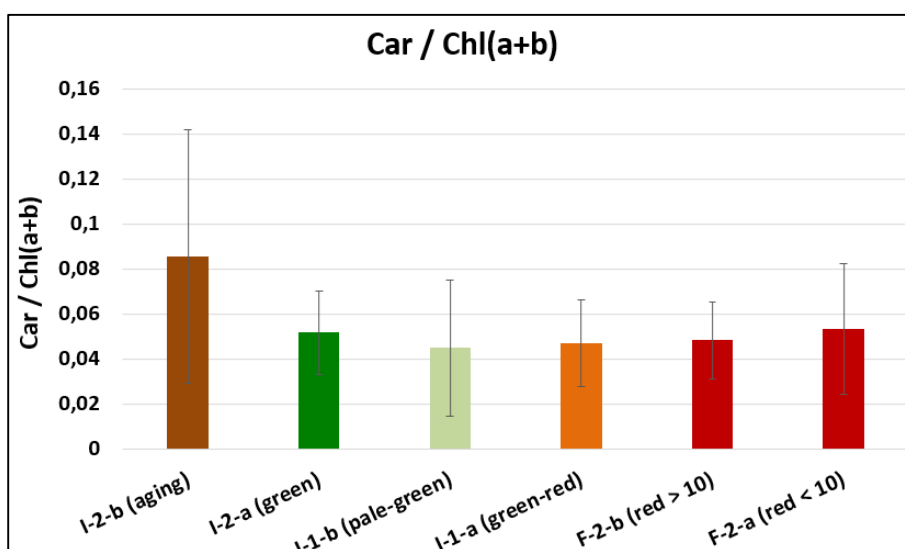


Figure 3.10: Ratio of Car to Chl a+b; error bars are calculated with error propagation.

Further measurements were performed to detect anthocyanidins. A serial dilution from standards to determine a calibration curve. A regression curve was calculated with the program statgraphics. The calibration function was:

$$c_{Antho}^{519} = (-0.0133992 + 0.304155 * E_{\lambda})^2$$

The function was applied for different E_{λ} . The concentration was calculated in mg/cm^2 , at the most matching wave-length 519 nm.

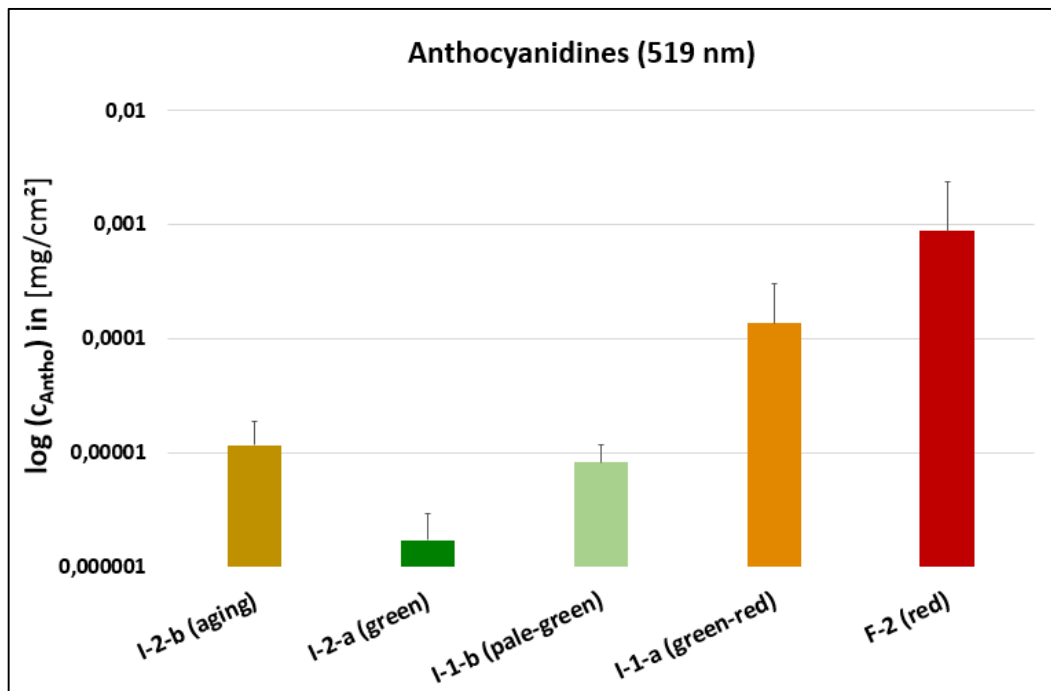


Figure 3.11: Content of anthocyanidins in mg/cm^2 at 519 nm (arithmetic mean and standard deviation (error bars)).

The chronological sequence showed a high amount of anthocyanidins (*Figure 3.11*) at the beginning of the leaf development. The amount of pigment per square centimetre decreased till the stage I-2-a (green) was reached. At the aging stage (I-2-b) the content was again increasing.

3.5. HPLC-UV/VIS

Several different substances were detected with the HPLC-UV/VIS measurements (Table 3.3).

The validation was done with an internal library. Mainly flavonoids were detected.

	aging (I-2-b)	green (I-2-a)	pale green (I-1-b)	green-red (I-1-a)	red > 10 (F-2-b)	red < 10 (F-2-a)
FLAVONOIDS						
flavonol cf.		X	X		X	
flavonoid dimer cf. 1	X	X	X	X		X
flavonoid cf. 2		X		X		X
flavonoid cf. 3		X	X			
flavonoid dimer cf. 4			X	X	X	
flavonoid, scutellarin 6,4' methyl der. cf. 5			X?			
flavanon cf. 1		X	X		X	
orientin(flavones) der. cf. 1				X		X
flavones cf. 1		X	X?			
flavones cf. 2			X	X		
flavones cf. 3	X	X	X	X	X	X
flavones cf. 4		X	X			
flavones cf. 5		X				
flavones cf. 6		X			X	
flavones – vitexin der. cf. 7		X	X			X
flavones cf. 8		X				
flavones cf. 9		X				
flavones cf. 10	x					
vitexin cf. 1	x	X	X	X	X	X
vitexin kaempferol der. cf. 2		X	X	X		X
vitexin der. cf. 3		x				
vitexin der. cf. 4		x		x		

	aging (I-2-b)	green (I-2-a)	pale green (I-1-b)	green-red (I-1-a)	red > 10 (F-2-b)	red < 10 (F-2-a)
apigenin 4 methyl der. <i>cf.</i> 1						
apigenin der. <i>cf.</i> 2		X		X		X
apigenin der. <i>cf.</i> 3		X	X	X	X	X
apigenin-4-methyl <i>cf.</i> 4	X			X	X	
apigenin-7-methyl, flavon <i>cf.</i> 5		X	X			
apigenin-7-O-rhamnogluco- side <i>cf.</i> 6				X		
genistein-5,7-dihydroxy-4- methoxyisoflavon <i>cf.</i>		X	X			
isorhamnetin-3-O-glycosid <i>cf.</i>		X				
Flavanoles						
catechin roaglaol <i>cf.</i> 1			X	X	X	X
(+)catechin monohydrate <i>cf.</i> 2			X	X	X	X
catechin der. <i>cf.</i> 3			X	X	X	X
catechin der. <i>cf.</i> 4		X	X	X	X	X
catechin der. <i>cf.</i> 5			X	X	X	X
catechin der. <i>cf.</i> 6			X	X	X	X
Anthocyanidins						
cyanidin der. <i>cf.</i> 1				X		X
cyanidin der. <i>cf.</i> 2						X
cyanidin der. <i>cf.</i> 3						X
cyanidin der. <i>cf.</i> 4						X
cyanidin 3-O glucoside <i>cf.</i> 5				X		
procyanidin B1 der. <i>cf.</i> 1		x	X	X	X	X
procyanidin B2 der. <i>cf.</i> 2			X	X	X	X
DIHYDROXYBENZOIC ACIDS						
gentisic acid <i>cf.</i>	X	X				
p-hydroxy-benzoic acid <i>cf.</i>	X	X	X	X	X	X

	aging (I-2-b)	green (I-2-a)	pale green (I-1-b)	green-red (I-1-a)	red > 10 (F-2-b)	red < 10 (F-2-a)
4_OH_benzoic acid cf.	X	X	X	X	X	X
CINNAMIC ACID – der.						
p-coumaric acid cf.	X	X		X		X
ALKALOID						
theobromine		x	X	X	X	X
STILBENE-derivatives						
stilbene structure cf. 1	X	X	X	X	X	X
resveratol der. stilbenoid cf. 2	X	X				
AMINO-ACIDS						
tryptophan cf. 1	X	X		X		
tryptophan der. cf. 2			X	X	X	
phenylalanin cf. 3	X					

Table 3.3: Results of HPLC-UV/VIS analysis. Detection of substance in most samples of one stage was signed as 'X'. Further, symbol 'x' means, that the detection was just in few samples or in low concentrations. The abbreviation cf. (lat. confer, determined uncertain) points out, that the spectrum could not be exactly attributed to metabolites in the UV/VIS library. Also, some derivatives (der.) were detected.

The smallest number of substances was detected in the stage aging (I-2-b). An accelerating amount of flavonoids could be detected during development and decreased in the aging stage. Several catechin derivatives could be mainly detected till stage pale-green. Further cyanidin der. are mostly observed in younger stages. Theobromine a main substance of cacao leaves, was not detected in aging leaf stage (I-2-b). Hence, phenylalanine (amino acid) was just detected in the aging stage. There was a match between gentisic acid in the older stages green and aging.

Some UV/VIS-spectra are pictured in *Figure 3.12*.

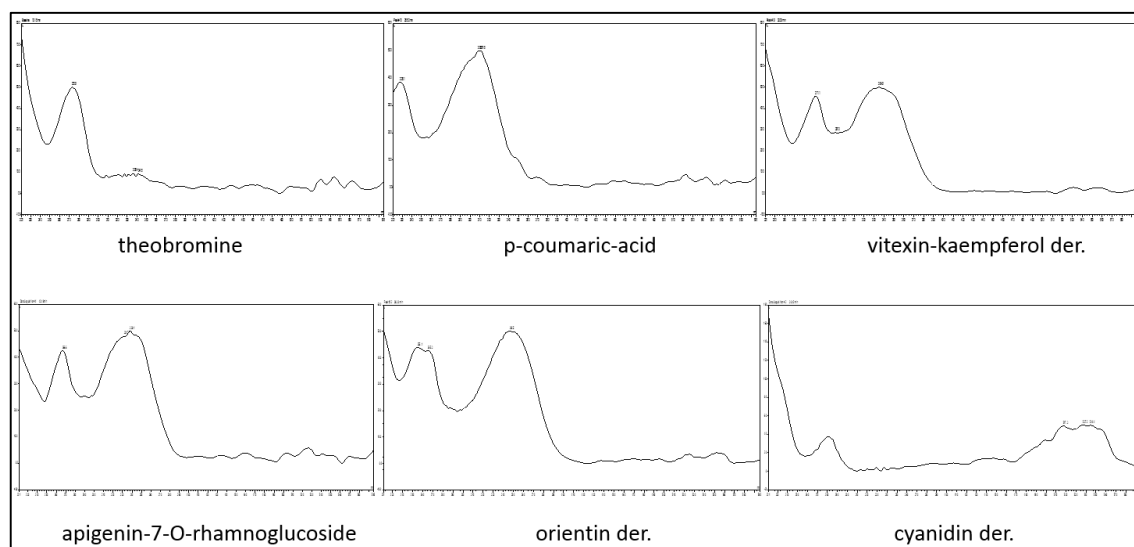


Figure 3.12: UV/VIS-spectra of several detected substances, see also Table 3.3.

3.6. Cation and anion chromatography

In the hot-water-extracts the cations and anions mainly of the vacuole are dissolved. This is the same case for the acid-extracts, in addition here the ions which are loose bound to the cell wall are extracted.

Five different types of cations were detected in the acid-extract-2 (AE) and the hot-water-extract-2 (HE). The two different extracts were compared in *Figure 3.13* (different scale bars). The main cation amount of acid-extract (AE) consisted of calcium and potassium, followed by magnesium. Hence the main amount from the hot-water-extract (HE) was potassium, followed by magnesium.

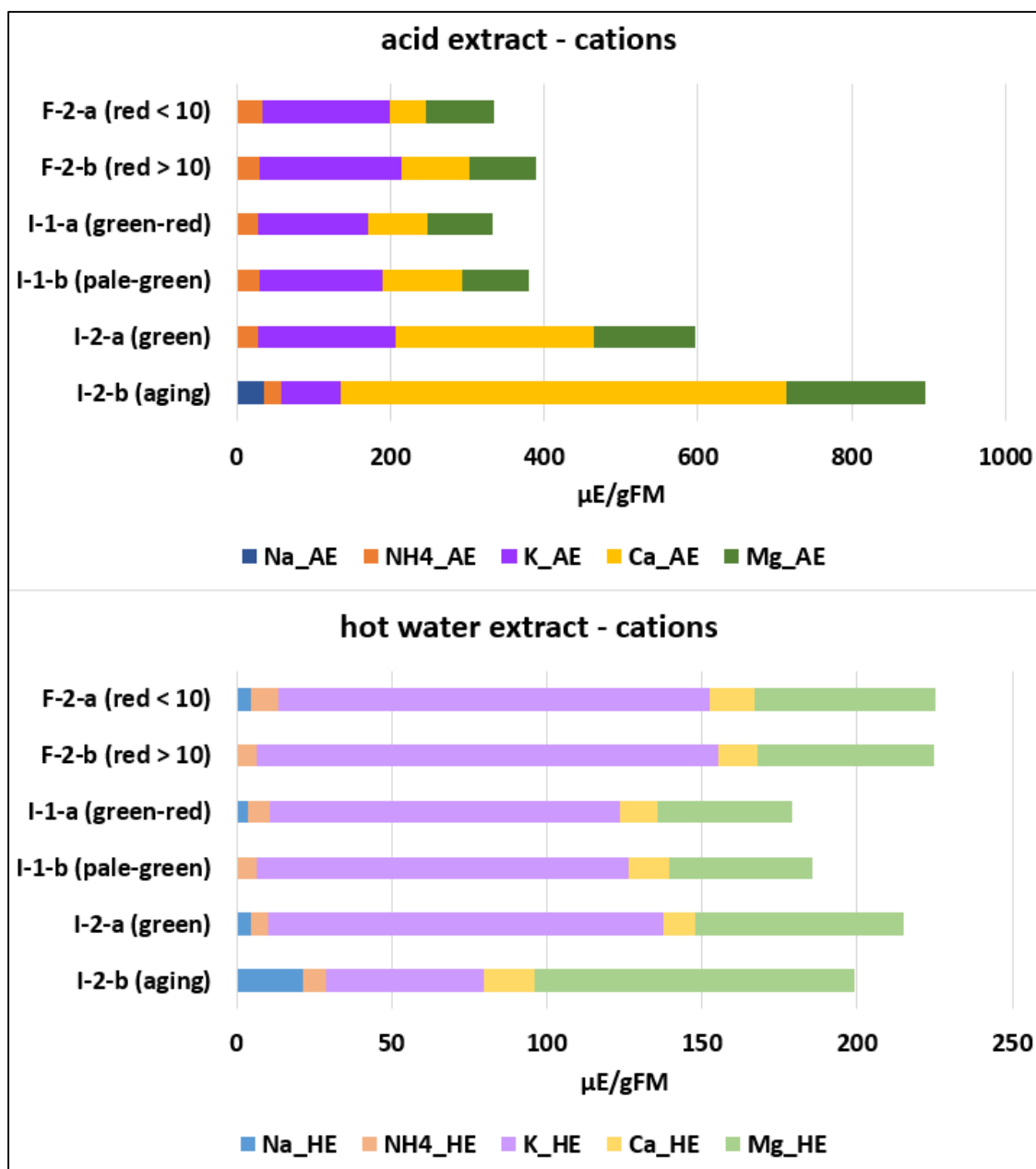


Figure 3.13: Different fragmentation of cations (medians). On top there are shown results from the acid-hot-water-extracts (AE) and at the bottom these ones of the hot-water-extracts (HE). The units are in micro equivalents per gram fresh mass [$\mu\text{E/gFM}$].

Total cation values of the acid-hot-water-extract is in average 2.4 times higher than the hot-water-extract. Sodium could not be measured sufficiently because the detection limit was reached (to high diluted). However, the other cations were measured entirely well and no other detection problems arose. The amount of ammonium in the AE (Figure 3.14) was much higher than in HE. Furthermore, the total amount of ammonium seems to be rather constant during

development. The potassium levels decrease significantly from stage green (I-2-a) to stage aging (I-2-b) (*Figure 3.14*).

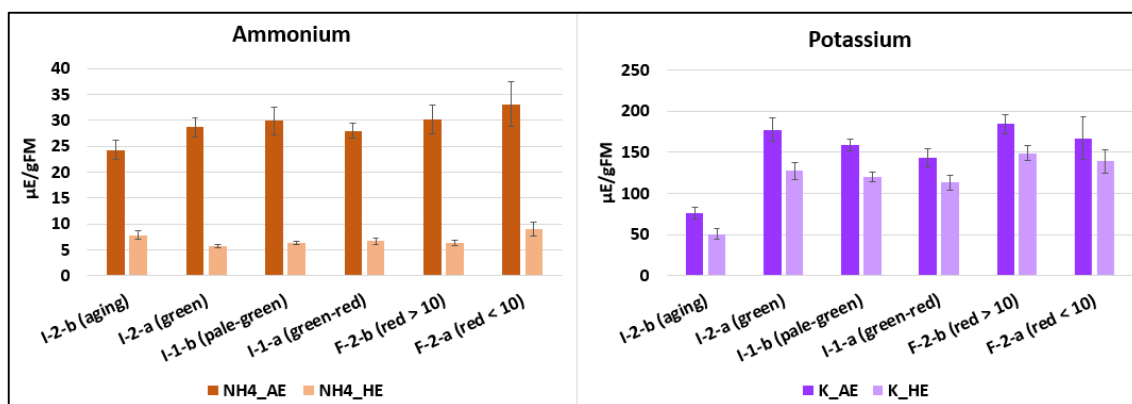


Figure 3.14: Comparison (median and 95 % confidence interval) between the AE and HE from ammonium (orange) and potassium (purple) during leaf development.

The amount of magnesium is shown in *Figure 3.15*. The highest concentration of magnesium were found in the oldest leaves. Relative constant values are reached until development stage pale-green (I-1-b). An increase of magnesium in the stage green is observed.

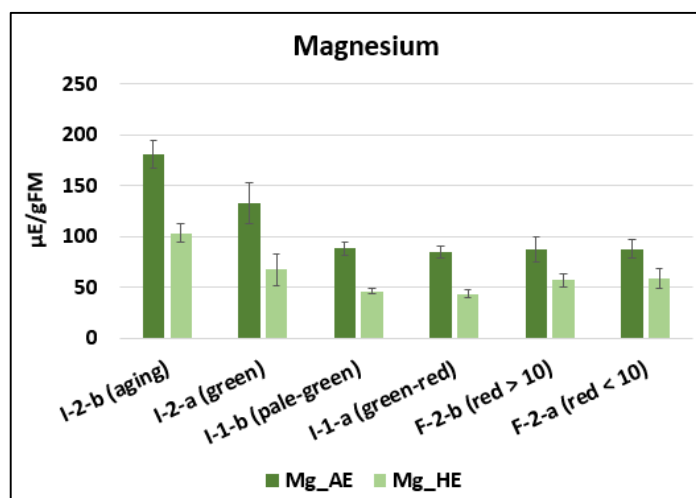


Figure 3.15: Differences (medians and 95 % confidence intervals) of magnesium concentrations in AE and HE are shown.

An enormous contrast between extracted calcium ions in acid or in hot water extract is shown in *Figure 3.16*. In the AE high concentrations of calcium could be extracted, whereas in the last two stages (green and aging) the maximum was reached.

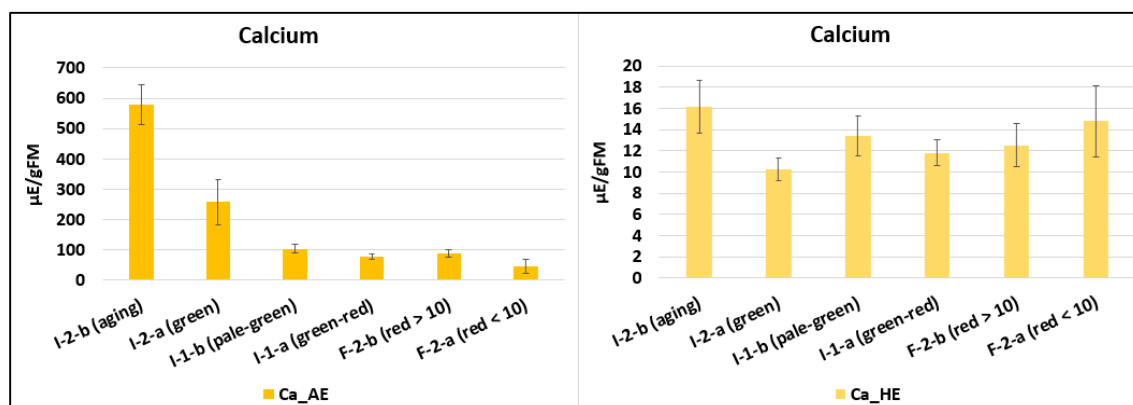


Figure 3.16: Calcium content (median and 95% confidence interval) in AE (left) and HE (right).

An overview of the anion measurements is shown in *Figure 3.17*. In total eleven different anions were measured. The amount is unequally distributed, the highest scores are these ones of nitrate, followed by lower values of oxalic acid, malic acid and phosphoric acid.

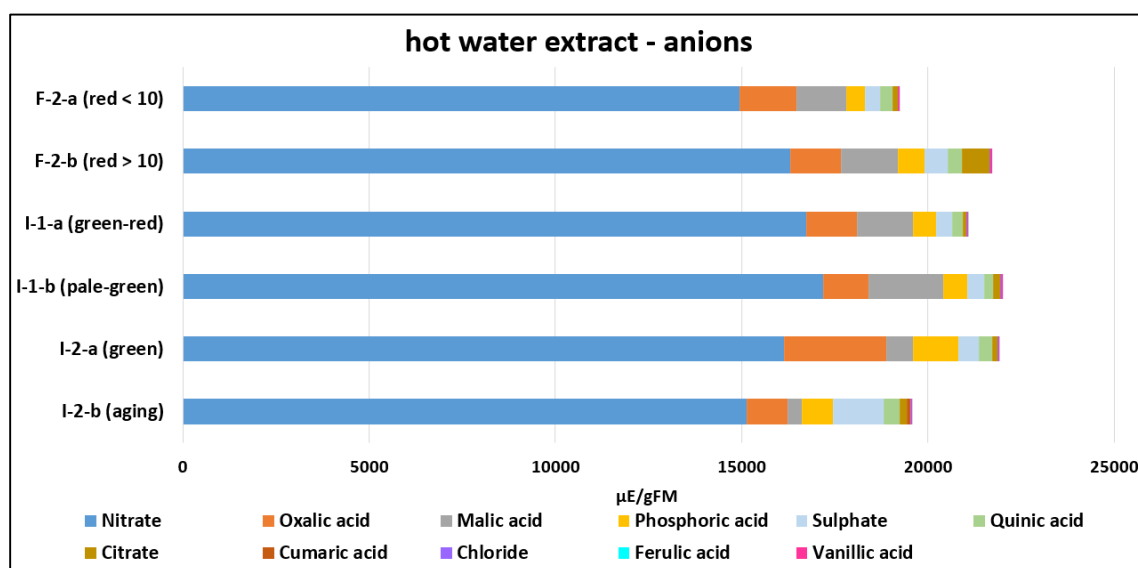


Figure 3.17: Anion measurements (median) of the hot-water-extracts.

Next figures are ordered with decreasing total anion concentration. The main anion concentrations – nitrate, oxalic acid, malic acid and phosphoric acid are shown in *Figure 3.18*. No significant contrast between the nitrate concentrations appeared. A higher amount of oxalic acid could be detected in the stage green (I-2-a). It seems that malic acid increases during development (F-2 till I-1-b) and decreases from stage green (I-2-a) to aging (I-2-b). Further, in the stage green (I-2-a) higher amounts of phosphoric acid (and oxalic acid) could be observed.

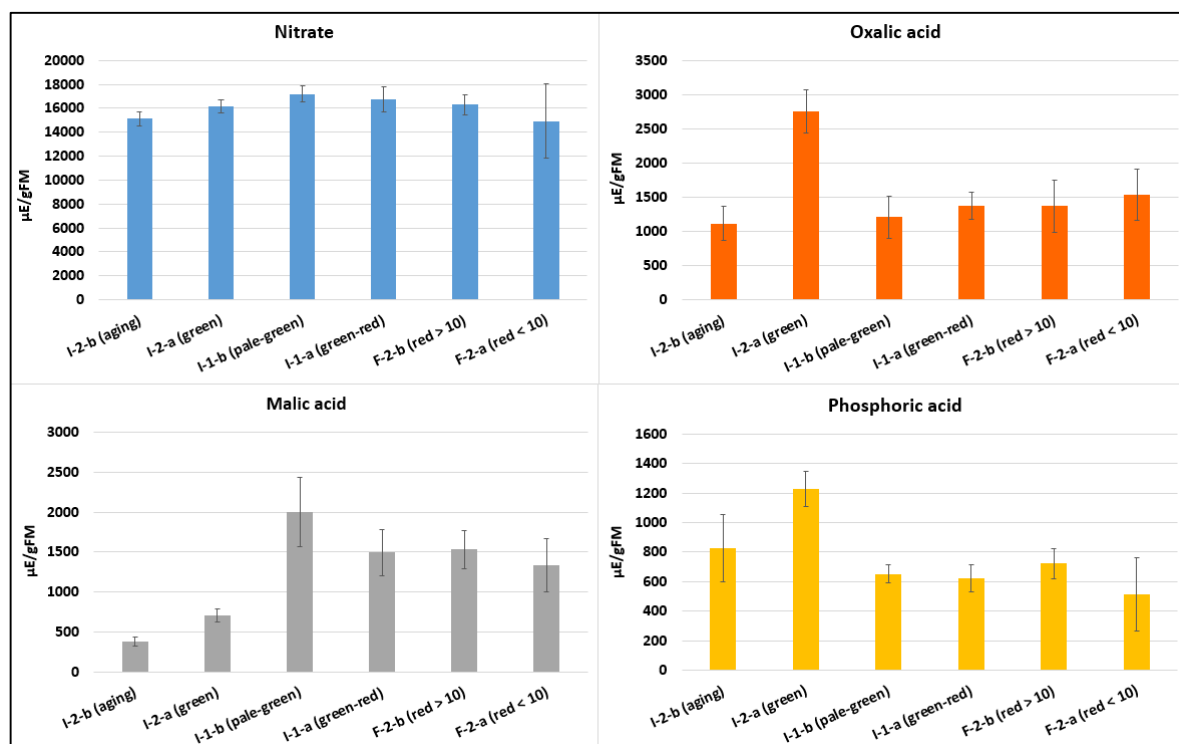


Figure 3.18: Concentrations of nitrate (blue), oxalic acid (orange), malic acid (grey) and phosphoric acid (yellow) in $\mu\text{E/gFM}$ (medians and 95 % confidence intervals).

All other anions appear in lower amounts, which is shown in *Figure 3.19*. A high sulphate and cumaric acid concentration could be detected in the senescence leaves (aging stage). Cumaric acid was present in higher concentrations in the stages green (median: $7.8 \mu\text{E/gFM}$) and aging (median: $105 \mu\text{E/gFM}$). In all other stages cumaric acid was detected in lower amounts. The amount of citrate was very high at the stage of red leaves which were taller than 10 cm (F-2-b).

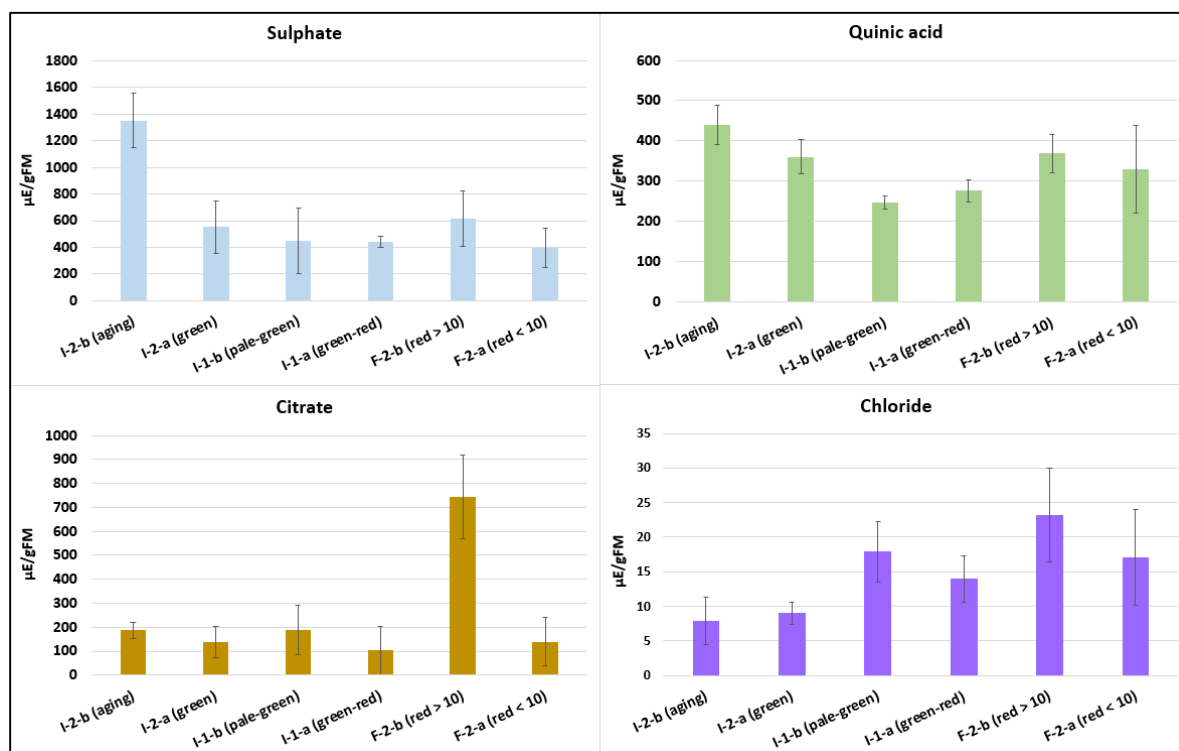


Figure 3.19: Concentrations of sulphate (blue), quinic acid (green), citrate (brown) and chloride (purple) in $\mu\text{E/gFM}$ are shown with their medians and 95 % confidence intervals.

Ferulic acid and vanillic acid were detected in the lowest amounts in all stages. There were no significant differences between the developing levels.

A detailed list of cation and anion concentrations can be found in *Table 8.1*.

3.7. Voltammetric measurements

The calculations of the integrated areas below the measurement curves are shown in *Figure 3.20*.

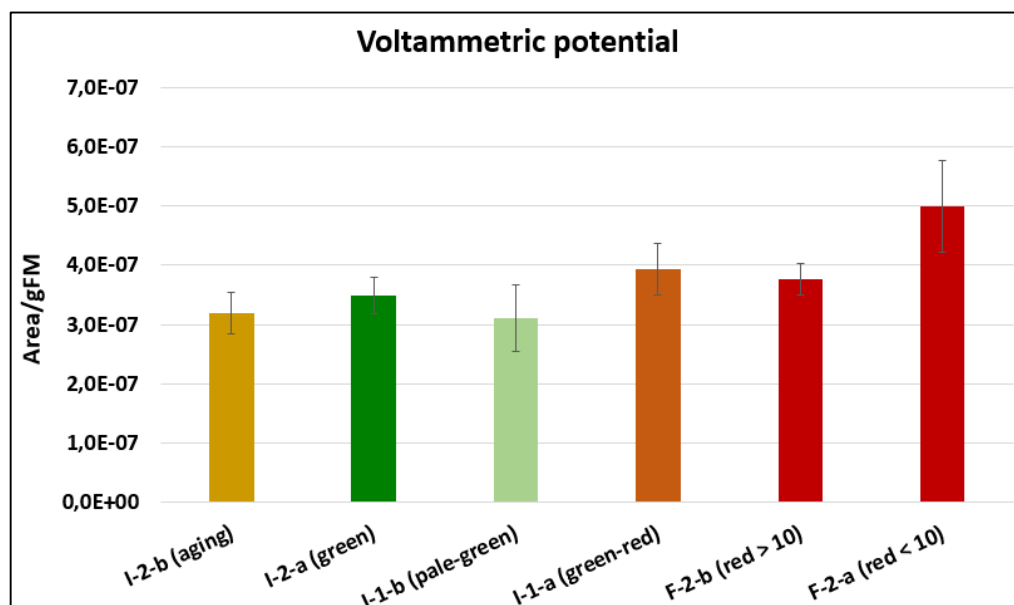


Figure 3.20: Voltammetric potential of the different stages (median and 95 % confidence interval (error bars)).

The voltammetric potential of HE-2 seems to be especially high for the youngest leaves (F-2-a). To demonstrate more details, results are split in five voltage ranges in *Figure 3.21*.

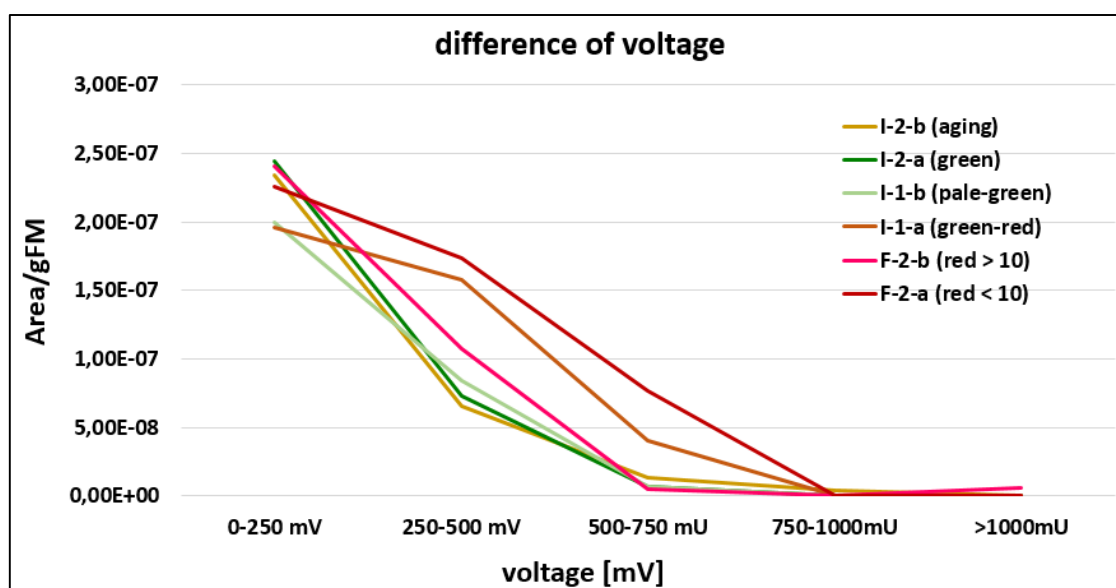


Figure 3.21: Medians of the integrated area at a gradual transformation of voltage (+ 250 mV).

In total six measuring curves of three stages are shown in *Figure 3.22*.

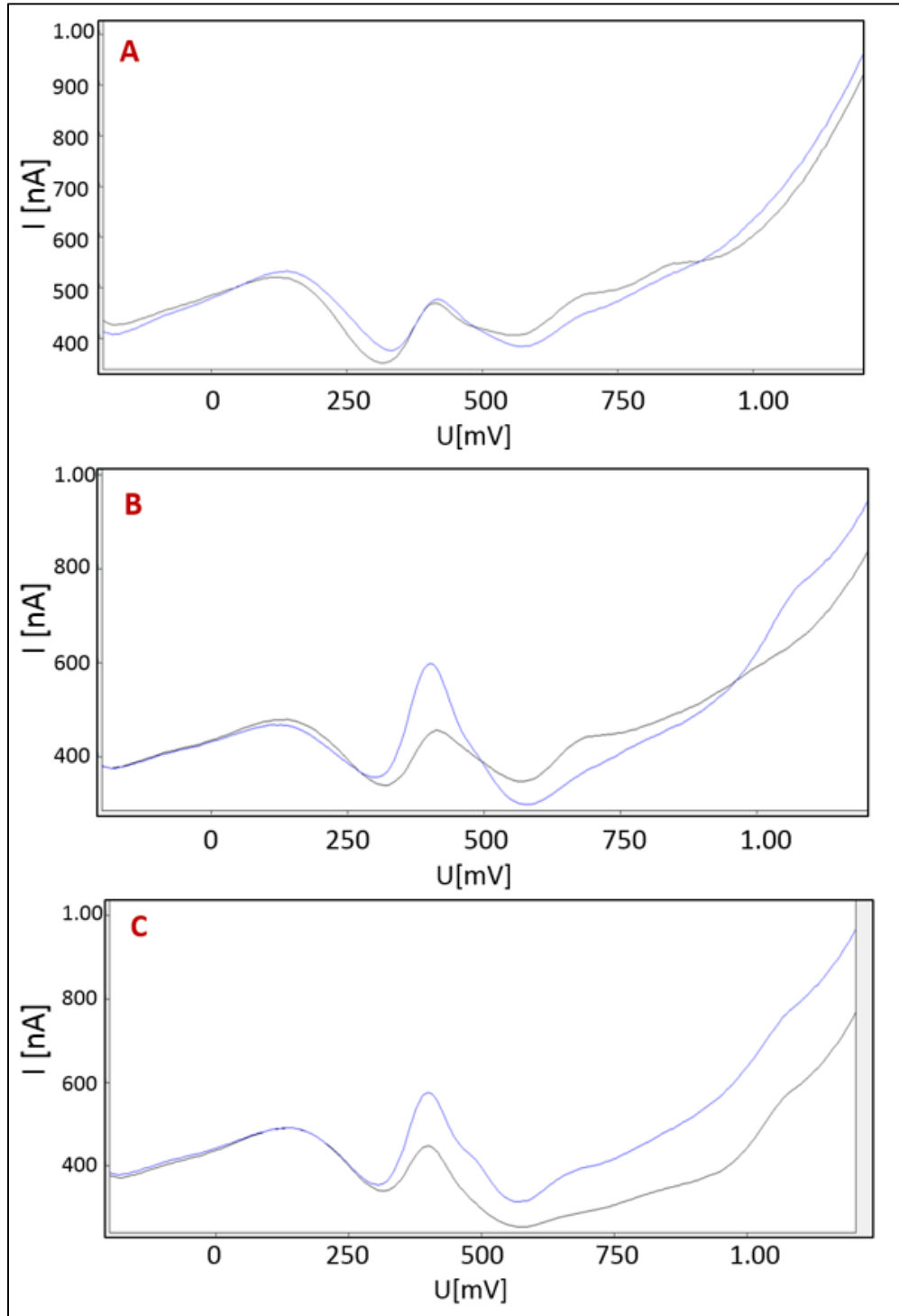


Figure 3.22: Measuring curves of two samples per stage (black and blue) A) stage aging (I-2-b); B) stage pale green (I-1-b); C) red > 10 cm (F-2-b).

3.8. Results LC-MS/MS Orbitrap XL

A principal component analysis (PCA) was done with cacao leaf LC-MS/MS data using the statistical toolbox COVAIN (WECKWERTH & SUN, 2012), which is integrated in MATLAB. The results from COVAIN analysis are shown in *Figure 3.23*. The separation of green (I-2-a) and aging (I-2-b) samples is significant to the younger ones. The developing leaves are moderately clustered together, so no smooth transition to the green leaves can be observed.

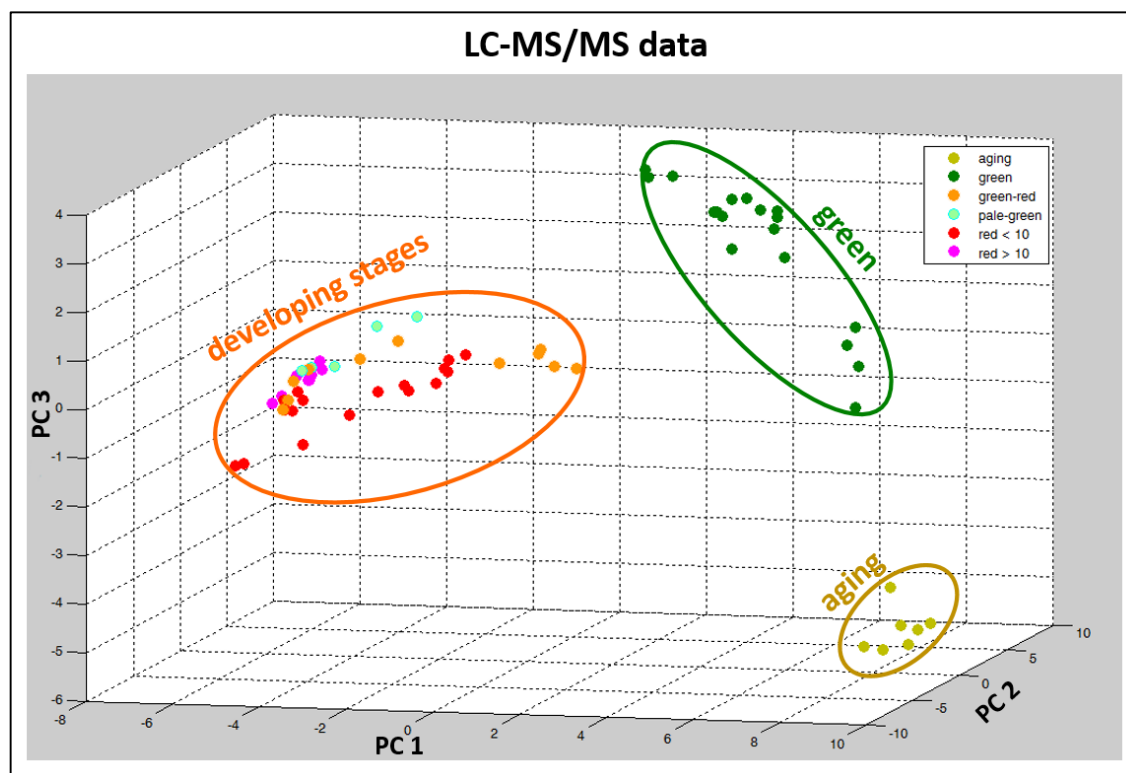


Figure 3.23: Principal component analysis of LC-MS/MS data; PC 1 (34.1 %), PC 2 (10.8 %) and PC 3 (7.0 %). Evaluation and figuring was done with COVAIN (WECKWERTH & SUN, 2012).

The LC-MS/MS data were further analysed with an internal library (EGELHOFER, unpublished) where MS2 spectra and retention times are compared against standards. Results are listed in *Table 3.4*.

	aging (I-2-b)	green (I-2-a)	Pale-green (I-1-b)	green-red (I-1-a)	red >10 (F-2-b)	red <10 (F-2-a)
cyanidin 5-O-glucoside		X		X	X	X
apigenin-7-glucoside	X	X		X	X	X
5,6,2',6'-tetra-O-methyl-flavon		X				
abscisic acid	X	X	X	X	X	X
heptadecanoic acid	X	X		X		X
theobromine				X	X	X
theophylline				X	X	X
eriodictyol	X					X
ferulic acid		X				
procyanidin A2	X	X	X	X	X	X
procyanidin B2		X	X		X	X

Table 3.4: Cacao leaf LC-MS/MS data results from an internal library.

3.9. Anatomical studies

Several anatomical cuttings were made. A surface cut could be found in *Figure 3.24*, some anthocyanidins are in special regions (mainly veins) of the leaves.

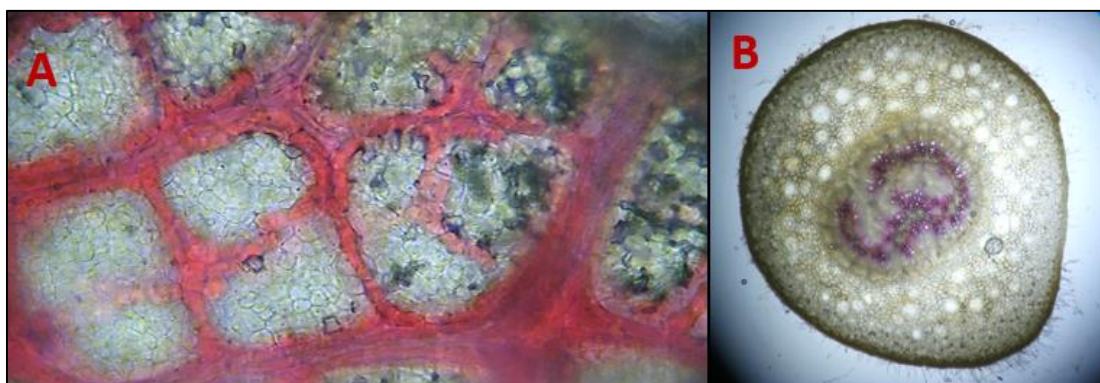


Figure 3.24: A) Surface cut of a young cacao leaf in stage F-2-b (red > 10) (x200); B) cross section through petiole, hairs are visible, xylem is stained red with phloroglucin and hydrochloric acid (x50).

In total, four types of trichomes were observed and demonstrated in *Figure 3.25*, *Figure 3.26* and *Figure 3.29*.

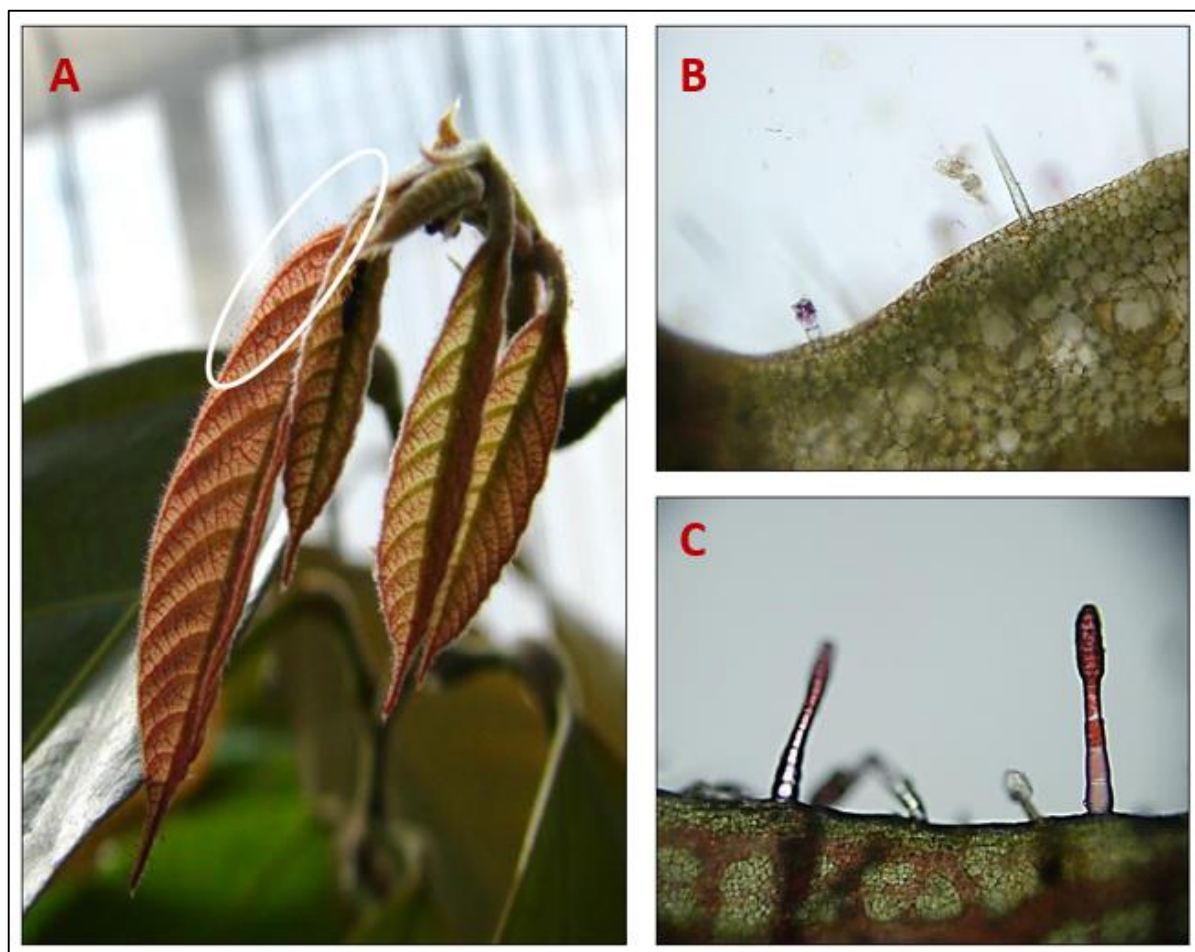


Figure 3.25: A) Trichomes visible at young leaves (stage red < 10); B) Small hair with a rounded multicellular head filled with anthocyanidins (left; in *Figure 3.26 B-ii*) and short stubby, single cellular cylindrical hair (right; in *Figure 3.26 B-iii*) (x200); C) Large hair with a larger multicellular head filled with anthocyanidins, only found on young hairs (in *Figure 3.26 B-iii*) (x400).

In *Figure 3.26 B* an overview of the four types of trichomes is given. In addition, some crystals were found in diverse cuttings.

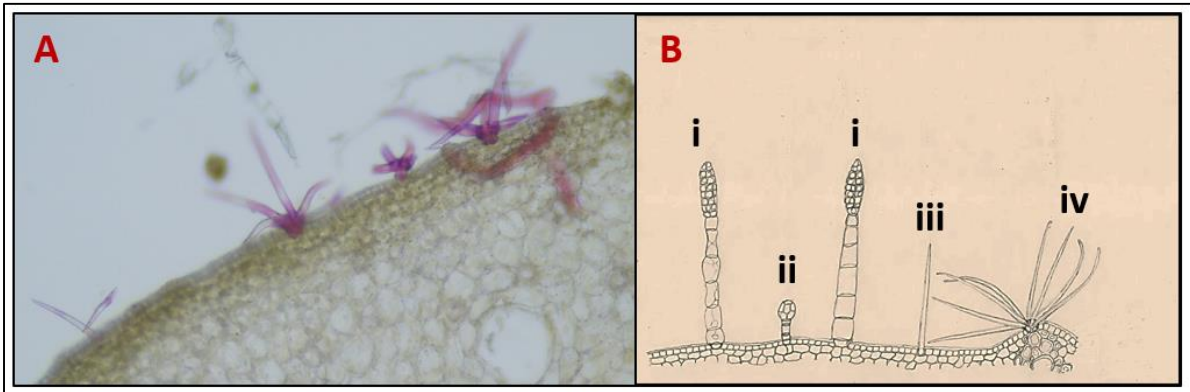


Figure 3.26: A) Fourth hair type: stellate shaped, multicellular hair (in B-iv) (x200); B) Anatomical drawing of all four hair types.

The number of counted stomata is presented in Figure 3.27, where fully developed stomata and stomata initial cells were counted.

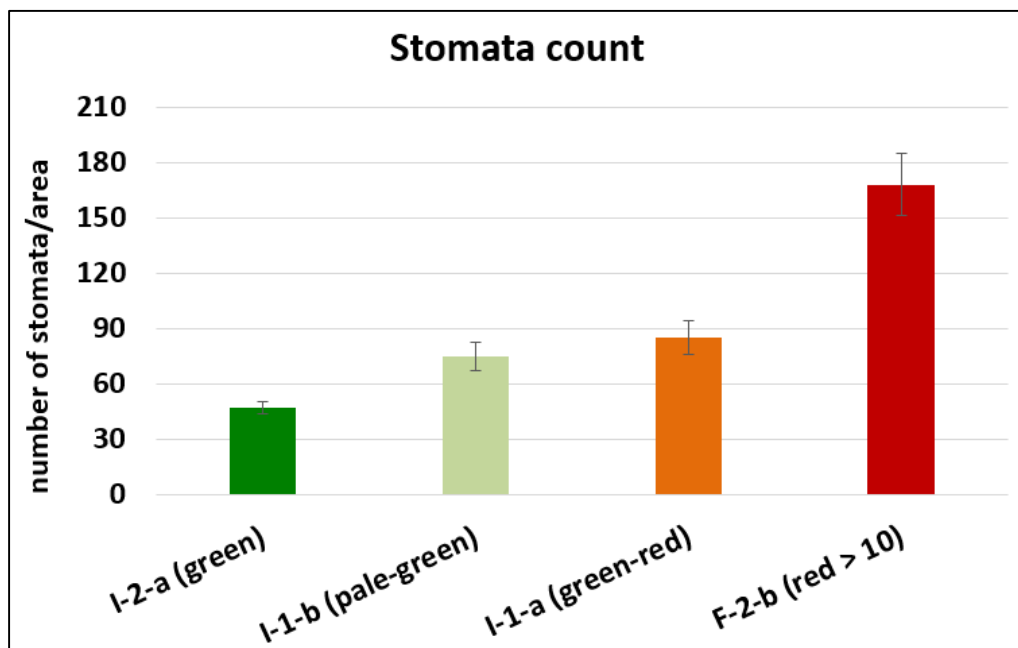


Figure 3.27: Stomata counting (medians and 95 % confidence intervals) of different cacao leaf stages, the observation area consecutively for all was $\sim 0.007 \text{ mm}^2$ (x400).

The sum of stomata per standardized area was decreasing during development. The median of stage F-2-b (red > 10) was 168 ± 16.9 and the counts of green leaves (I-2-a) was determined to be 47 ± 3.2 .

Stomata prints of four different stages are imaged in *Figure 3.28*, the decline of stomata in is visible.

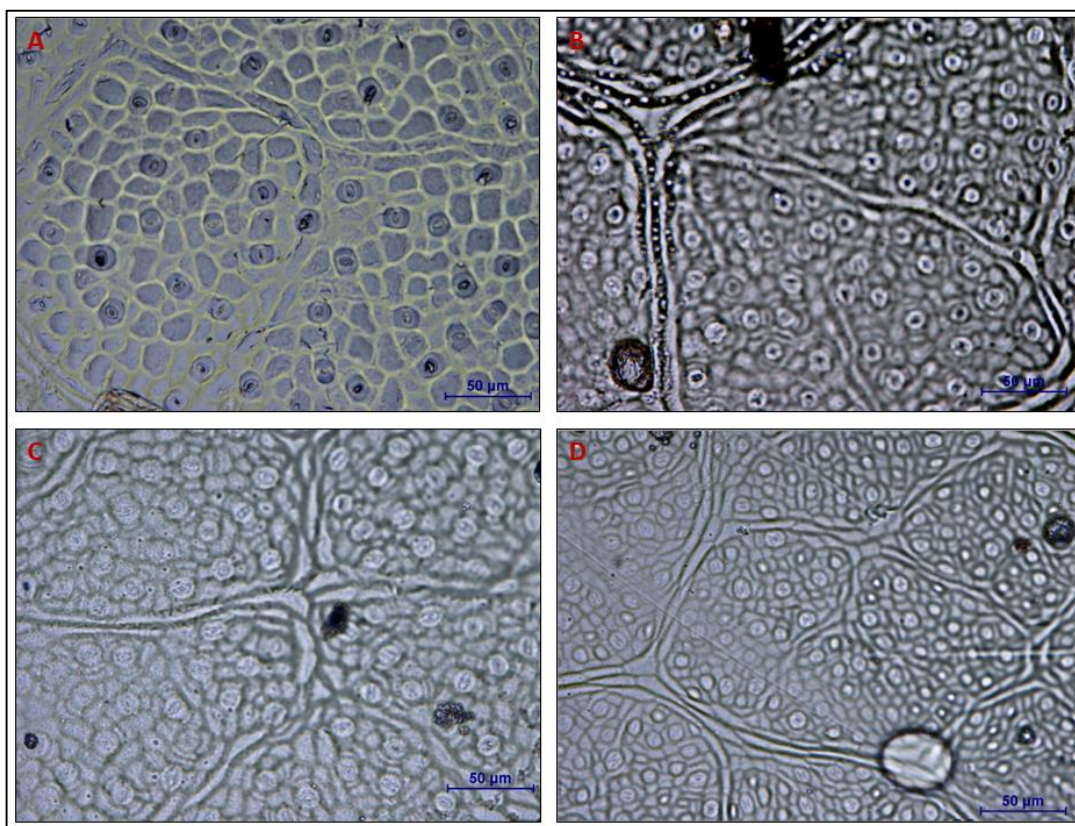


Figure 3.28: Stomata prints from four cacao leaf stages (x400) A) Green (I-2-a); B) Pale green (I-1-b); C) Green-red (I-1-a); D) Red > 10 (F-2-b).

Fully developed stomata could have been found in younger leaves (stage F-2-a) only along veins (*Figure 3.29*).

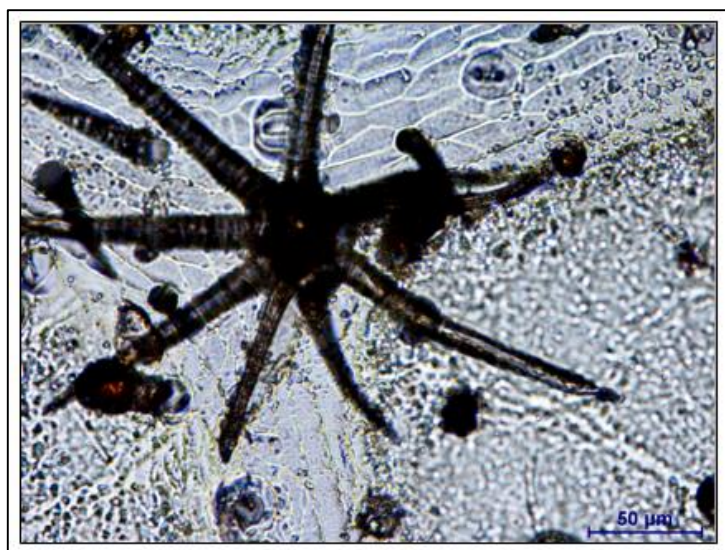


Figure 3.29: Stomata print of a leaf in stage red < 10. Fully developed stomata are located only on a middle vein and veins; A stellate shaped hair is in front (x400).

3.10. Statistical analysis

In detail, redox active compounds (voltammetric potential, some cations and anions) and fluorescence measurements (PEA) were analysed through OPLS-DA (Orthogonal Partial Least Squares Discriminant Analysis) and PCA-X (Principal Component Analysis). The analysis in *Figure 3.30* shows a clustering of the samples green (I-2-a), aging (I-2-b) and developing stages (pale-green (I-1-b) and green-red (I-1-a)).

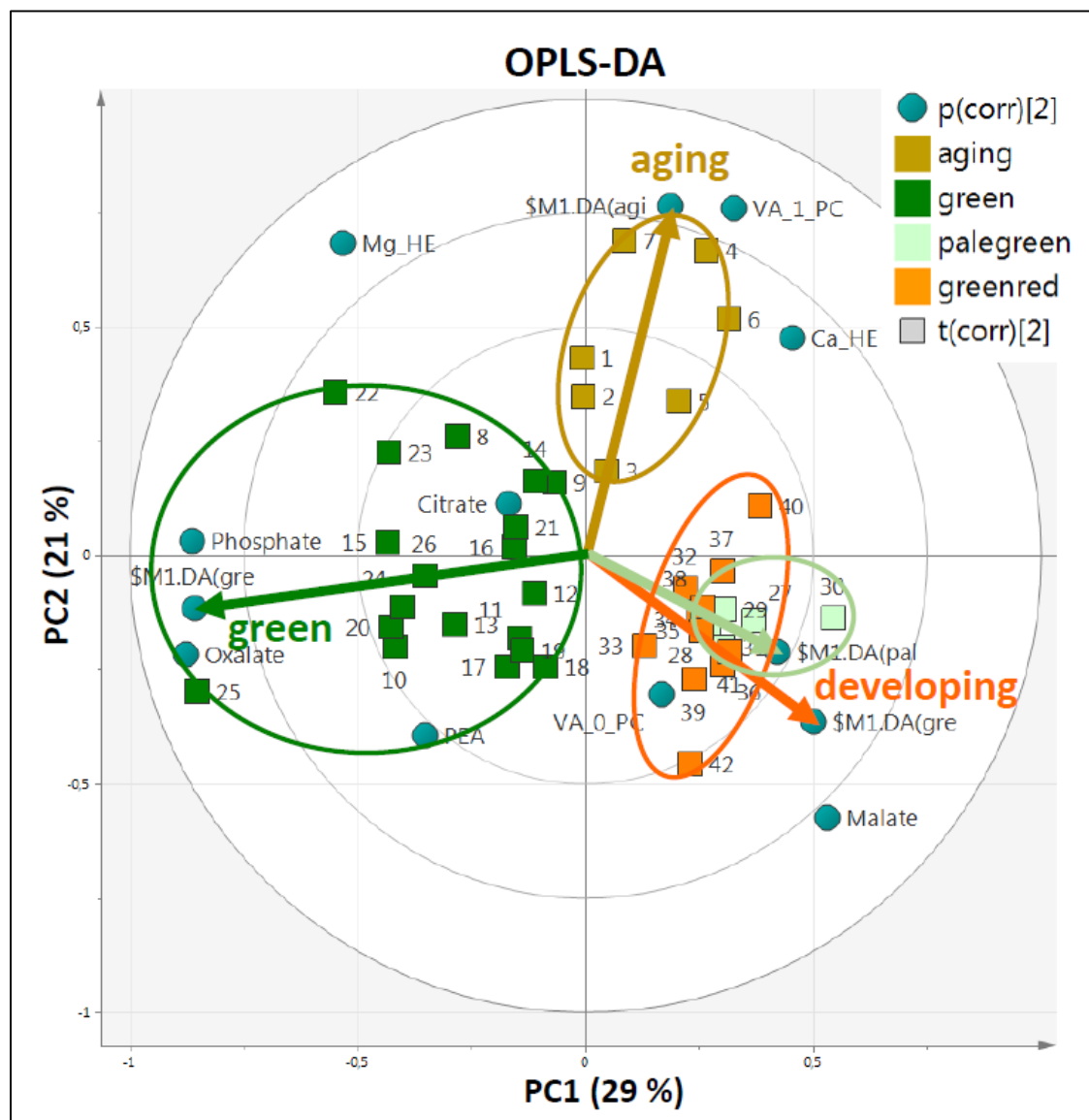


Figure 3.30: OPLS-DA analysis. The axes represent the two principal components (PC1 with 29 % and PC2 with 21 %). Analysis was performed with *statgraphics* and *SIMCA*.

The PCA-X analysis (*Figure 3.31*) shows similar results as these ones of the OPLS-DA, just component two varies about 1 %

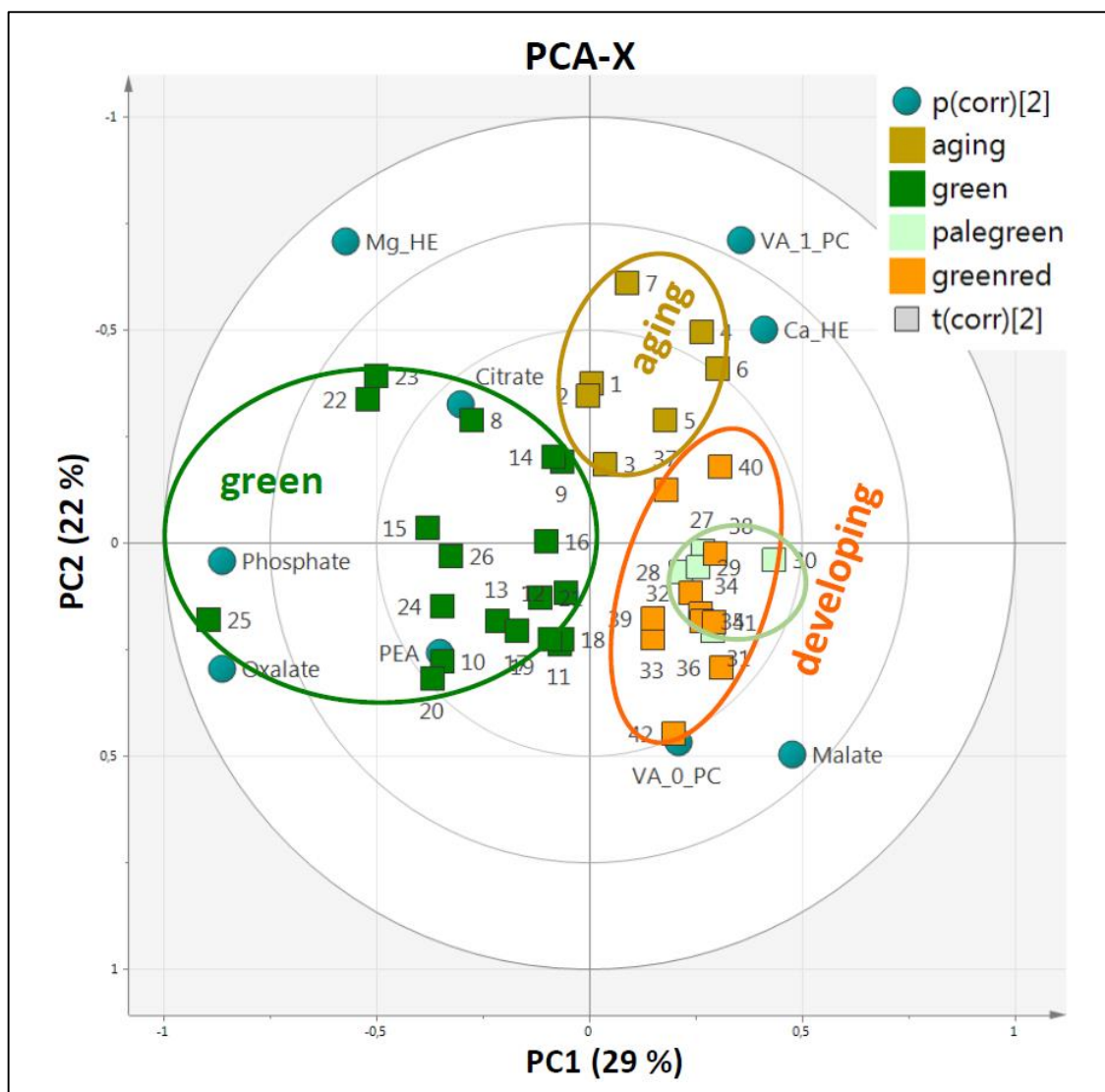


Figure 3.31: PCA-X analysis (PC1 with 29 % and PC2 with 22 %). The same basic pattern of clustering as in OPLS-DA analysis is found. Analysis was performed with statgraphics and SIMCA.

4. DISCUSSION

Fluorescence measurements

With the F_v/F_m values (*Figure 3.3*) and ETR measurements (*Figure 3.4*) a first statement of the constitution of the photosynthetic apparatus could be given. The F_v/F_m values of younger leaves is about 25 % smaller than that one of adult stage I-2-a (green) leaves. Similar, ETR measurements have shown a difference of about 23 %. It is mentionable, that both methods gain equal results. A disadvantage of the ETR measurements is the impracticality of measuring the accurate absorbance of the different leaf developing stages. As written in *chapter 2.4.2.*, the absorbance term ' a ' is within the ETR calculation. Accordingly, the results of the ETR measurements of younger stages in *Figure 3.4* may be even lower. If the absorbance would be smaller, the ETR data of the developing stages would differ even more.

Chlorophyll content and chlorophyll a to chlorophyll b ratio

Cacao leaves synthesize chlorophyll very slowly during their expansion and the major synthesis occurred only after full expansion had been reached. This fact is not typical for temperate plant, in which the chlorophyll content per unit reaches generally a maximum before the leaves are fully developed (BAKER & HARDWICK, 1973). Chlorophyll content could be used as a general indicator of plastid development in cacao. The maximum plastid development follows after the termination of leaf expansion, but not in flushing leaves (BAKER et al., 1975).

Further, HARDWICK & BAKER (1973) measured chlorophyll contents with an *in vivo* spectroradiometer method. They detected a chlorophyll content from 14 to 16 $\mu\text{g}/\text{cm}^2$ of flushing leaves to a maximum of 28 $\mu\text{g}/\text{cm}^2$ in older leaves. Their measured chlorophyll a and b content was increasing linearly in two phases (faster in the developing stage and slowly afterwards). Their calculation of the chlorophyll a : chlorophyll b ratio was maintained constantly at 2.26 ± 0.07 . Accordingly, differences occur during comparison between this computations and the results given in *Figure 3.6*. The total amount of chlorophyll disagrees through various stages. Additionally, a constant chlorophyll a : chlorophyll b ratio during all stages (*Figure 3.8*) was not shown. The percentage of chlorophyll b is higher in the developing stages, this corresponds maybe with the development of the antenna system. The variation can be explained by a work of HALE & ORCUTT (1987). They've assumed that the concentration

of chlorophyll in leaves represents developmental adaption to the environment. Previous studies of cacao have demonstrated a higher concentration of chlorophyll in cacao grown under shaded conditions compared with those ones grown under full sunlight (GUERS, 1974; GALYUON et al., 1996). Significant differences in chlorophyll contents of genotypes grown under identical conditions were also recorded by DAYMOND & HADLEY (2004). According to their data, the variance between the two Criollo trees C1 and C2 shown in *Figure 3.7 (C1 and C2)* fits to this theory.

Due to varied environmental situations data comparison can just be done within trends. These data here are compared in between distinctions of the different developing stages within same environmental conditions, which allows significant conclusions.

The difference in chlorophyll content per square centimetre between samples of developing stages compared to those ones of the green stage is immense (*Figure 3.6*). The total chlorophyll amount varied about the half. There was not observed a linear increase, but an abrupt rose between stage I-1-b (pale-green) and I-2-a (green), which correlates with visual impressions (*Figure 3.2*). At the stage I-1-b the leaves were not elongating any more, but a rapid greening until they were reaching stage I-2-a was visible. BAKER et al. (1975) assumed that chloroplasts of younger stages were still not that large as of the fully green stage.

A correlation between chlorophyll concentration and fluorescence measurements can be found. As mentioned before, no smooth transition between the stages I-1-b (pale-green) and I-2-a (green) was shown. The ETR and PEA data of the developing stages (I-1 and F-2) compared with the adult (green) one shows the same abrupt transition, as the chlorophyll concentrations.

When the leaves have stopped growing and reached the adult leaf stage I-2-a (green), the development of the photosynthetically active apparatus is completed. At 50 % lower chlorophyll concentrations, photosynthetic rates decrease about 25 % or more (due to the absorption factor).

Carotenoids:

BAKER et al. (1975) found in total five different carotenoids, three types of xanthophylls: lutein, neoxanthin, violaxanthin and two carotenes: α -carotene and β -carotene in measurable amounts in cacao leaves via thin layer chromatography. The development of carotenoids proceeded parallel with that one of chlorophyll. BAKER et al. (1975) assumed that both groups are photosynthetic pigments and are intimately associated with the chloroplast lamellae development and the photochemistry of photosynthesis.

In this study only the total amount of carotenoids was measured by photometry. The carotenoid concentrations in *Figure 3.9* is showing the same gain as the chlorophyll concentration (*Figure 3.6*). Especially the disparity between the pale-green stage (I-1-b) and the green stage (I-2-a) could be observed again. Only the carotenoid concentration of stage I-2-b (aging) differs, there the concentration is comparably high to those ones of the developing stages I-1 and F-2. The ratio between carotenoids to chlorophyll (a + b) is shown in *Figure 3.10*. For all stages that ratio is nearly the same value, therefore it can be considered, that the protection function of the photosystems (RICHTER, 1996) as well as capturing blue/green light and passing the energy from carotenoids to chlorophyll (OSTROUMOV et al., 2013) is the same during all stages.

Anthocyanidins:

The protecting function of phenolic compounds, especially anthocyanidins was discussed previously in *chapter 1.3.5*. The anthocyanidin concentration was a newly developed extraction method (described in *chapter 2.8*). Preliminary studies with different extraction solvents (H₂O: MeOH: CH₃COOH, MeOH: CHCl₃:H₂O, MeOH:HCl, MeOH:CH₃COOH and Acetone : H₂O) were not applicable for extraction of anthocyanidins (MeOH is equivalent to methanol). The extraction with 1 N HCl in a warm water bath was the most effective method. A comparative study with different cacao clones in terms of phenolics and anthocyanin concentration in seeds was done by NIEMENAK et al. (2006). They've found two different type of anthocyanidins: cyanidin-3-galactoside and cyanidin-3-arabinoside in cacao seeds with HPLC detection. Similarly for leaves, GRIFFITH (1958) found cyanidin derivatives. According to various methods and wavelength proposals in literature, a full spectral scan was done. The best fitting wavelength for detection of anthocyanidins was at 519 nm. The measured, anthocyanidin

concentrations in leaves (*Figure 3.11*) are showing explicit differences. The anthocyanidin concentration (in mg/cm²) is over 500 times higher in the F-2 (red) stage than in the I-2-a (green) stage. BIEZA & LOIS (2001) assumed that the high amount of anthocyanidins prevents leaf tissue damage from UV radiation. Leaves with high amounts of anthocyanidins as a potent antioxidant (GABRIELSKA et al., 1999) show a higher voltammetric potential (*Figure 3.20*). NEILL et al. (2002) also detected increased voltammetric currents in red leaves compared to green ones in *Elatostema rugosum*. They attribute it to the antioxidant behaviour of anthocyanidins against ROS (reactive oxygen species).

Metabolites from HPLC-UV/VIS and LC-MS/MS:

The HPLC-UV/VIS results are presented in *Table 3.3*. Various **vitexin** (apigenin-8-C-glucoside) derivatives as well **apigenin** derivatives were found. It is noteworthy that they mainly do not occur in the aging leave stage (I-2-b). JALAL & COLLIN (1977) have determined the major flavone in mature cacao leaves to be isovitexin (apigenin-6-C-glucoside). **Cumarinic acid**, **theobromine**, **ferulic acid** were also found what is also described by GRIFFITHS (1958) and JALAL & COLLIN (1977). Several **catechin** (flavan-3-ol) derivatives could be also detected. It has to be mentioned that they were mainly detected in younger stages. OSMAN et al. (2003) concluded that attributed to the high intensity of main catechin-polyphenols (e.g. epicatechin and derivatives), cacao leaves possess a better antioxidative performance than synthetic antioxidants. Their point of view was that specially in aqueous and oil based food applications cacao leaves extracts exhibit the potential to complement or replace synthetic antioxidants.

Several **cyandin** derivatives could be detected (cyandin der. 1 to 4; cyandin-3-O-glucoside). **Procyanidins** (procyanidin B1 and B2 der.) with HPLC-UV/VIS (*Table 3.4*) as well as cyanidin derivatives (cyanidin-5-O-glucoside) and **procyanidins** (procyanidin A2 and B2) with LC-MS/MS (*Table 3.4*). GRIFFITHS (1958) postulated red coloured cyanidin: 3-β-D-galactosidylcyanidin and 3-α-arabinosidylcyanidin (compare NIEMENAK et al., 2006 for seeds).

Only in young leaves **theophylline** (1,3-dimethylxanthine) was found, as well in Criollo cacao beans in high amounts (APGAR & TARKA, 1998). Theophylline causes relaxation of tracheal

smooth muscle and is pharmacologically used to manage asthma (SPILLER, 1998). SOTELO & ALVAREZ (1991) have found theophylline in Criollo leaves, what was in contrast not found by HAMMERSTONE et al. (1993).

Cation and Anion chromatography:

The distribution of nutrient elements varies between plant species and within one plant between different developmental stages as young and old leaves. Especially young leaves feature a high content of nutrients, older leaves often show high amount of less agile elements (e.g. Ca, Cu, B) (FINCK, 1975). These ions are highly responsible for i) the osmotic pressure (turgor) in the plant cell; ii) stabilizing the cell itself; iii) regulating the vacuole; and iv) building up the membrane potential (LÜTTGE & HIGINBOTHAM, 1979; EPSTEIN, 2004).

For further details on ion concentrations cf. MARSCHNER (1995) and EPSTEIN (2004).

Potassium (K^+):

The K^+ -ion is incorporated by plants in high rates. Plants absorb more potassium than any other mineral nutrient with the exception of nitrogen (TISDALE & NELSON, 1975; MÄSER et al., 2002; BRITTO & KRONZUCKER, 2008; SZCZERBA et al., 2008).

The high content of potassium (K^+) in plants is explainable by the unspecific competition with other cations (Na^+ , Mg^{2+} , Ca^{2+}), because K^+ is blocking the takeover. The agility of potassium in the plant is very good (MENGEL, 1984).

There are various functions in the metabolism in which potassium is included. A main character is that K^+ can permeate biological membranes. There is an essential meaning in the water supply (osmosis function, turgor), in the mass transport and as K^+ pump. Plants with a high presence of potassium show a more effective photophosphorylation and photoreduction (PFLÜGLER & MENGEL, 1972). The role of K^+ in photosynthetic ATP and NADPH formation is proved. The essential coenzymes ATP and NADPH are included in various processes. The increase of photosynthetic rate with increased K^+ concentration is based on the reduced CO_2 -resistance of the stomata and leaf tissue and the high activity of the RuBP-carboxylase activity (MENGEL, 1984; MARSCHNER, 1995). Also in enzyme activation, protoplasm swelling regulation

(LARCHER, 2001), charge pattern regulation (NULTSCH, 2000) and protein synthesis potassium plays a major role (MARSCHNER, 1995; EPSTEIN, 2004).

The concentration of potassium in cacao leaves (*Figure 3.14*) is very high compared to other ions. Variations between development stages were only found for stage I-2-b (aging). The reduced potassium content in senescence leaves may be due to the effect that potassium is transported back to living tissue. Also differences in the K^+ -rate between the acid-extracts and the hot-water-extracts were not that immense. So most of potassium seems to be located in living parts of a cell and not in the cell wall.

Ammonium (NH_4^+):

Nitrate and ammonium are the major sources of inorganic nitrogen taken up by the roots of higher plants. Ammonia also can derive from nitrate reduction or N_2 fixation (MARSCHNER, 1995).

Ammonium and its equilibrium partner ammonia ($NH_3 + H_2O \rightleftharpoons NH_4^+ + OH^-$) are toxic at quite low concentrations. The main pathway of detoxification is the formation of amino acids, amines and related compounds. The concentration of ammonium in the cytoplasm should be usually below 15 μM and there is an evidence that substantial amounts of ammonium may be stored in vacuoles. In the vacuoles the low pH prevents formation of ammonia (ROBERTS & PANG, 1992).

The measured NH_4^+ concentration (*Figure 3.14*) is moderate compared to other cation concentrations. The content seems to be quite constant during the development stages of leaves, except for the older stage. Here a little shift to less NH_4^+ concentrations in acid extracts and to higher NH_4^+ concentrations in the hot water extracts is observable.

Magnesium (Mg^{2+}):

The rate of uptake of Magnesium could be strongly depressed by other cations e.g. K^+ , NH_4^+ (KURVITS & KIRKBY, 1980) Ca^{2+} , Mn^{2+} (HEENAN & CAMPBELL, 1981) as well as by H_3O^+ (low pH) (MARSCHNER, 1995).

MENGEL (1984) described that the uptake of magnesium is usually lower than those ones of Ca^{2+} or K^+ , what is also confirmed by data shown in *Figure 3.13*.

The most familiar function of magnesium is certainly its role as a central atom of the chlorophyll molecule. The proportion of total magnesium bound to chlorophyll might even be higher than 50 % under scarce light conditions. As a rule, another 5-10 % of total magnesium in leaves is firmly bound to pectate (salt of the non-esterified pectic acid) or sparingly soluble salts in the vacuole. The remaining part is extractable with water. Magnesium also has an essential function in protein synthesis (MARSCHNER, 1995), as a bridging element for the aggregation of ribosome subunits (CAMMARANO et al., 1972) and the synthesis of RNA (MARSCHNER, 1995). At least 25 % of the total protein in leaf cells is located in chloroplasts. In order to that, deficiency of magnesium particularly affects the size, structure and function of chloroplasts, including electron transfer in photosystem II (McSWAIN et al., 1976). There are many processes of enzymes and enzyme reactions in which magnesium is interacting (e.g. PEP carboxylase) as well for the synthesis of ATP (phosphorylation) as a bridging component between ADP and the enzyme (MARSCHNER, 1995).

The content of magnesium in the samples of *T. cacao* (shown in *Figure 3.15*) is rather low in the developing stages (F-2, I-1). The high content of magnesium in the aging stage (I-2-b) might be attributed to the fact that the chlorophyll is decomposed (leaves were partially yellow), but the magnesium is still present inside the leaf. As already mentioned, potassium might block magnesium. So it might be that the plant first separates the potassium from the aging leaves and then the other nutrients are following succeedingly.

Calcium (Ca^{2+}):

Most plants have a low Ca^{2+} uptake, even at high concentrations in the soil. By cations like NH_4^+ , K^+ , Na^+ and Mg^{2+} the uptake of Ca^{2+} can be inhibited, therefore it can be interpreted as

the antagonist of K^+ and Mg^{2+} in cell sap (MENGEL, 1984). The mobilization of Ca^{2+} from older leaves to support the growth of roots doesn't follow that rule, because it is barely transported in the phloem but mainly with the transpiration stream. Four main functions of Calcium are described by BANGERTH (1979): it is i) stabilizing the cell wall and phospholipid membranes; ii) involved in construction of cell walls; iii) influencing enzymes as e.g. activator; iv) a part of some hormone reactions; v) charging pattern regulating (NULTSCH, 2000); and finally vi) regulating the degree of swelling (LARCHER, 2001; FINCK, 1975).

Cacao can accumulate high amounts of calcium oxalate in the stem (CEITA et al., 2007). Some crystals have been found in some leaf cuttings, it is estimated that they consist of calcium-oxalate. *Figure 3.16* shows the low availability of 'free' calcium. The distribution over all stages in the HE is moderately homogenous. An enormous amount of calcium was detected in acid extracts leaves of the aging stage. The main part of the Ca^{2+} in leaves seems to be bound in the cell walls.

Anions:

The largest anion concentrations accounted to nitrate (NO_3^-) followed by oxalic acid and malic acid (*Figure 3.17*).

Nitrate (NO_3^-):

As mentioned before, nitrate and ammonium are the major ion species of inorganic nitrogen uptake up by the roots of higher plants (MARSCHNER, 1995; EPSTEIN, 2004).

Nitrate is rather mobile in the xylem and can be stored. The accumulation of nitrate in vacuoles is of considerable importance for cation-anion balance and for osmoregulation. For fulfilling its essential functions as a plant nutrient, nitrate has to be reduced to ammonia (MARSCHNER, 1995).

Oxalic acid (C₂H₂O₄):

With increasing calcium supply the proportion of calcium oxalate increases in many plant species. Synthesis of oxalic acid for charge compensation in nitrate reduction and precipitation as calcium oxalate are common in plants (MARSCHNER, 1995). It is also found as membrane-bound crystals of the calcium salt or pectate salt (LÜTTGE & HIGINBOTHAM, 1979).

It is discussed that the oxalate-bound calcium might represent the dominant binding form of calcium (MARSCHNER, 1995).

The results in *Figure 3.18* are showing a high oxalic acid concentration in the green stage (I-2-a). In the other stages, developing and aging, the level seems to be fairly constant.

Malic acid (C₄H₆O₅):

Malate is acting as counter ion for cations in the vacuole. It is one of the acids which is built up in the citrate cycle. Another way of malate synthesis is possible during CO₂ fixation in the C₄ (carbon fixation with C₄) or CAM (Crassulacean acid metabolism) plants in the Calvin-Benson-cycle from oxaloacetate.

The measured concentrations of malic acid are shown in *Figure 3.18*. The concentration in the developing stages (F-2 till I-1-b (pale-green)) is higher than in the adult cacao leaf stage I-2-a (green). A possible hypothesis for high amounts of malic acid in the younger stages could be that cacao uses it during this phase as i) counter ion; ii) due to the lack of photosynthesis more dissimilation occur in the tissue; and/or as pure speculation iii) cacao changes its metabolism from C₃ metabolism to CAM. The last argument is supported of results from ABO-HAMED et al. (1983), which show that stomata of cacao leaves are built up late to restrict water loss.

Phosphoric acid (H₃PO₄):

Phosphorus is mainly uptaken by plants as H₂PO₄⁻ (depending on the pH). It is incorporated for example into organic compounds as nucleic acids (e.g. DNA and RNA), is bound to sugars (sugar phosphates) or builds the energy-rich molecule ATP. It is documented that plants which are suffering from phosphorus deficiency have a reduced leaf expansion and a lower number of

leaves, but the content of chlorophyll still remains constant. Nevertheless, under phosphorus deficiency the photosynthetic efficiency per chlorophyll unit is much lower (MARSCHNER, 1995). The content of phosphoric acid is demonstrated in *Figure 3.18*. The content of phosphorus is higher in the older adult leaves (green and aging) than in the younger ones.

Sulphate (SO_4^{2-}):

Atmospheric SO_2 is uptaken by the aerial parts of higher plants, but the most important source of sulphur is sulphate (SO_4^{2-}) absorption by roots. A reduction of sulphur is necessary for the incorporation into amino acids, proteins and coenzymes. Sulphate can also be utilized without reduction into essential organic structures e.g. sulpholipids in membranes (MARSCHNER, 1995). Sulphur is also responsible for protein-transforming disulfid bridges to stabilize conformation (NULTSCH, 2000). Sulphur deficiency can have severe influence on different plant features (MARSCHNER, 1995).

The sulphate concentrations which were measured for different cacao leaf stages are shown in *Figure 3.19*. The content of sulphate is quite low in both the developing stages and the green stage compared to these ones of the aging leaves. It could be assumed that sulphate is accumulating during leaf life. Sulphate might also be a counter ion for different substances in the aging stage.

Organic acids and carbonic acids:

Various organic acids (e.g. malic-, citric-, oxalic acid) are found in long distance transfer in phloem sap for utilizing sugars in small amount. For short and medium transport they occur either across membranes or via plasmodesmata. Plant tissue could be strongly acidic due to the accumulation of malic, citric, or other organic acids intermediates in the Krebs cycle. In addition, NO_3^- reduction to NH_3 cause problems of pH regulation in cells. With the concomitant of CO_2 dark fixation and formation of dicarboxylic acids – as malic acid – the problem of pH regulation during NO_3^- reduction is solved (SMITH & RAVEN, 1976). Furthermore such organic acids feature a high ability to complex ions (e.g. citric-, malic acid) and shuttle them more easily through membranes.

Carbonic acids, particularly phenylpropanoic acids as cinnamic-, p-cumaric-, caffeic- and ferulic acid, but also vanillic-, p-hydroxybenzoic-, quinic acid and many more arrive from the shikimat pathway. Their common property as organic acids is the remobilisation of ions from soil and between cells. These carbonic acids are ion sequestrates and further could be transferred into chinoid structures, which are important in redox reactions for balance of membranes and in cells itself (SCHLEE, 1986).

Chloride:

Cl⁻ is one of the abundant ions as K⁺ and Na⁺. It has a high influx in plasmalemma and tonoplast (LÜTTGE, 1973). Chloride is further in close correlation with photosynthetic CO₂ fixation. It also regulates stomata closing by stomata-vacuole outflow of Cl⁻ to decrease membrane potential (LÜTTGE & HIGINBOTHAM, 1979). Free available chloride (*Figure 3.19*) was detected in higher amounts in the younger stages.

General, remobilization of mineral nutrients from and into plant tissue occurs simultaneously during plant life span. In aging (senescing) leaves, as a rule, higher rates of export of mineral nutrients than rates of import are associated (S.107, MARSCHNER, 1995).

Anatomical studies:

Leaf hairs

Red pigmented leaves are at both leaf surfaces equipped with numerous hairs. ABO-HAMED et al. (1983) described four different main types of hairs:

- short stubby hairs (most of them)
- hairs with a red rounded multicellular head
- larger hairs as the former one, with a larger column and a larger red multicellular head and thin-walled single-celled pointed structures
- stellate shaped hairs (less frequent)

These types of hair are quite common for the family Malvaceae (METCALFE & CHALK, 1950). All four types were present in the young leaves and build a dense cover. During leaf expansion the density reduces, for the older stages only the stellate hairs and the shorter, stubby hairs were found (ABO-HAMED et al., 1983). The anatomical studies of cacao in this work have shown the same species of hairs (*Figure 3.25 and Figure 3.26*).

Stomata count:

The stomata of *T. cacao* are only present at the lower surface of the leaves (METCALFE & CHALK, 1950; HARDWICK et al., 1981; ABO-HAMED et al., 1983). They reported that at young, 4 days old flushed leaves fully developed stomata were located mainly at the mid-ribs and some were found at the primary lateral and minor veins. Visual observations, determination of stomatal number and density and width and length studies of the stomatal pore were made by ABO-HAMED et al. (1983). They found some correlations with the stomatal number and pattern of development with the leaf age. As a result they figured out that the transpiration loss via stomata in young leaves is low.

Indeed, also in the young stage (F-2-a, red < 10) stomata only could be found along veins (*Figure 3.29*). In stage F-2-b (red > 10) the increased number of stomata per area was counted (*Figure 3.27*) and during leaf development the number of stomata per square centimetre decreases (*Figure 3.28*). Subsequently, stomata are developed in F-2-b stage and with growing intercostal cells the stomata number decreases by square centimetre.

Statistical analysis

In *Figure 3.30* results from OPLS-DA method are shown. The arrowheads signal the centre of the discriminant functions for each special stage. A clustering of the stages green, aging and development is shown. The developing stages, here pale-green and green-red are assembled together. The vectors of phosphate, oxalate and the PEA are grouping the stage green (I-2-a). For the stage aging (I-2-b) the vectors calcium as well the voltammetric potential of 750 mV (VA_1_PC) are determining factors. The young leaves are batched via malate and the voltammetric potential till 750 mV. The vector magnesium is important for green and aging

stages, because at the opposite side of the developing stages magnesium was found. In total, different redox active compounds seem to be active (*Figure 3.20* and *Figure 3.21*).

Similar results are shown for OPLS-DA and PCA-X (*Figure 3.31*), for the clustering main diagnosing variables were chosen. In total, the photosynthetic performance is decreasing in the aging stage, Ca^{2+} is cumulating during leaf life and different redox active substances are important. The stage green is distinguished by phosphate, oxalate and a high photosynthetic performance. In the developing stages, mainly malate and other different redox active substances are respectable.

Conclusions:

In summary, the youngest stage (F-2-a, red < 10 cm) possess stomata only at the main, mostly green veins (*Figure 3.29*). The number of stomata per area (*Figure 3.27*) of stage F-2-b (red > 10 cm) is higher than these ones in the older stages. The stomata seem to evolve in the stage F-2-b. It could be estimated that the intercostal cells grow in between the stomata cells during aging processes (*Figure 3.28*). It is assumed that later on no further stomata are built up. The hairs (*Figure 3.25* and *Figure 3.26*) that were only present in younger stages possess partial anthocyanin colouration and allow therefore protection against UV-light for young leaves, as well transpiration (HARDWICK et al., 1981; ABO-HAMED et al., 1983) and maybe herbivory. Hypotheses regarding the high amounts of malic acid (*Figure 3.18*) in the younger stages are that cacao plants use malic acid during this phase as i) counter ion; ii) due to the lack of photosynthesis more dissimilation occur in the tissue; and/or as pure speculation iii) cacao changes its metabolism from C3 metabolism to CAM. The last argument is supported by results of ABO-HAMED et al. (1983), which show that stomata of cacao leaves are built up late to restrict water loss. The vertically hanging and soft leaves (without fully developed cuticula) have demonstrative high amounts of anthocyanidines (*Table 3.3*), catechines (*Table 3.3*) and theobromine (*Table 3.3* and *Table 3.4*). These substances possess a high antioxidant potential and gaining an UV- and light-stress and ROS protection (BIEZA & LOIS, 2001) of the partially developed leaves of this rainforest shadow plant. Also the different redox potentials (voltammetric measurements; *Figure 3.20*, *Figure 3.21* and *Figure 3.31*) from young to old leaves are supporting this theory. From the young leaves it is estimated that the photosynthetic apparatus is not fully developed, but the carotenoids to chlorophyll (a + b) ratio is nearly equal

at all stages (*Figure 3.10*). Consequently, the same amount of carotenoids per chlorophyll (a + b) molecule is nearly identical over all periods of the development. One of the various functions of carotenoids is the reduction of excited singlet oxygen. The antioxidant function and protection of the light harvesting systems by carotenoids seems to stay constant for all leaf ages. So the other antioxidant protection in older leaves is mainly done by flavonoids and epicatechines, as well in the younger ones with anthocyanidines, catechines and theobromine. The contents of magnesium (*Figure 3.15 and Figure 3.31*), oxalic acid (*Figure 3.18 and Figure 3.31*) and phosphoric acid (*Figure 3.18 and Figure 3.31*) are higher in the full developed stage I-2-a (green). These components indicate the maturation of leaves due to their function in metabolism. Therefore it can be postulated that the photosynthetic apparatus fully works and is supported by F_v/F_m (*Figure 3.3*) values which show 25 % higher rates than these ones of younger leaves. This is also indicated by the same gain in the ETR measurements (*Figure 3.4*). At this stage I-2-a (green) the leaf changes the position from vertically to horizontally, from soft to stiff and is protected by a thick cuticula.

5. OUTLOOK

Further measurements GC-MS (gas chromatography coupled with mass spectrometry) are planned with the same plant material. Together with the already performed LC-MS/MS measurements a good overview of different metabolites during the developing stages could be given. The internal server for labelling metabolites from LC-MS/MS measurements is still under construction. This tool would provide an exceeding detection of metabolites. Measurements of shotgun proteomics were done with most of the samples, the results still have to be analysed and interpreted.

Additional studies using the same methods within other species from cacao, which are cultivated in our greenhouse, are planned. Especially the relatively high amount of malate during developing stages should be studied in more detail.

6. ABSTRACT

6.1. Abstract (English)

Theobroma cacao L. (Malvaceae) is one of the most important crops worldwide, in the season 2013/14 about 4.16 million tons of cacao seeds were harvested (ICCO, 2013).

The intention of this study is to give an overview of photosynthetic performance (fluorescence measurements, PEA and Imaging PAM) as well to demonstrate changes in metabolites (HPLC-UV/VIS, LC/MS/MS, Cation and Anion chromatography, Voltammetry) during leaf development of two *Theobroma cacao* Criollo hybrids. Additionally, photometric measurements were done to determine contents of chlorophyll a, chlorophyll b, carotenoids and anthocyanidins. In particular, a new method is introduced for the extraction and detection of anthocyanidins.

Main differences during the stages of development could be shown by various analytic methods. Photosynthetic performance of fully green leaves is enhanced compared to developing stages. The same result was found for the concentration of chlorophyll molecules per leaf area. High amounts of magnesium, phosphate, oxalic acid and citrate were detected in adult, green leaves.

Higher values of anthocyanidins, malate and an increased voltammetric potential were discovered in younger stages. Furthermore stomata number per area was increased and a dense cover of trichomes could be shown via anatomical cuttings of early stages.

6.2. Zusammenfassung (Deutsch)

Die Kulturpflanze *Theobroma cacao* L. (Malvaceae) wird zu den wichtigsten der Welt gezählt. Es wird geschätzt, dass in der Saison 2013/14 in etwa 4.16 Millionen Tonnen Kakaosamen geerntet wurden (ICCO, 2013).

Diese Studie soll einen Überblick über die Photosyntheseaktivität (Fluoreszenzmessungen mittels PEA und Imaging PAM) sowie die Änderungen von Metaboliten (HPLC-UV/VIS, LC/MS/MS, Kationen- und Anionenchromatographie, Voltammetrie) während der Blattentwicklung von zwei *Theobroma cacao* Criollo Hybriden geben. Des Weiteren wurden photometrische Messungen zur Ermittlung des Gehaltes von Chlorophyll a, Chlorophyll b, Carotinoiden und Anthocyanidinen durchgeführt. Eine Errungenschaft stellt die neue Methode zur Extraktion und Detektion von Anthocyanidinen dar.

In den verschiedenen Blattentwicklungsstufen konnten zahlreiche Unterschiede mittels mehrerer Analysemethoden aufgezeigt werden. Die photosynthetischen Leistungen von grünen, ausgewachsenen Blättern sind im Vergleich zu denen jüngerer Blättern deutlich gesteigert. Ebenso war der Chlorophyllgehalt pro Flächeneinheit erhöht, des Weiteren konnten höhere Konzentrationen an Magnesium, Phosphat, Oxalsäure und Citronensäure detektiert werden.

Erhöhte Werte von Anthocyanidinen und Malat sowie ein erhöhtes voltammetrisches Potential wurden in jüngeren Blättern gemessen. Eine gesteigerte Anzahl an Stomata pro Flächeneinheit wurde ermittelt. Ein dichter Haarmantel an jungen Blättern konnte mittels anatomischen Schnitten gezeigt werden.

7. REFERENCES

- ABO-HAMED S., COLLIN H.A., HARDWICK K. (1983): Biochemical and physiological aspects of leaf development in cocoa (*Theobroma cacao* L.) – Growth, Orientation, Surface structure and water loss from developing flush leaves. *New Phytol.* (1983) **95**: 9-17.
- ALMEIDA A.-A.F. DE & VALLE R.R. (2008): Ecophysiology of the cacao tree. *Braz. J. Plant Physiol.* (2008) **19** (4): 425-448.
- APGAR J.L. & TARKA S.M.Jr. (1998): Methylxanthine Composition and Consumption Patterns of Cocoa and Chocolate Products. In: SPILLER G.A. (1998): Caffein, *CRC Press LCC*, US: 179.
- ARGOUT X., FOUET O., WINCKER P., GRAMACHO K., LEGAVRE T., SABAU X., RITERUCCI A.M., DA SILVA C., CASCARDO J., ALLEGRE M., KUHN D., VERICA J., COURTOIS B., LOOR G., BABIN R., SOUNIGO O., DUCAMP M., GUILTINAN M.J., RUIZ M., ALEMANNIO L., MACHADO R., PHILLIPS W., SCHNELL R., GILMOUR M., ROSENQUIST E., BUTLER D., MAXIMOVA S., LANAUD C. (2008): Towards the understanding of the cocoa transcriptome: Production and analysis of an exhaustive dataset of ESTs of *Theobroma cacao* L. generated from various tissues and under various conditions. *BMC Genomics* (2008) **9**: 512.
- ARGOUT X., SALSE J., AURY J.M., GUILTINAN M.J., DROC G., GOUZY J., ALLEGRE M., CHAPARRO C., LEGAVRE T., MAXIMOVA S.N., ABROUK M., MURAT F., FOUET O., POULAIN J., RUIZ M., ROGUET Y., RODIER-GOUD M., BARBOSA-NETO J.F., SABOT F., KUDRNA D., AMMIRAJU J.S.S., SCHUSTER S.C., CARLSON J.E., SALLET E., SCHIEX T., DIEVART A., KRAMER M., GELLEY L., SHI ZI, BÉRARD A., VIOT C., BOCCARA M., RISTERUCCI A.M., GUIGNON V., SABAU X., AXTELL M.J., MA Z., ZHANG Y, BROWN S., BOURGE M., GOLSER W., SONG X., CLEMENT D., RIVALLAN R.1, TAHI M., AKAZA J.M., PITOLLAT B., GRAMACHO K., D'HONT A., BRUNEL D., INFANTE D., KEBE I., COSTET P., WING R., MCCOMBIE W.R., GUIDERDONI E., QUETIER F., PANAUD O., WINCKER P., BOCS S. & LANAUD C. (2011): The genome of *Theobroma cacao*. *Nature Genetics* (2011) **43** (2).
- BANGERTH F. (1979): Calcium-related physiological disorders of plants. *Annu. Rev. Phytopathol.* (1979) **17**: 97-122.
- BAKER N.R. & HARDWICK K. (1973): Biochemical and physiological aspects of leaf development in cocoa (*Theobroma cacao*) I. Development of chlorophyll and photosynthetic activity. *New Phytol.* (1973) **72**: 1315-1324.

- BAKER N.R., HARDWICK K., JONES P. (1975): Biochemical and physiological aspects of leaf development in cocoa (*Theobroma cacao*) II. Development of chloroplast ultrastructure and carotenoids. *New Phytol.* (1975) **75**: 513-518.
- BIEZA K. & LOIS R. (2001): An Arabidopsis Mutant Tolerant to Lethal Ultraviolet-B Levels Shows Constitutively Elevated Accumulation of Flavonoids and Other Phenolics. *Plant Physiology* (2001) **126**: 1105-1115.
- BJÖRKMAN O. & DEMMIG B. (1987): Photon yield of O₂ –evolution and chloroplast fluorescence characteristics at 77 K among vascular plants of diverse origins. *Planta* (1987) **170**: 489-504.
- BRITTO D.T. & KRONZUCKER H.J. (2008): Cellular mechanisms of potassium transport in plants. *Physiol. Plant* (2008) **133**: 637-650.
- CALDWELL M.M. (1981): Plant responses to ultraviolet radiation. Physiological ecology I. *Encyclopedia of plant physiology series II: Springer-Verlag*, Heidelberg, Germany: 170-197.
- CAMMARANO P., FELSANI A., GENTILE M., GUALERZI C., ROMEO C., WOLF G. (1972): Formation of active hybrid 80-S particles from subunits of pea seedlings and mammalian liver ribosomes. *Biochem. Biophys. Acta* (1972) **281**: 625-642.
- CAMPBELL N.A., REECE J.B., URRY L.A., CAIN M.L., WASSERMAN S.A., MINORSKY P.V., JACKSON R.B. (2009): Biologie. *Pearson*, München, Germany.
- CEITA G.O., MACÊDO J.N.A., SANTOS T.B., ALEMANNO L., Da SILVA GESTEIRA A., MICHELI F., MARIANO A.C., GRAMACHO K.P., Da COSTA SILVA D., MEINHARDT L.W., MAZZAFERA P., PEREIRA G.A.G., De MATTOS CASCARDO J.C. (2007): Involvement of calcium oxalate degradation during programmed cell death in *Theobroma cacao* tissues triggered by the hemibiotrophic fungus *Moniliophthora perniciosa*. *Plant Science* (2007) **173**: 106–117.
- COE S.D. (1994): America's First Cuisines. *University of Texas Press*, U.S.
- COE S.D. & COE M.D. (1996): The true history of chocolate. *Thames and Hudson*, London, U.K.
- COLOMBO M.L., PINORINI-GODLY M.T., CONTI A. (2012): Botany and Pharmacognosy of the Cacao Tree. In: PAOLETTI R., POLI A., CONTI A., VISIOLI F. (2012): Chocolate and health. *Springer-Verlag Italia*: 42pp.
- COOK N.C. & SAMMAN S. (1996): Flavonoids – Chemistry, metabolism, cardioprotective effects, and dietary sources. *Nutritional Biochemistry* (1996) **7**: 66-76.

- CUATRECASAS J. (1964): Cacao and its allies: A taxonomic revision of the genus *Theobroma*. *United States national museum Volume 35 (6)*: 379-614. In: *Systematic Plant Studies (1964)* – Smithsonian Institution Press, Washington D.C., U.S.
- DAVIES K.M. & SCHWINN K.E. (2006): Molecular biology and biotechnology of flavonoid biosynthesis. In: ANDERSON O.M., MARKHAM K.R. (2006): Flavonoids. Chemistry, Biochemistry and application. *CRC Press, Taylor & Francies Group (2006)*: 143-218.
- DAYMOND A.J. & HADLEY P. (2004): The effects of temperature and light integral on early vegetative growth and chlorophyll fluorescence of four contrasting genotypes of cacao (*Theobroma cacao*). *Ann. Appl. Biol. (2004)* **145**: 257-262.
- DELZENNE N.M. (2001): Le chocolat, un remède ancien remis au goût du jour. *Journal de Pharmacie de Belgique (2001)* **56 (5)**: 119-124. In: SCHAARSCHMIDT C. (2008): Theobromin – Zur Geschichte und Gegenwart eines Wirkstoffs. *Ludwig-Maximilians-Universität München (2008)*.
- DILLINGER T.L., BARRIGA P., ESCÁRCEGA S., JIMENEZ M., SALAZAR LOWE D., GRIVETTI L.E. (2000): Food of the Gods: Cure for Humanity? A Cultural History of the Medicinal and Ritual Use of Chocolate. *Journal of Nutrition (2000)* **130**: 2057-2072.
- DÖRFLER H. (2011): Comparative metabolic studies in *Arabidopsis thaliana* via GC-MS and LC-MS. *Diplomarbeit Universität Wien*.
- EPSTEIN E. & BLOOM A.J. (2004): Mineral Nutrition of Plants: Principles and Perspectives. Sunderland MA: *Sinauer Association*.
- ESAKI S., TANAKA R., KAMIYA S. (1983): Structure-Taste Relationships of Flavanone and Dihydrochalcone Glycosides Containing (1 → 2) Linked Disaccharides. *Agric. Biol. Chem. (1983)* **47 (10)**: 2319-2328.
- FAO (2003): Food and Agriculture Organization www.fao.org.
- FINCK A. (1975): Pflanzenernährung in Stichworten. *Verlag Ferdinand Hirt*, Kiel, Germany.
- GABRIELSKA J., OSZMIANŚKIB J., KOMOROWSKAC M., LANGNER M. (1999): Anthocyanin Extracts with Antioxidant and Radical Scavenging Effect. *Z. Naturforsch. (1999)* **54c**: 319 -324.
- GENTY B., BRIANTAIS J.M., BAKER N.R. (1989): The relationship between the quantum yield of photosynthetic electron transport and quenching of chlorophyll fluorescence. *Biochim Biophys. Acta (1989)* **990**: 87-92.

- GITZ D.C. & BAKER J.T. (2009): Methods for Creating Stomatal Impressions Directly onto Archivable. *Agronomy Journal* (2009) **101** (1): 232-236.
- GOVINDJEE (1995): Sixty-three years since Kautsky: Chlorophyll a fluorescence. *Aust. J. Plant Physiol.* (1995) **22**: 131-160.
- GOVINDJEE (2004): Chlorophyll a Fluorescence: A Bit of Basics and History. In: GOVINDJEE, PAPAGEORGIOU G.C. (2004) Chlorophyll a Fluorescence: A Signature of Photosynthesis. *Springer, Netherlands*: 1-42.
- GRAZIANO M.M. (1998): Food of the Gods as Mortals' medicine: The uses of chocolate and cocoa products. *Pharmacy in History* (1998) **40**: 132-146.
- GREATHOUSE D.C., LAETSCH W.M., PHINNEY B.O. (1971): The shoot growth rhythm of a tropical tree *Theobroma cacao*. *American Journal of Botany* (1971) **58**: 281-286.
- GRIFFITHS L.A. (1958): Phenolic Acids and Flavonoids of *Theobroma cacao* L. Separation and Identification by Paper Chromatography. *Biochem. J.* (1958) **70** (1): 120-125.
- GRIVETTI L.E. & SHAPIRO H.-Y. (2009): Chocolate: History, Culture, and Heritage. *John Wiley & Sons*, New Jersey, U.S.
- GALYUON I. K.A., McDAVID C.R., LOPES F.B., SPENCE J.A. (1996): The effects of irradiance level on cocoa (*Theobroma cacao* L.): gas exchange and chlorophyll fluorescence. *Tropical Agriculture* (1996) **73**: 29-33.
- GUERS J. (1974): Influence des conditions d'éclairement et de temperature sur la teneur en chlorophylles et l'activité photosynthétique des feuilles de cacaoyer. *Café, Cacao, Thé* **18**: 157-166. In: DAYMOND A.J., HADLEY P. (2004): The effects of temperature and light integral on early vegetative growth and chlorophyll fluorescence of four contrasting genotypes of cacao (*Theobroma cacao*). *Ann. Appl. Biol.* (2004) **145**: 257-262.
- HÄDER D. P. & TEVINI M. (1987): General Photobiology. Pergamon Press, Oxford, U.K.
- HALE M.G. & ORCUTT D.M. (1987): The Physiology of Plants Under Stress. *Wiley & Sons*, New York U.S.: 206pp.
- HAMMERSTONE JR J.F., ROMANCZYK JR L.J. and AITKEN W.M. (1993): Purine Alkaloid Distribution Within *Herrania* and *Theobroma*. *Phytochemistry* (1994) **35** (5): 1237-1240.
- HANSATECH INSTRUMENTS Ltd. (2014): permission to use this information is courtesy of Hansatech Instruments Ltd. (www.hansatech-instruments.com)

- HARBORNE J.B. (1965): Flavonoids: distribution and contribution to plant colour. In: GOODWIN T.W. (1965): Chemistry and biochemistry of plant pigments. *Academic Press*, London, U.K.: 247-278.
- HARBORNE J.B. (1967): The anthocyanins pigments. In: Comparative biochemistry of the flavonoids. *Academic Press Inc.*, London: 1-36pp.
- HARBORNE J.B. (1973): Phytochemical Methods. *Chapman & Hall*, London, U.K.
- HARBORNE J.B. (1991): Flavonoid pigments. In: ROSENTHAL G.A. & BERENBAUM M.R. (1991): Herbivores: Their interaction with secondary plant metabolites. *Academic Press*, San Diego, U.S.: 389-429.
- HARDWICK K. & BAKER N.R. (1973): In vivo measurement of chlorophyll content of leaves. *New Phytol.* (1973) **72**: 51-54.
- HARDWICK K., BAKER N.R., BIRD K.J. (1981). Control of chloroplast formation and photosynthetic performance in developing cocoa (Var Amelanado and Amazon) leaves. *Proceedings 7th International Cocoa Research Conference*, Douala, Cameroon. In: ABO-HAMED S., COLLIN H.A., HARDWICK K. (1983): Biochemical and physiological aspects of leaf development in cocoa (*Theobroma cacao* L.) – Growth, Orientation, Surface structure and water loss from developing flush leaves. *New Phytol.* (1983) **95**: 9-17.
- HEENAN D.P. & CAMPBELL L.C. (1981): Influence of potassium and manganese on growth and uptake of magnesium by soybeans (*Glycine max* (L.) Merr. Cv Bragg). *Plant Soil* (1981) **61**: 447-456.
- HENDERSON J.S., JOYCE R.A., HALL G.R., HURST W.J., McGOVERN P.E. (2007): Chemical and archaeological evidence for the earliest cacao beverages. *PNAS* (2007) **104** (48): 18937-18940.
- HESSE M., MEIER H., ZEEH B. (1995): Spektroskopische Methoden in der organischen Chemie *Georg Thieme Verlag*, Stuttgart, Germany: 1-26.
- HURST W.J., TARKA S.M., POWIS T.G. VALEDZ F., HESTER T.R. (2002): Cacao usage by the earliest Maya civilization. *Nature* (2002) **418**: 289-290.
- ICCO (2006): permission to use this picture is courtesy of the International Cocoa Organization (www.icco.org)
- ICCO (2013): International Cocoa Organization; www.icco.org.
- JALAL M.A.F. & COLLIN H.A. (1977): Polypehnnols of mature plant, seedling and tissue cultures of *Theobroma cacao*. *Phytochemistry* (1977) *Pergamon Press*, U.K. **16**: 1377-1380.

- JANZEN D. (1979): New horizons in the biology of plant defenses. In: ROSENTHAL G.A. & BERENBAUM M.R. (1991): Herbivores: Their interaction with secondary plant metabolites. Vol I. *Academic Press*, San Diego, U.S.
- KIRK J.T.O. & ALLEN R.L. (1965): *Biochem. Biophys. Res. Commun.* (1965) **21**: 523-530.
- KURVITS A. & KIRKBY E.A. (1980): The uptake of nutrients by sunflower plants (*Helianthus annuus*) growing in a continuous flowing culture system, supplied with nitrate or ammonium as nitrogen source. *Z. Pflanzenernähr. Boden.* (1980) **143**: 140-149.
- LACHENAUD P., MOOLEEDHAR V., COUTURIER C. (1997): Les cacaoyers spontanés de Guyane. Nouvelles prospections. *Plant. Rech. Dévelop.* (1997) **4**: 25-30.
- LARCHER W. (2001): Ökophysiologie der Pflanzen: Leben, Leistung und Streßbewältigung der Pflanzen in ihrer Umwelt. *UTB*, Stuttgart, Germany.
- LC RESOURCES (2005): permission to use this picture is courtesy of LC RESOURCES (www.lcresources.com)
- LEE D.W., BRAMMEIER S., SMITH A.P. (1987): The Selective Advantages of Anthocyanins in Developing Leaves of Mango and Cacao. *Biotropica* (1987) **19** (1): 40-49.
- LEVIN D.A. (1971): Plant phenolics: an ecological perspective. *Amer. Nat.* (1971) **10**: 157-181.
- LINDOO S.J. & CALDWELL M.M. (1978): UV-B radiation induced inhibition of leaf expansion and promotion of anthocyanin production. Lack of involvement of the low irradiance phytochrome system. *Plant Physiol.* (1978) **61**: 278-282.
- LOVELOCK C.E., KURSAR T.A., SKILLMAN J.B., WINTER K. (1998): Photoinhibition in tropical forest understorey species with short- and long-lived leaves. *Functional Ecology* (1998) **12**: 553-560.
- LÜTTGE U. (1973): Stofftransport der Pflanzen. *Springer-Verlag*, Heidelberger Taschenbücher, Germany.
- LÜTTGE U. & HIGINBOTHAM N. (1979): Transport in Plants. *Springer Verlag*, New York (U.S.), Heidelberg, Berlin, Germany.
- LÜTTGE U., KLUGE M., THIEL G. (2010): Botanik – Die umfassende Biologie der Pflanzen *WILEY-VCH Verlag GmbH & Co. KGaA*, Weinheim, Germany: 190pp.
- MARI A., LYON D., FRAGNER L., MONTORO P., PIACENTE S., WIENKOOP S., EGELHOFER V., WECKWERTH W. (2013): Phytochemical composition of *Potentilla anserina* L. analyzed by an integrative GC-MS and LC-MS metabolomics platform. *Metabolomics* (2013) **9**:599–607

- MÄSER P., GIERTH M., SCHROEDER J.I. (2002): Molecular mechanisms of potassium and sodium uptake in plants. *Plant Soil* (2002) **247**: 43-54.
- McCLURE J.W. (1975): Physiology and functions of flavonoids. In: HARBORNE J.B., MABRY T.J., MABRY H. (1975): The flavonoids. *Chapman and Hall*, London, U.K.: 971-1055.
- McSWAIN B.D., TSUJIMOTO H.Y., ARNON D.I. (1976): Effects of magnesium and chloride ions on light-induced electron transport in membrane fragments from a blue-green alga. *Biochim. Biophys. Acta* (1975) **423**: 313-322.
- MENGEL K. (1984): Ernährung und Stoffwechsel der Pflanze. *Gustav Fischer Verlag*, Stuttgart, Germany.
- METCALFE C.R. & CHALK L. (1950): Anatomy of the Dicotyledons. Vol. I. *Clarendon Press, Oxford* (1950), U.K.: 242pp.
- MEYER U., KÖLLNER B., WILLENBRINK J., KRAUSE G.H.M. (1997): Physiological changes on agricultural crops induced by different ambient ozone exposure regimes. *New Phytol.* (1997) **136**: 645-652.
- MIYAJI K.-I., DA SILVA W.S., ALVIM P.DE T. (1997): Longevity of leaves of a tropical tree, *Theobroma cacao*, grown under shading, in relation to position within the canopy and time emergence. *New Phytol.* (1997) **135**: 445-454.
- MORAN R., PORATH D. (1980): Chlorophyll Determination in Intact Tissues Using N,N-Dimethylformamide. *Plant Physiol.* (1980) **65**: 478-479.
- MRABET Y. (2009): permission to use this picture is courtesy of *MRABET Yassine*
- NAGORNAYA R.V. & KOTSUR N.V. (1970): Absorption of radiant energy by anthocyanin-containing plants. *Nauk. Pr. Ukr. Silskogospod. Akad.* (1970) **31**: 103-112.
- MARSCHNER H. (1995): Mineral Nutrition of Higher Plants – Second Edition. *ACADEMIC PRESS LIMITED*, London, U.K.
- NASA (National Aeronautics and Space Administration) (2004): permission to use this picture is courtesy of [visibleearth.nasa](http://visibleearth.nasa.gov/) (<http://visibleearth.nasa.gov/>)
- NEILL S.O., GOULD K.S., KILMARTIN P.A, MITCHELL K.A., MARKHAM K.R. (2002): Antioxidant activities of red versus green leaves in *Elatostema rugosum*. *Plant, Cell and Environment* (2002) **25**: 539–547

- NIEMENAK N., ROHSIUS C., ELWERS S., NDOUMOU D.O., LIEBEREI R. (2006): Comparative study of different cocoa (*Theobroma cacao* L.) clones in terms of their phenolics and anthocyanins contents. *Journal of Food Composition and Analysis* (2006) **19**: 612-619.
- NOVAK B., SCHULZ B. (2009): Taschenlexikon tropischer Nutzpflanzen und ihrer Früchte. *Quelle & Meyer*, Wiebelsheim, Germany.
- NULTSCH W. (2000): Allgemeine Botanik. *Georg Thieme Verlag*: Stuttgart, Germany.
- ORCHARD J.E., COLLIN H.A., HARDWICK K. (1980): Biochemical and physiological aspects of leaf development in cocoa (*Theobroma cacao*) IV. Changes in growth inhibitors. *Plant Science Letters* (1980) **18**: 299-305 In: ABO-HAMED S., COLLIN H.A., HARDWICK K. (1983): Biochemical and physiological aspects of leaf development in cocoa (*Theobroma cacao* L.) – Growth, Orientation, Surface structure and water loss from developing flush leaves. *New Phytol.* (1983) **95**: 9-17.
- OSMAN H., NASARUDIN R., LEE S.L. (2003): Extracts of cocoa (*Theobroma cacao* L.) leaves and their antioxication potential. *Food Chemistry* (2004) **86**: 41-46.
- OSTROUMOV E.E., MULVANEY R.M., COGDELL R.J., SCHOLES G.D. (2013): Broadband 2D electronic spectroscopy reveals a carotenoid dark state in purple bacteria. *Science* (2013) **340**: 52-56.
- OTTO M. (2000): Analytische Chemie. *Wiley-VCH*, Weinheim, Germany: 381pp.
- OXBOROUGH K. & BAKER N.R. (1997): Resolving chlorophyll a fluorescence images of photosynthetic efficiency into photochemical and non-photochemical components – calculation of qP and F_v'/F_m' without measuring F_o' . *Photosynthesis Research Kluwer Academic Publishers, Netherlands* (1997), Netherlands **54**: 135-142.
- PAOLETTI R., POLI A., CONTI A., VISIOLI F. (2012): Chocolate and health. *Springer-Verlag Italia*: 42pp.
- PÉREZ-GREGORIO M.R., REGUEIRO J., ALONSO-GONZÁLEZ E., PASTRANA-CASTRO L.M., SIMAL-GÁNDARA J. (2011): Influence of alcoholic fermentation process on antioxidant activity and phenolic levels from mulberries (*Morus nigra* L.). *Food Science and Technology* (2011) **44**: 1793-1801.
- PFLÜGLER R. & MENGEL K. (1972): The photochemical activity of chloroplasts from various plants with different potassium nutrition. *Plant and Soil* (1972) **36**: 417-425. In: MENGEL K. (1984): Ernährung und Stoffwechsel der Pflanze. *Gustav Fischer Verlag*, Stuttgart, Germany.
- PORRA R.J. (2002): The chequered history of the development and use of simultaneous equations for the accurate determination of chlorophylls a and b. *Photosynthesis Research Kluwer Academic Publishers, Netherlands* (2002) **73**: 149-156.

- PRICE J.R. & STURGESS V.C. (1938): CCXIV A survey of anthocyanins. VI. *Biochem. J.* (1938) **32**: 1658-1660. In: LEE D. W., BRAMMEIER S., SMITH A.P. (1987): The Selective Advantages of Anthocyanins in Developing Leaves of Mango and Cacao. *Biotropica* (1987) **19** (1): 40-49.
- RAUF A. & SHRAMA U. (1980): Hill activity and anthocyanin levels in *Mangifera indica*. *Phytochemistry* (1980) **19**: 1270-1271. In: LEE D. W., BRAMMEIER S., SMITH A.P. (1987): The Selective Advantages of Anthocyanins in Developing Leaves of Mango and Cacao. *Biotropica* (1987) **19** (1): 40-49.
- RAVEN P.H., EVERT R.F., EICHHORN S.E. (2006): *Biologie der Pflanzen*. Walter de Gruyter GmbH & Co. KG, Berlin, Germany: 159.
- RICHARDS P.W. (1952): The tropical rainforest. *Cambridge University Press*, London, U.K. In: LEE D. W., BRAMMEIER S., SMITH A.P. (1987): The Selective Advantages of Anthocyanins in Developing Leaves of Mango and Cacao. *Biotropica* (1987) **19** (1): 40-49.
- RICHTER G. (1996): *Biochemie der Pflanzen*. Georg Thieme Verlag, Stuttgart, Germany.
- ROBERTS J.K.M. & PANG M.K.L. (1992): Estimation of ammonium ion distribution between cytoplasm and vacuole using nuclear magnetic resonance spectroscopy. *Plant Physiol.* (1992) **100**: 1571-1574.
- SALT D.E., BAXTER I., LAHNER B. (2008): Ionomics and the Study of the Plant Ionome. *Annu. Rev. Plant Biol.* (2008) **59**: 709-33.
- SANTOS R.C., PIRES J.L., CORREA R.X. (2011): Morphological characterization of leaf, flower, fruit and seed traits among Brazilian *Theobroma L.* species. Published online (2011) *Springer Science Buisness Media B.V. (2011) and Genet Resour Crop Evol* (2012) **59**: 327-345.
- SAUNDERS J.A., MISCHKE S., LEAMY E.A., HEMEIDA A.A. (2004): Selection of international molecular standards for DNA fingerprinting of *Theobroma cacao*. *Theor. Appl. Genet.* (2004) **110**: 41-47.
- SCHOPFER P. (1986): *Experimentielle Pflanzenphysiologie Band 1 Einführung in die Methoden*. Springer-Verlag, Berlin Heidelberg, Germany: 82pp.
- SCHOPFER P. (1989): *Experimentielle Pflanzenphysiologie Band 2 Einführung und Anwendungen*. Springer-Verlag, Berlin Heidelberg, Germany: 33pp.
- SCHOPFER P. & BRENNICKE A. (2010): *Pflanzenphysiologie*. Spektrum Akademischer Verlag, Heidelberg, Germany: 176pp.

- SCHREIBER U. (2004): Pulse-Amplitude-Modulation (PAM) Fluorometry and Saturation Pulse Method: An Overview In: GOVINDJEE, PAPAGEORGIOU G.C. (2004): Chlorophyll a Fluorescence: A Signature of Photosynthesis. *Springer*, Netherlands: 279-319.
- SCHREIBER U., BILGER W., NEUBAUER C. (1994): Chlorophyll fluorescence as a non-intrusive indicator for rapid assessment of in vivo photosynthesis. In: SCHULZE E.D., CALDWELL M.M.: Ecophysiology of Photosynthesis. Series Ecological Studies. *Springer-Verlag*, Berlin, Germany **100**: 49-70.
- SCHLEE D. (1986): Ökologische Biochemie. *Springer Verlag*, Berlin, Heidelberg (Germany), New York (U.S.), Tokyo (Japan).
- SCHWEDT G. (1996): Taschenatlas der Analytik. *Georg Thieme Verlag*, Stuttgart, Germany: 108pp.
- SEESING M. & TAUSCH M.W. (2004): permission to use this picture is courtesy of Prof. TAUSCH: Universität Duisburg-Essen, Germany [Lit: Tausch, von Wachtendonk: Chemie SII, *Buchner Verlag*, Bamberg, Germany 1993]
- SEIGLER D.S. (1998): Plant Secondary Metabolism. *Kluwer Academics Publisher* (1998), Boston, Dordrecht, London: 151-192.
- SMITH A.M. (1909): On the internal temperatures of leaves in tropical insolation, with special reference to the effect of their colour on temperature; also observations on the periodicity of the appearance of young coloured leaves of trees growing in Peradinaya Gardens. *Ann. Roy. Bot. Gard. Peradinaya* (1909) **4**: 229-297. In: LEE D. W., BRAMMEIER S., SMITH A.P. (1987): The Selective Advantages of Anthocyanins in Developing Leaves of Mango and Cacao. *Biotropica* (1987) **19** (1): 40-49.
- SMITH F.A. & RAVEN J.A. (1976): Transport and regulation of cell pH. *Enc. Plant Physiol.* **2A**: 317-346.
- SOTELO A. & ALVAREZ R.G. (1991): Chemical Composition of Wild Theobroma Species and Their Comparison to the Cacao Bean. *J. Agric. Food Chem.* (1991), **39**: 1940-1943.
- SPILLER G.A. (1998): Basic Metabolism and Physiological Effects of the Methylxanthines. In: SPILLER G.A. (1998): Caffein, *CRC Press LCC*, U.S.: 225pp.
- STRASSER R.J. (2004): Analysis of the Chlorophyll a Fluorescence Transient. In: GOVINDJEE, PAPAGEORGIOU G.C. (2004) Chlorophyll a Fluorescence: A Signature of Photosynthesis. *Springer*, Netherlands: 321-362.
- SZCZERBA M.W., BRITTO D.T., KRONZUCKER H.J. (2008): K⁺ transport in plants: physiology and molecular biology. *J. Plant Physiol.* (2008) **166**: 447-466.

- TISDALE S.L. & NELSON W.L. (1975): Soil Fertility and Fertilizer. *Macmillan*, New York, U.S.
- TERASHIMA I., FUJITA T., INOUE T., CHOW W.S., OGUCHI R. (2009): Green light drives leaf photosynthesis more efficiently than red light in strong white light: revisiting the enigmatic question of why leaves are green. *Plant Cell Physiol.* (2009) **50**: 684-697.
- VALEUR B. & BERBERAN-SANTOS M.N. (2012): Molecular Fluorescence Principles and Applications. *Wiley-VCH Verlag & Co*, Weinheim, Germany: 13pp.
- VOGEL M. (1975): Recherche du déterminisme du rythme de croissance du cacaoyer. *Café, Cacao, Thé* (1975) **19**: 265-290. In: ABO-HAMED S., COLLIN H.A., HARDWICK K. (1983): Biochemical and physiological aspects of leaf development in cocoa (*Theobroma cacao* L.) – Growth, Orientation, Surface structure and water loss from developing flush leaves. *New Phytol.* (1983) **95**: 9-17.
- WASHBURN D. K., WASHBURN W.N., SHIPKOVA P.A. (2011): The prehistoric drug trade: widespread consumption of cacao in Ancestral Pueblo and Hohokam communities in the American Southwest. *Journal of Archaeological Science* (2011) **38**: 1634-1640.
- WECKWERTH W. (2003): Metabolomics in systems biology. *Annu. Rev. Plant Biol.* (2003) **54**: 669-689.
- WECKWERTH W. & SUN X. (2012): COVAIN: a toolbox for uni- and multivariate statistics, time-series and correlation network analysis and inverse estimation of the differential Jacobian from metabolomics covariance data. *Metabolomics* (2012) **8**: 81-93.
- WORLD AGROFORESTRY CENTER (2012): www.worldagroforestry.org.
- YATSUHASHI H., HASHIMOTO T., SHIMUZU S. (1982): Ultraviolet action spectrum for anthocyanin formation in broom sorghum first internodes (*Sorghum bicolor*). *Plant Physiol.* (1982) **70**: 735-741. In: LEE D. W., BRAMMEIER S., SMITH A.P. (1987): The Selective Advantages of Anthocyanins in Developing Leaves of Mango and Cacao. *Biotropica* (1987) **19** (1): 40-49.
- ZIEGLER E. & EGGLE K. (1965): Zur quantitativen Analyse der Chloroplastenpigmente. I. Kritische Überprüfung der spektralphotometrischen Chlorophyll-Bestimmung. *Beiträge zur Biologie der Pflanze. Beiträge zur Biologie der Pflanzen* (1965) **41**: 11-37.

8. APPENDICES

8.1. Results overview - list of cations and anions

F-2-a (red < 10)	F-2-b (red > 10)	I-1-a (green-red)	I-1-b (pale-green)	I-2-a (green)	I-2-b (aging)	CATIONS [μE/gFM]
d	d	d	d	d	d	Na ⁺ _HE
d	d	d	d	d	d	Na ⁺ _AE
9.0 ± 1.4	6.3 ± 0.6	6.7 ± 0.6	6.4 ± 0.3	5.7 ± 0.3	7.9 ± 0.8	NH ₄ ⁺ _HE
33.1 ± 4.3	30.2 ± 2.8	28.0 ± 1.5	29.9 ± 2.7	28.7 ± 1.8	24.3 ± 1.8	NH ₄ ⁺ _AE
138.9 ± 14.4	149.1 ± 9.2	113.2 ± 9.2	119.7 ± 6.1	127.2 ± 10.6	50.7 ± 6.1	K ⁺ _HE
167.1 ± 26.1	184.2 ± 11.9	143.0 ± 10.8	159.4 ± 7.2	177.3 ± 14.2	76.3 ± 7.2	K ⁺ _AE
14.8 ± 3.4	12.5 ± 2	11.8 ± 1.2	13.4 ± 1.9	10.2 ± 1.1	16.2 ± 2.5	Ca ²⁺ _HE
46.3 ± 23.7	88.4 ± 11.4	77.8 ± 9.8	103.3 ± 14.7	257.9 ± 74.9	580.2 ± 65.1	Ca ²⁺ _AE
58.2 ± 9.9	57.0 ± 6.7	43.3 ± 4.1	46.0 ± 2.9	67.4 ± 15.7	103.4 ± 9.1	Mg ²⁺ _HE
87.5 ± 9	87.2 ± 12.2	84.5 ± 6.4	87.9 ± 6.8	132.8 ± 20.1	180.5 ± 13.8	Mg ²⁺ _AE
						ANIONS [μE/gFM]
14935.3 ± 3104.8	16298.9 ± 809.9	16727.5 ± 1040.9	17195.8 ± 687.3	16128.8 ± 546.1	15127.0 ± 605.2	Nitrate
1539.2 ± 377.6	1367.7 ± 385	1373.1 ± 195.2	1209.0 ± 308.1	2759.4 ± 316.5	1113.1 ± 252	Oxalic acid
1334.4 ± 331.9	1533.9 ± 240.0	1494.3 ± 292.1	1999.1 ± 434.9	702.3 ± 82.3	379.1 ± 58.4	Malic acid
511.4 ± 247.8	721.7 ± 104.7	622.8 ± 91.3	653.5 ± 63.4	1226.6 ± 119.4	828.7 ± 227.5	Phosphoric
397.0 ± 149.5	615.3 ± 211	439.9 ± 43.4	449.4 ± 246.9	552.0 ± 197.5	1353.4 ± 202.6	Sulphate
329.8 ± 109.9	368.9 ± 47.3	276.1 ± 26.8	247.5 ± 16.2	360.5 ± 42.2	439.9 ± 49.7	Quinic acid
139.5 ± 101.5	744.5 ± 174.1	102.7 ± 101.8	189.0 ± 102.4	138.8 ± 66.2	186.7 ± 32.9	Citrate
17.1 ± 6.9	23.2 ± 6.8	14.0 ± 3.3	17.9 ± 4.3	9.0 ± 1.6	7.9 ± 3.5	Chloride
d	d	d	d	7.8 ± 15.5	105.8 ± 9.6	Cumaric acid
d	d	d	d	d	d	Ferulic acid
d	d	d	d	d	d	Vanillic acid

Table 8.1: List of detected cations and anions (median ± 95% confidence interval), 'd' means detected at detection limit

8.2. Results overview – fluorescence, photometry, voltammetry and anatomy

		I-2-b (aging)	I-2-a (green)	I-1-b (pale-green)	I-1-a (green-red)	F-2-b (red > 10)	F-2-a (red < 10)
	F_v/F_m	0.4 ± 0.1	0.8 ± 0	0.6 ± 0	0.6 ± 0	0.6 ± 0	0.6 ± 0
	ETR [$\mu\text{mol}/\text{m}^2\text{s}$] at irradiance 784 [$\mu\text{mol}/\text{m}^2\text{s}$] PAR	-	53.3 ± 0.2	40.7 ± 5.4	40.6 ± 2.7	40.5 ± 1.1	41.0 ± 1.7
	pH	$5.4 \pm 0.1^*$	$5.7 \pm 0.1^*$	$5.7 \pm 0.1^*$	$5.7 \pm 0.2^*$	$6.0 \pm 0^*$	$5.7 \pm 0.2^*$
	$c(\text{H}_3\text{O}^+)$ [$\mu\text{mol}/\text{l}$]	3.8 ± 0.8	2.0 ± 0.2	1.8 ± 0.5	2.1 ± 0.6	1.0 ± 0.1	2.3 ± 1.0
	Chl a [$\mu\text{g}/\text{cm}^2$]	3.9 ± 1.5	16.7 ± 2.9	6.2 ± 1.5	6.8 ± 0.8	6.5 ± 0.5	5.9 ± 1
	Chl b [$\mu\text{g}/\text{cm}^2$]	2.5 ± 0.5	5.7 ± 0.8	3.7 ± 0.5	4.3 ± 0.2	4.4 ± 0.2	4.5 ± 1.1
	Carotenoids [$\mu\text{g}/\text{cm}^2$]	0.6 ± 0.1	1.1 ± 0.2	0.5 ± 0.1	0.5 ± 0	0.5 ± 0	0.6 ± 0.1
	Chl a/Chl b	1.6 ± 0.7	2.9 ± 0.6	1.7 ± 0.5	1.6 ± 0.3	1.5 ± 0.2	1.3 ± 0.4
	Car/Chl (a + b)	0.09 ± 0.06	0.05 ± 0.02	0.04 ± 0.03	0.05 ± 0.02	0.05 ± 0.02	0.05 ± 0.03
	Anthocyanidins [mg/cm^2]	$1.17\text{E-}05 \pm 7.30\text{E-}06$	$1.72\text{E-}06 \pm 1.20\text{E-}06$	$8.30\text{E-}06 \pm 3.40\text{E-}06$	$1.38\text{E-}04 \pm 1.65\text{E-}04$	$8.76\text{E-}04 \pm 1.50\text{E-}03$	$8.76\text{E-}04 \pm 1.50\text{E-}03$
	Voltammetric potential [Area/gFM]	$3.19\text{E-}07 \pm 3.45\text{E-}08$	$3.48\text{E-}07 \pm 3.06\text{E-}08$	$3.11\text{E-}07 \pm 5.59\text{E-}08$	$3.94\text{E-}07 \pm 4.31\text{E-}08$	$3.77\text{E-}07 \pm 2.65\text{E-}08$	$4.99\text{E-}07 \pm 7.73\text{E-}08$
	Stomata per area ($\sim 0.007 \text{ mm}^2$)	d	$47 \pm 3.2^*$	$75 \pm 7.6^*$	$85 \pm 9.1^*$	$168 \pm 16.9^*$	d

Table 8.2: Overview of some results shown in chapter 3. Most of them are presented with their median or arithmetic mean (*) and their appendant 95% confidence interval; 'd' means detected, but not further analysed, '-' means not measured.

8.3. List of figures

Figure 1.1: In red the latitude from about 20 ° North and South is plotted; the equator is marked in orange. (Adapted with Photoshop from a satellite world map from the NASA: http://visibleearth.nasa.gov/ 2004)	1
Figure 1.2: T. cacao flower development: A) Cauliflower cluster at a trunk; B) Flower with anthers; C) Flower bud, flower cross sections and flower top view. (©Engelmeier)	2
Figure 1.3: T. cacao flower development: A) Flower top view with anthers and floral formula drawing of * S5 P5 A(5+5) G(5); B) Drawing and flower cross section through flower bud. (©Engelmeier).....	3
Figure 1.4: T. cacao A) 1 day old Criollo cacao fruit on a trunk 1 cm long, still with petals; B) Forastero cacao fruit, 2 cm long and 3 days old; C) Criollo cacao, 2 months old, 22 cm. Developing and colouring Forastero cacao fruit: D) 2 months old, 19 cm; E) 3 months old, 19 cm. (©Engelmeier).....	4
Figure 1.5: T. cacao fruit development: A) Opened Forastero cacao fruit with creamy coloured pulp which covers every seed; B) Cacao seed covered with pulp, seed and cross section of anthocyanidin rich seed cotyledons; C) Hypocotyl germination of young T. cacao seed. (©Engelmeier).....	5
Figure 1.6: T. cacao tree in the greenhouse of the Department: The developing leaves are bright coloured and hanging down vertically, beneath adult dark green leaves in nearly horizontal position. (©Engelmeier)	6
Figure 1.7: T. cacao leaf flushing: A) Leaf bud with first flushing leaf (red arrow); B) Leaf expanding during the first days; C) Shiny about one week old leaf coloured in orange; D) 10 days old leaves with anthocyanidin coloured parts and shadowed leaf parts are still transparent greenish; E) 2 week old red to orange leaves with green nerves; F) Red leaves on a twig during expansion, about a week old; G) 1 week old leaf which is still enough transparent to see fingers behind it. (©Engelmeier)	7
Figure 1.8: Production and net exports of cacao beans in 2005/06 (ICCO, 2006).....	10
Figure 1.9: Schematic overview of the light and dark reaction in a chloroplast of a C3 plant. (Based on Engelmeier, unpublished).....	12
Figure 1.10: Derivation of a chlorophyll molecule A) pyrrol; B) porphyrin; C) chlorophyll a (black) and b (black with COH group in red). Structural formulae are constructed with ChemSketch.....	13
Figure 1.11: Two carotenes A) α -carotene B) β -carotene. Structural formulae are constructed with ChemSketch.....	14
Figure 1.12: Two xanthophylls A) Lutein B) Violaxanthin. Structural formulae are constructed with ChemSketch.....	15
Figure 1.13: A) Phenol B) Flavan – ground structure C) Flavone D) Flavonol. Structural formulae are constructed with ChemSketch.	16
Figure 1.14: A) anthocyanidin, the basic structure of anthocyanins and B) cyanidin. Structural formulae are constructed with ChemSketch.	17

Figure 1.15: Absorption spectra of chlorophyll a, b and carotenoids. The maximal absorbances are typically in the region of blue and red. Around green light, there is less absorbance (green-gap). (Based on CAMPBELL et al. 2009)	19
Figure 1.16: A) Perrin and Jablonski scheme: Different possibilities for an excited Chl a molecule (Chl a*) to return to the electronic ground state S ₀ . B) During deactivation of triplet chlorophyll molecules, excited singlet oxygen (¹ O ₂ [*]) is formed. It is transformed to original stage (³ O ₂) with usage of singlet carotene (¹ Car), which is then transformed to triplet carotene (³ Car*). The triplet carotene is formed to singlet carotene by the release of thermal energy. (Based on HÄDER & TEVINI, 1987 and SCHOPFER & BRENNICKE, 2010)	20
Figure 1.17: Energy transfer from the antenna to the reaction centre (© Engelmeier, unpublished). .	22
Figure 1.18: Not cyclic electron chain. Mn for manganese cluster; P680 for a pair of chlorophyll a at the reaction centre; Pheo for pheophytin for primary electron acceptor of PS II; Q for plastochinone electron acceptor of PS II; PQ for plastochinone pool; Cyt for cytochrome; Pcy for plastocyanin; P700 for a pair of Chl a; Chl a for primary electron acceptor of PS I – monomer; Fd for ferredoxin; FNR for ferredoxin - NADP reductase. (Adapted from Engelmeier, unpublished)	23
Figure 1.19: Overview of the working steps.	25
Figure 1.20: At the F ₀ state, reaction centres are opened, the leaf is illuminated with saturating light till all reaction centres are closed (F _m). (Adapted from: HANSATECH INSTRUMENTS Ltd, 2014)	26
Figure 1.21: Set-up of a photometric analyser. A) Light source; B) Monochromatic illuminator (prism or grating); C) Aperture; D) Cuvette with the liquid sample; F) Light detector; G) Measuring amplifier with the extinction outcome E _λ ; I ₀) Intensity of the irradiating light; I) Intensity of the transmitted light. © SEESING & TAUSCH (2004).....	27
Figure 1.22: Schematic Diagram of a High Performance Liquid Chromatograph.....	29
Figure 1.23: Simple illustration of a photodiode array detector (PDA), which is linked to the HPLC system and detected with a photodiode (light sensor). (Adapted from: LC RESOURCES, 2005).....	29
Figure 2.1: The classification of the different leaf stages. At the stages F-2 to I-1-a differences between the two trees can be determined (right: C1 and left: C2). The picture of the leaf initiation (F-1) is enhanced.....	34
Figure 2.2: Extraction of metabolites – individual colouring during maturity.	44
Figure 3.1: Climate plotting of temperature (°C, red) and relative humidity (% rh, blue) analysed by Temp Data logger, 5 days are zoomed out in scheme.	46
Figure 3.2: Leaf classification with an approximate time bar. Leaf initiation is zoomed out.	46
Figure 3.3: Results of PEA measurements: the shown data represent the median; error bars correspond to the 95 % confidence interval (t-values).	47

Figure 3.4: Imaging PAM: the data points are the medians; the 95 % confidence interval corresponds to the error bars.....	48
Figure 3.5: Median and 95 % confidence interval (error bar) of the calculated proton concentrations [$\mu\text{mol/l}$].....	49
Figure 3.6: Median and 95 % confidence interval (error bars) of concentrations of chlorophyll a (Chl a), chlorophyll b (Chl b) and carotenoids.	50
Figure 3.7: Comparison between the two trees C1 (n = 14) and C2 (n = 5) in stage I-2-a (green). Medians and 95 % confidence intervals (error bars) are shown.	51
Figure 3.8: Chl a to Chl b ratio; error bars are calculated with error propagation.	51
Figure 3.9: Carotenoids photometry of different development stages; medians and 95 % confidence intervals (error bars) are shown (zoomed out of Figure 3.6).	52
Figure 3.10: Ratio of Car to Chl a+b; error bars are calculated with error propagation.	52
Figure 3.11: Content of anthocyanidins in mg/cm^2 at 519 nm (arithmetic mean and standard deviation (error bars)).....	53
Figure 3.12: UV/VIS-spectra of several detected substances, see also Table 3.3.	57
Figure 3.13: Different fragmentation of cations (medians). On top there are shown results from the acid-hot-water-extracts (AE) and at the bottom these ones of the hot-water-extracts (HE). The units are in micro equivalents per gram fresh mass [$\mu\text{E/gFM}$].	58
Figure 3.14: Comparison (median and 95 % confidence interval) between the AE and HE from ammonium (orange) and potassium (purple) during leaf development.....	59
Figure 3.15: Differences (medians and 95 % confidence intervals) of magnesium concentrations in AE and HE are shown.....	59
Figure 3.16: Calcium content (median and 95% confidence interval) in AE (left) and HE (right).	60
Figure 3.17: Anion measurements (median) of the hot-water-extracts.	60
Figure 3.18: Concentrations of nitrate (blue), oxalic acid (orange), malic acid (grey) and phosphoric acid (yellow) in $\mu\text{E/gFM}$ (medians and 95 % confidence intervals).	61
Figure 3.19: Concentrations of sulphate (blue), quinic acid (green), citrate (brown) and chloride (purple) in $\mu\text{E/gFM}$ are shown with their medians and 95 % confidence intervals.	62
Figure 3.20: Voltammetric potential of the different stages (median and 95 % confidence interval (error bars)).....	63
Figure 3.21: Medians of the integrated area at a gradual transformation of voltage (+ 250 mV).	63
Figure 3.22: Measuring curves of two samples per stage (black and blue) A) stage aging (I-2-b); B) stage pale green (I-1-b); C) red > 10 cm (F-2-b).	64
Figure 3.23: Principal component analysis of LC-MS/MS data; PC 1 (34.1 %), PC 2 (10.8 %) and PC 3 (7.0 %). Evaluation and figuring was done with COVAIN (WECKWERTH & SUN, 2012).	65

- Figure 3.24:** A) Surface cut of a young cacao leaf in stage F-2-b (red > 10) (x200); B) cross section through petiole, hairs are visible, xylem is stained red with phloroglucin and hydrochloric acid (x50). 66
- Figure 3.25:** A) Trichomes visible at young leaves (stage red < 10); B) Small hair with a rounded multicellular head filled with anthocyanidins (left; in Figure 3.26 B-ii) and short stubby, single cellular cylindrical hair (right; in Figure 3.26 B-iii) (x200); C) Large hair with a larger multicellular head filled with anthocyanidins, only found on young hairs (in Figure 3.26 B-iii) (x400). 67
- Figure 3.26:** A) Fourth hair type: stellate shaped, multicellular hair (in B-iv) (x200); B) Anatomical drawing of all four hair types. 68
- Figure 3.27:** Stomata counting (medians and 95 % confidence intervals) of different cacao leaf stages, the observation area consecutively for all was ~ 0.007 mm² (x400). 68
- Figure 3.28:** Stomata prints from four cacao leaf stages (x400) A) Green (I-2-a); B) Pale green (I-1-b); C) Green-red (I-1-a); D) Red > 10 (F-2-b). 69
- Figure 3.29:** Stomata print of a leaf in stage red < 10. Fully developed stomata are located only on a middle rip and veins; A stellate shaped hair is in front (x400). 69
- Figure 3.30:** OPLS-DA analysis. The axes represent the two principal components (PC1 with 29 % and PC2 with 21 %). Analysis was performed with statgraphics and SIMCA. 70
- Figure 3.31:** PCA-X analysis (PC1 with 29 % and PC2 with 22 %). The same basic pattern of clustering as in OPLS-DA analysis is found. Analysis was performed with statgraphics and SIMCA. 71

8.4. List of tables

Table 1.1: Overview and definition of fluorescence concerning abbreviations (GENTY et al., 1989; SCHREIBER et al., 1994)	26
Table 3.1: Arithmetic means and standard deviations (σ) of pH measurements.	49
Table 3.2: Differences from stages green and green-red in between the two trees C1 and C2 (medians \pm 95 % confidence interval).....	50
Table 3.3: Results of HPLC-UV/VIS analysis. Detection of substance in most samples of one stage was signed as 'X'. Further, symbol 'x' means, that the detection was just in few samples or in low concentrations. The abbreviation cf. (lat. confer, determined uncertain) points out, that the spectrum could not be exactly attributed to metabolites in the UV/VIS library. Also, some derivatives (der.) were detected.....	56
Table 3.4: Cacao leaf LC-MS/MS data results from an internal library.....	66
Table 8.1: List of detected cations and anions (median \pm 95% confidence interval), 'd' means detected at detection limit	100
Table 8.2: Overview of some results shown in chapter 3. Most of them are presented with their median or arithmetic mean (*) and their appendant 95% confidence interval; 'd' means detected, but not further analysed, '-' means not measured.....	101

8.5. *Curriculum Vitae et Studiorum*

Lisa Maria Haberl

Personal Information

Date of birth: January, 6th 1990

Place of birth: Schärding am Inn, Austria

Nationality: Austria

Education:

2000-2008: Bundesrealgymnasium Schärding am Inn (main focus natural science)

Since 2008: University of Vienna

Studies in Biology and Mathematics for teacher professions

Working experience:

Tutorial functions in different lectures at the Department of Molecular Systems Biology:

2011-2014: “Pflanzenphysiologie für LA-BU” (Plant physiological practical course for teachers)

2012-2014: “Pflanzenphysiologische Übungen” (Plant physiological practical course)

2012-2014: “Experimente in Pflanzenphysiologie: Schulversuchsübungen” (Experiments in plant physiology for school)